THE DISCOVERY AND FUNCTIONAL STUDIES OF TWO DIPHTHAMIDE BIOSYNTHETIC GENES

A Dissertation

Presented to the Faculty of the Graduate School

of Cornell University

In Partial Fulfillment of the Requirements for the Degree of

Doctor of Philosophy

by

Xiaoyang Su

May 2013

THE DISCOVERY AND FUNCTIONAL STUDIES OF TWO DIPHTHAMIDE BIOSYNTHETIC GENES

Xiaoyang Su, Ph. D.

Cornell University 2013

Diphthamide is a post-translationally modified histidine residue found in eukaryotic and archael elongation factor 2 (EF2). Diphtheria toxin (DT) and the *Pseudomonas* exotoxin A (ETA) catalyze the ADP-ribosylation reaction on the diphthamide residue of EF-2 and therefore inactivate EF-2 and stop ribosomal protein synthesis. Proposed biosynthetic pathway of diphthamide has three steps. In eukaryotes, there are five participating genes, namely DPH1 – DPH5, have been identified. The first step requires four proteins, Dph1-4, while the second step requires a single protein, Dph5. In contrast, the enzyme required for the last amidation step has remained unknown even three decades after the structure of diphthamide was revealed.

I started my work on the first step modification. Yeast Dph1 and Dph2 were expressed and purified and were shown to be active in S-adenosyl methionine (SAM) cleavage, but not in the 3-amino-3-carboxypropyl (ACP) group transfer. Yeast ORF YBR246W was then studied, which was reported to be required for diphthamide biosynthesis. Our results showed that diphthine accumulates in the YBR246W deletion strain. Therefore YBR246W is required for the amidation step of diphthamide biosynthesis. Following this functional study, I discovered the diphthamide synthetase, YLR143W using yeast co-fitness analysis. We have been able to show that YLR143W catalyzes the diphthine amidation reaction *in vitro*. The nitrogen source of this reaction is ammonium and

AMP is generated. The human orthologue ATPBD4 is also a diphthamide synthetase. Further study revealed that YBR246W's activity is required prior to the activity of YLR143W. So there should be a minimum of four steps in diphthamide biosynthetic pathway.

The final part of my thesis describes our work on a human sirtuin SIRT5. Sirtuins are a family of NAD-dependent deacetylases. Our crystallography and biochemical studies showed that Sirt5 prefers to catalyze demalonylation and desuccinylation instead of deacetylation. A number of lysine succinylation sites were identified on bovine glutamate dehydrogenase (GDH) and other proteins. Sirt5 was shown to regulate succinylation and activity of carbamoyl-phosphate synthase 1 (CPS1).

BIOGRAPHICAL SKETCH

Xiaoyang Su was born in Beijing, China in 1981. He graduated from Tsinghua University in 2004, majored in Biology. He got a Master's degree from Tsinghua University in 2007 by studying the role of metal ions in Alzheimer's disease under the supervision of Dr. Yan-Mei Li. He joined the Department of Chemistry and Chemical Biology at Cornell University in 2007 and started working in Dr. Hening Lin's group. His graduate study was kindly supported by Tsang Fellowship in 2009. He won the Tunis Wentink Prize for Outstanding Graduate Students in 2012 and the Chinese Government Scholarship for Outstanding Self-Financed Students in 2012. His thesis entitled "The discovery and functional studies of two diphthamide biosynthetic genes" was supervised by Dr. Hening Lin.

ACKNOWLEDGMENTS

My entire work was made possible under the supervision of Dr. Hening Lin. I sincerely appreciate his support in every aspect. His guidance on experiment design, troubleshooting, result analysis, manuscript and presentation preparation has been an invaluable lesson to me. I want to give my appreciation to my committee members, Prof. Steven E. Ealick and Prof. Brian Crane for their suggestions and helps.

Dr. Jintang Du helped me greatly when I started working in this lab. I learn a lot of techniques from him. Dr. Hong Jiang not only provided the Rh-NAD molecule for my experiments, but also gave me critical suggestions on experiment design and data analysis. Dr. Xuling Zhu helped me a lot with the glovebox experiments and SDS-PAGE gel autoradiography. Dr. Colleen M. Kuemmel gave me suggestions on the yeast bioinformatics tools and resource. Zhewang Lin made distinguished contribution to this work and it is a true pleasure to work with him. I would like to thank the undergraduate students who worked with me. Their work facilitated and enriched my research. Kyle Horak helped me making some of the yeast Dph1/Dph2 mutants. Wankyu Lee helped me purified eEF-2 from a number of yeast DPH gene deletion strains. Diana Cheung helped me with the cloning of GDH and the CPS1 activity assay. Emily Dando helped me in the Dph2 mutagenesis study. All the Lin lab members contribute to a friendly, cooperative and productive environment that I truly enjoyed in.

My research has been greatly facilitated by our collaborators. Dr. Sheng Zhang, Dr. Wei Chen and Robert Sherwood helped me with mass spectrometry and proteomics studies. Special thanks go to Dr. Wei Chen for enormous help in technical support and data analysis. I would like to thank Dr. Quan Hao and Dr. Yeyun Zhou for solving the

structure of Sirt5. Dr. Johan Auwerx and Dr. Jiujiu Yu provided us samples from Sirt5 knock-out mice. Dr. Richard A. Cerione provided valuable insight on our Sirt5 work. Dr. Scott D. Emr and Dr. Yufeng Shi provided helpful discussion on our diphthamide projects and a number of deletion strains.

Finally, I would like to thank my family and friends for their supports. I had good days and bad days. No matter what happened, they were always with me. Without them being so supportive, I could not have achieved anything.

TABLE OF CONTENTS

Biographical Sketch iii

Acknowledgements iv

Table of Contents vi

Chapter 1: An Overview of Diphthamide Biosynthesis

Introduction 1

Structure determination of diphthamide and the identification of DPH genes 1

Activity and function of the DPH genes 3

The biological function of diphthamide 6

Dissertation statement 8

References 10

Chapter 2: YBR246W Is Required for The Third Step of Diphthamide Biosynthesis

Abstract 17

Introduction 18

Results and discussion 20

Methods 31

References 37

Chapter 3: A Chemogenomic Approach Identified Yeast YLR143W as Diphthamide Synthetase

Abstract 41

Introduction 42

Results 44
Discussion 58
Methods 61
References 68

Chapter 4: A Revisit of The Function of Dph7

Abstract 74
Introduction 75
Results 76
Discussion 79
Methods 82
References 85

Chapter 5: Functional Studies of Yeast Dph1-4

Abstract 88
Introduction 89
Results 90
Discussion 99
Methods 101
References 108

Chapter 6: Sirt5 Is an NAD-Dependent Protein Lysine Demalonylase and Desuccinylase

Abstract 111
Introduction 112

Results and discussion 113

Methods 140

References 153

Appendix A: Permissions for Full Paper Reproduction (Chapter 2) 157

Appendix B: Permissions for Full Paper Reproduction (Chapter 6) 158

LIST OF FIGURES

1.1 The structure of diphthamide and ADP-ribosylation reaction 2

1.2 The proposed biosynthetic pathway of diphthamide 3

2.1 Biosynthesis pathway of diphthamide 19

2.2 *In vitro* ADP-ribosylation using Rh-NAD 21

2.3 Growth assay of DPH gene deletion strains transformed with pLMY101 22

2.4 DT sensitivity assays of WT and deletion strains 22

2.5 DT sensitivity assays of WT and deletion strains 23

2.6 *In vitro* ADP-ribosylation assay with high concentration of DT 25

2.7 ADP-ribosylatability of eEF-2 from *Δdph5* 25

2.8 ADP-ribosylation assay using endogenous eEF-2 26

2.9 Extracted ion chromatograms of the unmodified peptides 27

2.10 MS/MS spectra of the unmodified peptide 28

2.11 Extracted ion chromatograms of diphthamide and diphthine from different strains 28

2.12 MS/MS spectra of diphthamide and diphthine containing peptides 29

3.1 Biosynthetic pathway of diphthamide in eukaryotes 43

3.2 The top 8 co-fitness correlations 44

3.3 The top 8 co-fitness correlations to YLR143W deletion strain 46

3.4 Diphthine accumulates in *Δylr143w* yeast strain 47

3.5 The Rh-NAD labeling of total lysates from various parental strains 47

3.6 The structure of the eEF-2-Exotoxin A complex 49

3.7 The sequence alignment of Exotoxin A and Diphtheira toxin 50

3.8 Growth assay using DT mutants 50

3.9 Diphtheria toxin sensitivity assay 51

3.10 Control plates of diphtheria toxin sensitivity assay 51

3.11 The mass spectrum of the eEF-2 peptide containing diphthine 52

3.12 The MS/MS spectrum of the diphthine containing peptide 52

3.13 YBR246W and YLR143W restore diphthamide biosynthesis in their deletion strains 54

3.14 Ectopic expression of YLR143W or human ATPBD4 restores diphthamide biosynthesis in the *Δylr143w* strain 54

3.15 YLR143W uses ATP and NH_4^+ for the amidation reaction 55

3.16 Clustal Omega protein sequence alignment result 57

3.17 AMP is formed in the diphthine amidation reaction 58

3.18 Proposed reaction pathway for YLR143W-catalyzed diphthine amidation reaction 58

4.1 eEF-2 from *Δdph7* cannot be amidated by purified Dph6 77

4.2 Dph5 purified from *E. coli* 78

4.3 Activity assay of purified Dph5 78

4.4 Amidation assay of diphthine produced by Dph5 79

4.5 Structure of diphthamide on eEF-2 may be in R-configuration 81

4.6 Proposed diphthamide biosynthetic pathway 82

5.1 Sequence alignment of Dph1 and Dph2 proteins from different species 91

5.2 Mutagenesis study of Dph2 92

5.3 Mutagenesis study of Dph1 92

5.4 Expression and purification of yeast Dph1-Dph2 in pET duet-1 and pET28b 94

5.5 The UV spectra of Dph1/Dph2 95

5.6 Purified yeast Dph1-Dph2 can cleave SAM 96

5.7 Expression and purification of yeast Dph3 and Dph4 97

5.8 The UV spectra of Dph3 97

5.9 Dph3 characterized by UV-Vis spectroscopy 98

5.10 The ^{14}C labeling assay of eEF-2 99

6.1 The sirtuins catalyzed NAD-dependent deacylation reaction 112

6.2 The structure of Sirt5 revealed an unusual acyl pocket 116

6.3 Overall structure of Sirt5 in complex with an H3K9 thioacetyl peptide 116

6.4 The rationale for predicting that malonyl/succinyl peptides could be better substrates for Sirt5 118

6.5 Sirt5 catalyzed the hydrolysis of malonyl and succinyl lysine 119

6.6 Sirt1 and Sirt5 catalyzed-hydrolysis of different acyl peptides monitored using LC-MS 122

6.7 Sirt1 and Sirt5-catalyzed deacetylation, demalonylation and desuccinylation of H3 K9 peptides were examined by HPLC 123

6.8 In the absence of Sirt5 or NAD, malonyl and succinyl peptides could not be hydrolyzed 124

6.9 LC-MS of synthetic unmodified H3K9 peptide 125

6.10 HPLC traces for the demalonylation reactions with H3K9 WW peptide were monitored at 280 nm and 215 nm 126

6.11 Sirt2, Sirt3, Sirt6, and Sirt7 did not catalyze the hydrolysis of malonyl and succinyl lysine 127

6.12 Time courses and sample HPLC traces from kinetic studies for Sirt5-catalyzed deacylation reactions 130

6.13 Sirt5-succinyl peptide-NAD ternary structure showing that the succinyl group interacted with Tyr102 and Arg105 131

6.14 Succinyl lysine was detected in bovine liver mitochondria 133

6.15 Succinyl lysine modification could be detected in CPS1 and GDH peptides 137

6.16 Relative quantitation analysis was achieved by extracted ion chromatograms 138

6.17 Tyr and Arg residues are conserved in most Class III sirtuins 139

LIST OF TABLES

2.1 Yeast strains used in Chapter 2 36

3.1 Yeast strains used in Chapter 3 66

6.1 Acetyl peptides used to assay the deacetylase activity of sirtuins 114

6.2 The kinetic parameters of four human sirtuins on H3 K9 acetyl peptide 115

6.3 The kinetic parameters of Sirt5 on acetyl, malonyl, and succinyl peptides with different sequences 128

6.4 Acetyl, thioacetyl, malonyl, and succinyl peptides used for Sirt5 crystallization and kinetics studies 129

6.5 The kinetic parameters of mutant Sirt5 132

6.6 Acetyl, malonyl, and succinyl GDH peptides identified by LC-MS/MS 135

6.7 Acetyl, malonyl, and succinyl peptides identified 136

CHAPTER 1

AN OVERVIEW OF DIPHTHAMIDE BIOSYNTHESIS

Introduction

Diphthamide is a post-translationally modified histidine residue found in eukaryotic and archael elongation factor 2 (EF2). It is named after the fact that it is the target of diphtheria toxin produced by *Corynebacterium diphtheriae*. Diphtheria toxin (DT) and the *Pseudomonas* exotoxin A (ETA) catalyzes the ADP-ribosylation reaction on the diphthamide residue of EF-2 using nicotinamide adenine dinucleotide (NAD) as the ADP-ribosyl donor(*1*). EF-2 catalyzes the translocation step and the ADP-ribosylation of EF-2 inactivates it, stopping protein synthesis and leads to cell death(*2, 3*).

Structure determination of diphthamide and the identification of DPH genes

The study of diphthamide started with the elucidation the DT modification site. It was first discovered that the target residue of diphtheria toxin is not an ordinary amino acid residue(*4*). It was further revealed that diphthamide exists only on EF-2 and there is one diphthamide residue per EF-2 protein(*5*). The modification sites were determined in both rat and yeast. The surrounding residues were found to be highly conserved(*5*). The structure of ADP-ribosyl diphthamide was determined using NMR and later confirmed by fast atom bombardment mass spectrometry(*6, 7*). The structure of diphthamide was proposed as 2-[3-carboxyamido-3-(trimethylammonio)propyl]histidine (Figure 1). The structure determination has also been confirmed by X-ray crystallography(*3, 8*). However, there is a noteworthy discrepancy on the

stereochemistry of diphthamide. Crystal structure of the eEF-2 showed R configuration on the third carbon of diphthamide side chain*(3, 8)*.

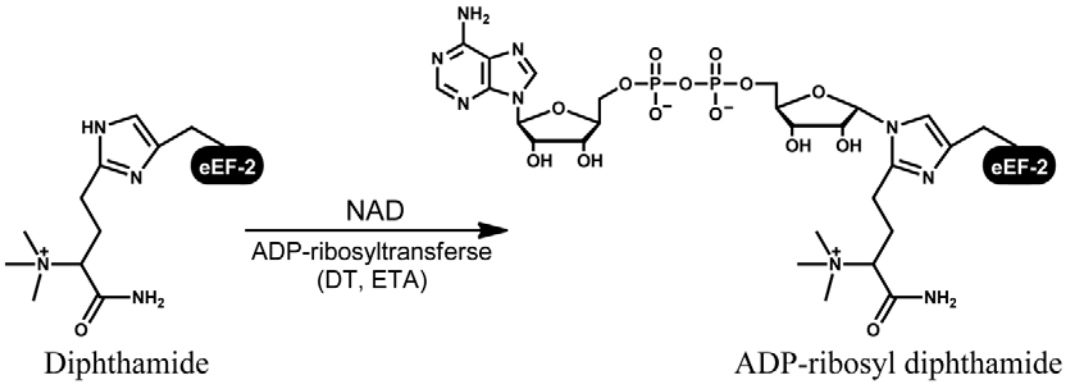

Figure 1.1 The structure of diphthamide and ADP-ribosylation reaction.

The structure determination allowed the proposal of the diphthamide biosynthetic pathway. By using biosynthetic labeling technique, it became clear that the backbone and the three methyl groups of diphthamide come from S-adenosylmethionine (SAM)(*9*). The study of diphtheria toxin resistant mutants of CHO-K1 Chinese hamster ovary cells revealed that there are a minimum of three steps(*10*). A genetic screening method for diphthamide deficient strains was developed based on the toxin sensitivity of the yeast spheroplasts(*11*). Five complementation groups were found and they were designated *dph1*, *dph2*, *dph3*, *dph4* and *dph5*. Heterozygous diploid produced by mating wild-type and the mutants showed that the resistant phenotype is recessive to the sensitive phenotype(*11*). It became clear later that Dph1-4 are responsible for the first step(*12*) (Figure 1.2), which is the transfer of the 3-amino-3-carboxypropyl (ACP) group. Dph5 is a methyltransferase that produces diphthine intermediate(*12*). Diphthine can be ADP-ribosylated, but the reaction rate was only 3% of the diphthamide ADP-ribosylation reaction(*12*). It was also

suggested that there is a diphthine amidation step following the Dph5 trimethylation. But the amidation enzyme remained unknown for almost three decades. It was speculated that the missing of diphthamide synthetase in the genetic screening was because diphthine can already be ADP-ribosylated by the toxin. Therefore, the original screening condition did not allow the emerge of the gene(s) responsible for the amidation reaction.

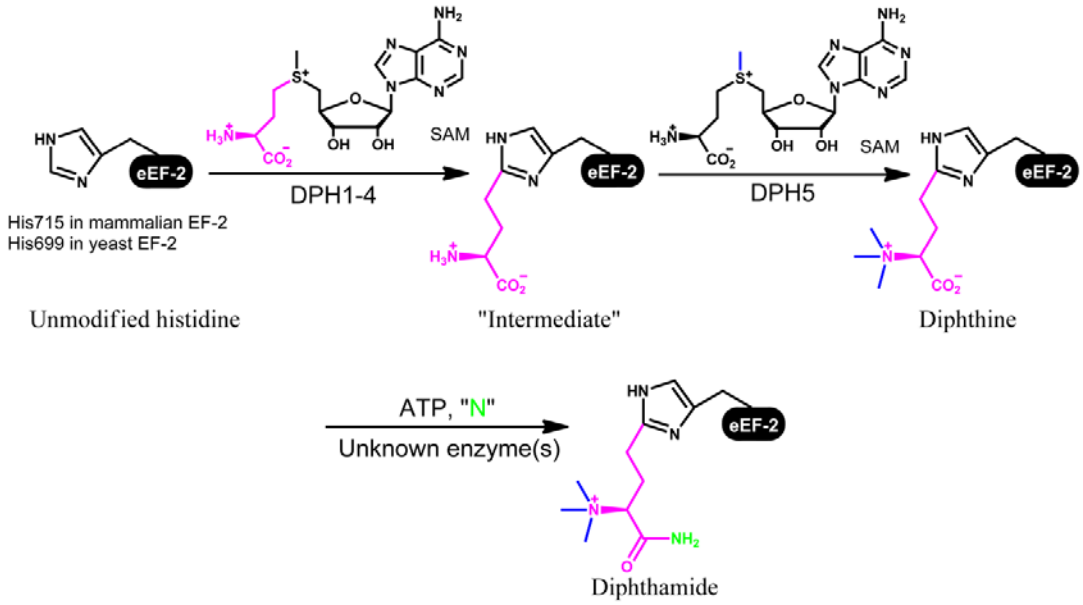

Figure 1.2 The proposed biosynthetic pathway of diphthamide. The origin of each functional group is colored.

Activity and function of the DPH genes

The first step of diphthamide biosynthesis is the transfer of the ACP group from SAM to the C2 position of the imidazole ring of the histidine residue being modified in EF-2. This reaction has been reconstituted in vitro and studied in great detail using the enzyme from an archaeal species *Pyrococcus horikoshii*(*13*). Unlike yeast, *Pyrococcus horikoshii* has only one gene to catalyze this step. The *Pyrococcus horikoshii* Dph2 (PhDph2) is homologous to eukaryotic Dph1 and

Dph2. Crystal structure of PhDhp2 homodimer was solved. PhDph2 forms a homodimer and contains one [4Fe-4S] cluster per monomer. Each PhDph2 monomer consists of three domains with similar folding pattern. The basic domain folding pattern is a four-stranded parallel β-sheet with three flanking α-helices(*13*). PhDph2 lacks the CX3CX2C motif which is present in most radical SAM enzymes(*14*), but contains three cysteine residues Cys59, Cys163 and Cys287 that are spatially closed and coordinate the [4Fe-4S] cluster. PhDph2 has been found to be active only under anerobic condition. PhDph2 does not generate 5'-deoxyadenosyl radical as most radical SAM enzymes do. Instead, PhDph2 cleaves the $C_{\gamma,Met}$–S bond of SAM to form 5'-deoxy-5'-methylthioadenosine (MTA) and ACP radical. The ACP radical attacks the histidine residue to give the final product.

In *Saccharomyces cerevisiae* the first step is considerably more complicated than in *Pyrococcus horikoshii*. There are 4 genes known to be required for this step, DPH1-4. Dph1 and Dph2 are homologous to each other and presumably form a heterodimer. Dph1/Dph2 dimer may work in a different way than PhDph2. It has been shown that PhDph2 forms a homodimer but only one active monomer is required for the activity(*15*). In yeast, both Dph1 and Dph2 are required. The PhDph2 has three cysteine residues coordinating the [4Fe-4S] cluster. These three cysteine residues are well conserved in Dph1, while the Dph2 has only the first and the third cysteine residues in place. The functional implication of this asymmetry awaits further study. It is not clear whether Dph1/Dph2 dimer is sufficient for the ACP transfer *in vitro*. It is also not clear whether other protein factors are required for this step.

Dph3 from Saccharomyces cerevisiae is as small as 82 amino acids. However, there are two domains, a N-terminal cystathionine β-synthase (CBS) domain and a C-terminal Zn ribbon domain(*16*). The solution structure of Dph3 structure was reported, which comprises a 3_{10} helix, two turns, two α helices and two β sheets(*17*). The C-terminal Zn ribbon domain has 4 conserved cysteine residues arranged in Cys-X-Cys-X_{19}-Cys-X_2-Cys motif. The Zn ribbon domain was found to bind both zinc and iron. Dph3 can be reduced by E. coli rubredoxin reductase NorW, suggesting its role as a rubredoxin-like electron carrier(*16*).

Dph3 has been studied for functions other than diphthamide biosynthesis. Δ*dph3* grows slower compared to other DPH gene deletion strains, implying that it has multiple functions(*18*). So far, people have shown that several DPH3 binding partners, including Elongator complex(*19, 20*), DelGEF (*21*) and yeast homologues of endophilin and amphiphysin(*22*). The physical interactions of Dph3 imply a variety of physiological functions, spanning from transcription regulation to endocytosis and secretion. The study of biochemical role of Dph3 in diphthamide biosynthesis is likely to shed light on its other cellular functions and vice versa.

Yeast Dph4 has an N-terminal J domain which is commonly found in co-chaperone proteins. The C-terminal of Dph4 is the CSL zinc finger(*23*). The J domain is required for the activity of Dph4. However, a chimeric version of Dph4 with the J domain from Ydj1 is also active(*23*). The cysteine residue in the CSL tripeptide is also important for its activity. The CSL zinc finger in Dph4 is shown to bind Fe more tightly than Zn. Iron binding induces the oligomerization of Dph4. The iron containing Dph4 is redox-active(*24*).

Dph5 is a methyltransferase which catalyzes the trimethylation of the amino group(*25*). The product of this step was named diphthine. Like most other methyltransferases, Dph5 uses SAM as the methyl group donor. eEF-2 from Δ*dph5* has a very weak activity as the substrate for ADP-ribosylation, about 10^6 times weaker than the eEF-2 from the wild-type strain(*26*). The diphthine-containing eEF-2 which was obtained by *in vitro* methylation using purified Dph5 is a much better substrate for ADP-ribosylation, about 30 times weaker than wild-type eEF-2*(12)*. Diphthine amidation was reconstituted *in vitro* using yeast cell lysate. It was revealed that this reaction is ATP-dependent. The identity of the nitrogen source was elusive.

Pyrococcus horikoshii Dph5 (PhDph5) was also studied in diphthine formation. PhDph5 was able to catalyze the trimethylation reaction in a highly processive manner. Interestingly, it was found that diphthine on PhEF-2 is not stable. It tends to lose the trimethylamino group in a reaction that is similar to Hofmann elimination(*27*). This reaction does not happen readily on yeast diphthine. The exact mechanism and implication of this reaction is unknown. However, this may help to explain the weak activity of archeal EF-2 as substrates in ADP-ribosylation reactions(*28*).

The biological function of diphthamide

The biological function of diphthamide has been elusive. Diphthamide modification makes cell susceptible to bacterial toxins, yet it is highly conserved among archaea and eukaryotes. The formation of diphthamide involves multiple proteins and enzymatic steps. It is hard to believe that such a system exists only to be exploited by bacterial toxins. These facts suggest a fundamental role of diphthamide. However, in yeast none of the DPH genes is essential. Therefore the true

function of diphthamide is mysterious. It has long been speculated that diphthamide is the target of endogenous ADP-ribosyltransferases. Bacterial toxin induced ADP-ribosylation shuts down ribosomal protein synthesis and kills host cells. It has been reported that diphthamide can also be ADP-ribosylated by endogenous ADP-ribosyltransferase and this is a regulatory mechanism for cellular protein synthesis(*29*). The endogenous ADP-ribosyltransferase activity was found from both polyoma virus-transformed baby hamster kidney (pyBHK) cells (*29*) and beef liver(*30*). However, later studies showed that the eEF-2 ADP-ribosylation activity from pyBHK cells was independent of diphthamide modification(*31, 32*). It has also been reported that interleukin-1β may act as an activator of the endogenous ADP-ribosylation(*33*). To the best knowledge of the authors, there has not been any endogenous diphthamide ADP-ribosyltransferase cloned and characterized.

Despite the fact that yeast strains lacking DPH genes grow normally, DPH genes have much more important functions in mammals. DPH1 gene has been found to be frequently deleted in ovarian and breast cancer, hence the alias OVCA1 (ovarian cancer gene 1)(*34-36*). Overexpression of OVCA1 suppresses the colony formation of ovarian cancer cells, presumably by cell cycle arrest at G1 phase(*37*). It was further demonstrated that OVCA1 overexpression in ovarian cancer cells A2780 leads to down-regulation of cyclin D1, and up-regulation of p16(*38*). OVCA1 homozygous mutant mice die at birth due to developmental delay and multiple organ defects. OVCA1 heterozygous mice develop cancer spontaneously(*39*). Similar to DPH1, DPH3 homozygous deletion leads to embryonic death(*40*) and DPH4 homozygous mutants were

retarded in growth and development(*41*). These developmental defects has been attributed to the deficiency of diphthamide(*42*).

Diphthamide has been found to be important in maintaining translational fidelity. The lack of diphthamide results in elevated -1 frameshift in protein synthesis(*43*). Diphthamide resides in the tip of domain IV of eEF2 which is in close proximity with the tRNA in the P-site(*44*). The positive charge brought by diphthamide modification helps eEF-2 to maintain conformational integrity(*42*). These discoveries provide a molecular insight of diphthamide function in development and tumorigenesis.

It is not clear whether diphthamide modification is a regulated process or not. However, evidences were provided that 5'-deoxy-methylthioadenosine inhibits diphthamide biosynthesis(*45*). This is probably because of the inhibition on the first step.

Dissertation statement

My graduate work touches on several steps of diphthamide biosynthesis. In Chapter 2, I describe my work on the first step modification. We have expressed and purified yeast Dph1 and Dph2 and showed that the proteins are active in SAM cleavage, but not in ACP group transfer. Chapter 3 described the functional study of yeast ORF YBR246W, which was reported to be required for diphthamide biosynthesis. Our results showed that diphthine accumulates in the YBR246W deletion strain. Therefore YBR246W is required for the amidation step of diphthamide biosynthesis. In Chapter4, I described the discovery of diphthamide synthetase, YLR143W,

using yeast co-fitness analysis. We have been able to show that YLR143W catalyzes the diphthine amidation reaction *in vitro*. The nitrogen source of this reaction is ammonium and AMP is generated. The human orthologue ATPBD4 is also a diphthamide synthetase. In Charpter 5, I further discussed the possible biochemical role of YBR246W. We found that there are actually two diphthine-containing eEF-2 species, one can be amidated and the other one cannot. So there should be a minimum of four steps in diphthamide biosynthetic pathway. YBR246W works after Dph5 and before YLR143W. Chapter 6 describes our work on a human sirtuin SIRT5. Sirtuins are a family of NAD-dependent deacetylases. Our crystallography and biochemical studies showed that Sirt5 prefers to catalyze demalonylation and desuccinylation instead of deacetylation. a number of lysine succinylation sites were identified on bovine glutamate dehydrogenase (GDH) and other proteins. Sirt5 was shown to regulate succinylation and activity of carbamoyl-phosphate synthase 1 (CPS1).

REFERENCES

1. Collier, R. J. (2001) Understanding the mode of action of diphtheria toxin: a perspective on progress during the 20th century, *Toxicon 39*, 1793-1803.

2. Honjo, T., Nishizuka, Y., and Hayaishi, O. (1968) Diphtheria toxin-dependent adenosine diphosphate ribosylation of aminoacyl transferase II and inhibition of protein synthesis, *J Biol Chem 243*, 3553-3555.

3. Jorgensen, R., Merrill, A. R., and Andersen, G. R. (2006) The life and death of translation elongation factor 2, *Biochem Soc Trans 34*, 1-6.

4. Robinson, E. A., Henriksen, O., and Maxwell, E. S. (1974) Elongation factor 2. amino acid sequence at the site of adenosine diphosphate ribosylation, *J. Biol. Chem. 249*, 5088-5093.

5. Van Ness, B. G., Howard, J. B., and Bodley, J. W. (1978) Isolation and properties of the trypsin-derived ADP-ribosyl peptide from diphtheria toxin-modified yeast elongation factor 2, *J Biol Chem 253*, 8687-8690.

6. Van Ness, B. G., Howard, J. B., and Bodley, J. W. (1980) ADP-ribosylation of elongation factor 2 by diphtheria toxin. NMR spectra and proposed structures of ribosyl-diphthamide and its hydrolysis products, *J. Biol. Chem. 255*, 10710-10716.

7. Van Ness, B. G., Howard, J. B., and Bodley, J. W. (1980) ADP-ribosylation of elongation factor 2 by diphtheria toxin. Isolation and properties of the novel ribosyl-amino acid and its hydrolysis products, *J. Biol. Chem. 255*, 10717-10720.

8. Jorgensen, R., Yates, S. P., Teal, D. J., Nilsson, J., Prentice, G. A., Merrill, A. R., and Andersen, G. R. (2004) Crystal structure of ADP-ribosylated ribosomal translocase from *Saccharomyces cerevisiae*, *J. Biol. Chem. 279*, 45919-45925.

9. Dunlop, P. C., and Bodley, J. W. (1983) Biosynthetic labeling of diphthamide in *Saccharomyces cerevisiae*, *J. Biol. Chem. 258*, 4754-4758.

10. Moehring, T. J., Danley, D. E., and Moehring, J. M. (1984) In vitro biosynthesis of diphthamide, studied with mutant Chinese hamster ovary cells resistant to diphtheria toxin, *Mol Cell Biol 4*, 642-650.

11. Chen, J. Y., Bodley, J. W., and Livingston, D. M. (1985) Diphtheria toxin-resistant mutants of *Saccharomyces cerevisiae.*, *Mol. Cell. Biol. 5*, 3357-3360.

12. Chen, J. Y., and Bodley, J. W. (1988) Biosynthesis of diphthamide in Saccharomyces cerevisiae. Partial purification and characterization of a specific S-adenosylmethionine:elongation factor 2 methyltransferase, *J Biol Chem 263*, 11692-11696.

13. Zhang, Y., Zhu, X., Torelli, A. T., Lee, M., Dzikovski, B., Koralewski, R. M., Wang, E., Freed, J., Krebs, C., Ealick, S. E., and Lin, H. (2010) Diphthamide biosynthesis requires an organic radical generated by an iron-sulphur enzyme, *Nature 465*, 891-896.

14. Frey, P. A., Hegeman, A. D., and Ruzicka, F. J. (2008) The radical SAM superfamily, *Crit. Rev. Biochem. Mol. Biol. 43*, 63 - 88.

15. Zhu, X., Dzikovski, B., Su, X., Torelli, A. T., Zhang, Y., Ealick, S. E., Freed, J. H., and Lin, H. (2011) Mechanistic understanding of Pyrococcus horikoshii Dph2, a [4Fe-4S]

enzyme required for diphthamide biosynthesis, *Mol. BioSystems 7*, 74-81.

16. Proudfoot, M., Sanders, S. A., Singer, A., Zhang, R., Brown, G., Binkowski, A., Xu, L., Lukin, J. A., Murzin, A. G., Joachimiak, A., Arrowsmith, C. H., Edwards, A. M., Savchenko, A. V., and Yakunin, A. F. (2008) Biochemical and structural characterization of a novel family of cystathionine [beta]-synthase domain proteins fused to a Zn ribbon-like domain, *J. Mol. Biol. 375*, 301-315.

17. Sun, J., Zhang, J., Wu, F., Xu, C., Li, S., Zhao, W., Wu, Z., Wu, J., Zhou, C.-Z., and Shi, Y. (2005) Solution structure of Kti11p from *Saccharomyces cerevisiae* reveals a novel zinc-binding module, *Biochemistry 44*, 8801-8809.

18. Bar, C., Zabel, R., Liu, S., Stark, M. J., and Schaffrath, R. (2008) A versatile partner of eukaryotic protein complexes that is involved in multiple biological processes: Kti11/Dph3, *Mol Microbiol 69*, 1221-1233.

19. Fichtner, L., and Schaffrath, R. (2002) KTI11 and KTI13, Saccharomyces cerevisiae genes controlling sensitivity to G1 arrest induced by Kluyveromyces lactis zymocin, *Mol Microbiol 44*, 865-875.

20. Greenwood, C., Selth, L. A., Dirac-Svejstrup, A. B., and Svejstrup, J. Q. (2009) An iron-sulfur cluster domain in Elp3 important for the structural integrity of elongator, *J Biol Chem 284*, 141-149.

21. Sjolinder, M., Uhlmann, J., and Ponstingl, H. (2004) Characterisation of an evolutionary conserved protein interacting with the putative guanine nucleotide exchange factor DelGEF and modulating secretion, *Exp Cell Res 294*, 68-76.

22. Krogan, N. J., Cagney, G., Yu, H., Zhong, G., Guo, X., Ignatchenko, A., Li, J., Pu, S., Datta, N., Tikuisis, A. P., Punna, T., PeregrÃ-n-Alvarez, J. M., Shales, M., Zhang, X., Davey, M., Robinson, M. D., Paccanaro, A., Bray, J. E., Sheung, A., Beattie, B., Richards, D. P., Canadien, V., Lalev, A., Mena, F., Wong, P., Starostine, A., Canete, M. M., Vlasblom, J., Wu, S., Orsi, C., Collins, S. R., Chandran, S., Haw, R., Rilstone, J. J., Gandi, K., Thompson, N. J., Musso, G., St Onge, P., Ghanny, S., Lam, M. H. Y., Butland, G., Altaf-Ul, A. M., Kanaya, S., Shilatifard, A., O'Shea, E., Weissman, J. S., Ingles, C. J., Hughes, T. R., Parkinson, J., Gerstein, M., Wodak, S. J., Emili, A., and Greenblatt, J. F. (2006) Global landscape of protein complexes in the yeast Saccharomyces cerevisiae, *440*, 637.

23. Sahi, C., and Craig, E. A. (2007) Network of general and specialty J protein chaperones of the yeast cytosol, *Proc Natl Acad Sci U S A 104*, 7163-7168.

24. Thakur, A., Chitoor, B., Goswami, A. V., Pareek, G., Atreya, H. S., and D'Silva, P. (2012) Structure and mechanistic insights into novel iron-mediated moonlighting functions of human J-protein cochaperone, Dph4, *J Biol Chem 287*, 13194-13205.

25. Mattheakis, L., Shen, W., and Collier, R. (1992) DPH5, a methyltransferase gene required for diphthamide biosynthesis in *Saccharomyces cerevisiae*., *Mol. Cell. Biol. 12*, 4026-4037.

26. Mattheakis, L. C., Shen, W. H., and Collier, R. J. (1992) DPH5, a methyltransferase gene required for diphthamide biosynthesis in Saccharomyces cerevisiae, *Mol Cell Biol 12*, 4026-4037.

27. Zhu, X., Kim, J., Su, X., and Lin, H. (2010) Reconstitution of diphthine synthase activity in vitro, *Biochemistry 49*, 9649-9657.

28. Pappenheimer, A. M., Jr, Dunlop, P. C., Adolph, K. W., and Bodley, J. W. (1983) Occurrence of diphthamide in archaebacteria, *J. Bacteriol. 153*, 1342-1347.

29. Lee, H., and Iglewski, W. J. (1984) Cellular ADP-ribosyltransferase with the same mechanism of action as diphtheria toxin and Pseudomonas toxin A, *Proc. Natl. Acad. Sci. USA 81*, 2703-2707.

30. Iglewski, W. J., Lee, H., and Muller, P. (1984) ADP-ribosyltransferase from beef liver which ADP-ribosylates elongation factor-2, *FEBS Lett 173*, 113-118.

31. Fendrick, J. L., Iglewski, W. J., Moehring, J. M., and Moehring, T. J. (1992) Characterization of the endogenous ADP-ribosylation of wild-type and mutant elongation factor-II in eukaryotic cells, *Eur. J. Biochem. 205*, 25-31.

32. Muhammet, B., scedil, K., R. N., inodot, and vanç Ergen, E. B. (2006) Endogenous ADP-ribosylation for eukaryotic elongation factor 2: evidence of two different sites and reactions, *Cell Biochemistry and Function 24*, 369-380.

33. Jager, D., Werdan, K., and Muller-Werdan, U. (2011) Endogenous ADP-ribosylation of elongation factor-2 by interleukin-1beta, *Mol Cell Biochem 348*, 125-128.

34. Phillips, N. J., Ziegler, M. R., Radford, D. M., Fair, K. L., Steinbrueck, T., Xynos, F. P., and Donis-Keller, H. (1996) Allelic deletion on chromosome 17p13.3 in early ovarian cancer, *Cancer Res. 56*, 606-611.

35. Phillips, N. J., Ziegler, M. R., and Deaven, L. L. (1996) A cDNA from the ovarian cancer

critical region of deletion on chromosome 17p13.3, *Cancer Lett. 102*, 85.

36. Chen, C. M., and Behringer, R. R. (2001) Cloning, structure, and expression of the mouse Ovca1 gene, *Biochem Biophys Res Commun 286*, 1019-1026.

37. Bruening, W., Prowse, A. H., Schultz, D. C., Holgado-Madruga, M., Wong, A., and Godwin, A. K. (1999) Expression of OVCA1, a candidate tumor suppressor, is reduced in tumors and inhibits growth of ovarian cancer cells, *Cancer Res 59*, 4973-4983.

38. Kong, F., Tong, R., Jia, L., Wei, W., Miao, X., Zhao, X., Sun, W., Yang, G., and Zhao, C. (2011) OVCA1 inhibits the proliferation of epithelial ovarian cancer cells by decreasing cyclin D1 and increasing p16, *Mol Cell Biochem 354*, 199-205.

39. Chen, C.-M., and Behringer, R. R. (2004) Ovca1 regulates cell proliferation, embryonic development, and tumorigenesis, *Genes Dev. 18*, 320-332.

40. Liu, S., Wiggins, J. F., Sreenath, T., Kulkarni, A. B., Ward, J. M., and Leppla, S. H. (2006) Dph3, a small protein required for diphthamide biosynthesis, is essential in mouse development, *Mol Cell Biol 26*, 3835-3841.

41. Webb, T. R., Cross, S. H., McKie, L., Edgar, R., Vizor, L., Harrison, J., Peters, J., and Jackson, I. J. (2008) Diphthamide modification of eEF2 requires a J-domain protein and is essential for normal development, *J Cell Sci 121*, 3140-3145.

42. Liu, S., Bachran, C., Gupta, P., Miller-Randolph, S., Wang, H., Crown, D., Zhang, Y., Wein, A. N., Singh, R., Fattah, R., and Leppla, S. H. (2012) Diphthamide modification on eukaryotic elongation factor 2 is needed to assure fidelity of mRNA translation and mouse development, *Proc Natl Acad Sci U S A*.

43. Ortiz, P. A., Ulloque, R., Kihara, G. K., Zheng, H., and Kinzy, T. G. (2006) Translation elongation factor 2 anticodon mimicry domain mutants affect fidelity and diphtheria toxin resistance, *J. Biol. Chem. 281*, 32639-32648.

44. Spahn, C. M., Gomez-Lorenzo, M. G., Grassucci, R. A., Jorgensen, R., Andersen, G. R., Beckmann, R., Penczek, P. A., Ballesta, J. P., and Frank, J. (2004) Domain movements of elongation factor eEF2 and the eukaryotic 80S ribosome facilitate tRNA translocation, *EMBO J 23*, 1008-1019.

45. Yamanaka, H., Kajander, E. O., and Carson, D. A. (1986) Modulation of diphthamide synthesis by 5'-deoxy-5'-methylthioadenosine in murine lymphoma cells., *Biochim. Biophys. Acta 888*, 157-162.

CHAPTER 2

YBR246W IS REQUIRED FOR THE THIRD STEP OF DIPHTHAMIDE BIOSYNTHESIS

Abstract

Diphthamide, the target of diphtheria toxin, is a post-translationally modified histidine residue that is found in archaeal and eukaryotic translation elongation factor 2. The biosynthesis and function of this modification has attracted the interest of many biochemists for decades. The biosynthesis has been known to proceed in three steps. Proteins required for the first and second steps have been identified, however, the protein(s) required for the last step remained elusive. Here we demonstrate that the YBR246W gene in yeast is required for the last step of diphthamide biosynthesis, as the deletion of YBR246W leads to the accumulation of diphthine, which is the enzymatic product of the second step of the biosynthesis. This discovery will provide important information to finally complete the full biosynthesis pathway of diphthamide.

Introduction

Diphthamide is a post-translationally modified histidine found on archaeal and eukaryotic translational elongation factor 2 (eEF-2)(*1-4*). Diphthamide is the target of the diphtheria toxin (DT), which is an exotoxin produced by *Corynebacterium diphtheria(5)*. The toxin ADP-ribosylates diphthamide and therefore inactivates eEF-2 to stop ribosomal protein synthesis. While being highly conserved from archaea to eukaryotes, the biological function of diphthamide remains poorly understood. The diphthamide modification has been reported to regulate translational fidelity in protein synthesis and the lack of diphthamide results in increased -1 frameshift mutation(*6*). However, no significant phenotype other than the toxin sensitivity has been linked to the lack of diphthamide modification in yeast.

The biosynthetic pathway of diphthamide has been elucidated in yeast and mammalian cells by biochemical and genetic studies(*7-15*). There are three steps in the diphthamide biosynthesis and five participating genes, namely DPH1 – DPH5, have been identified (Figure 2.1). The first step requires four proteins, Dph1-4, while the second step requires a single protein, Dph5. In contrast, the enzyme required for the last amidation step has remained unknown even three decades after the structure of diphthamide was revealed.

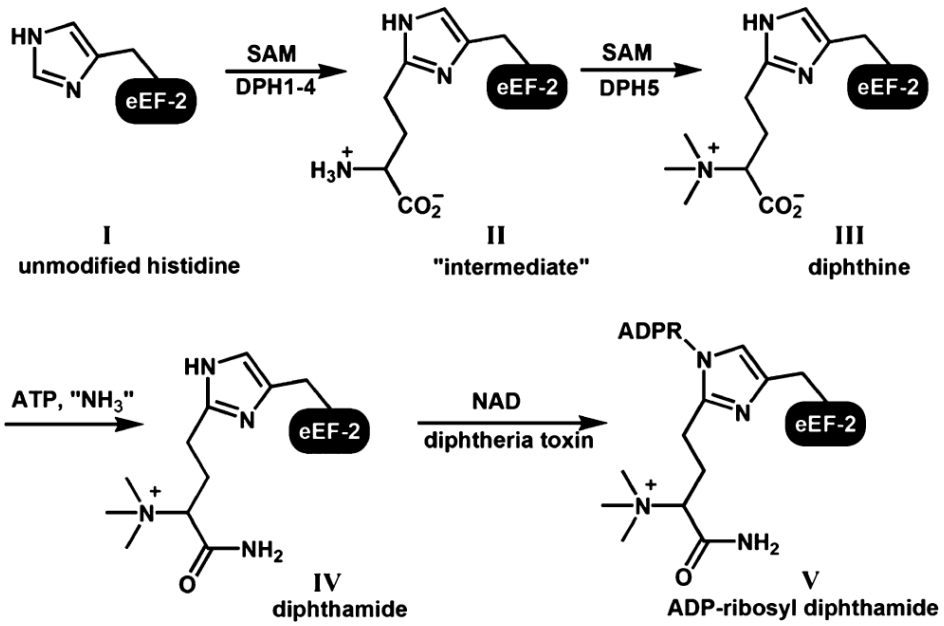

Figure 2.1 Biosynthesis pathway of diphthamide.

Recently, we have reconstituted the first and second step of diphthamide biosynthesis in vitro using proteins from a thermophilic archaea, *P. horikoshii(16-18)*. Archaeal diphthamide biosynthesis differs from the eukaryotic system in that among the four proteins (Dph1-Dph4) required for the first step, only one (Dph2) is present in archaea. *P. horikoshii* Dph2 (PhDph2) forms a homodimer in vitro, and uses a [4Fe-4S] cluster to generate a 3-amino-3-carboxypropyl radical to catalyze the first step of diphthamide biosynthesis(*16*). Based on what was learned from PhDph2 and that eukaryotic Dph1 and Dph2 are homologous and exist in a complex, we hypothesized that eukaryotic Dph1 and Dph2 forms a heterodimer and is functionally equivalent to PhDph2 homodimer(*16*). Dph3 and Dph4 most likely are required for the assembly of the [4Fe-4S] cluster or maintaining the [4Fe-4S] cluster in the correct redox state. Interestingly, one more protein, the product of yeast open reading frame (ORF) YBR246W, recently was reported

to be required for the first step of diphthamide biosynthesis(*19*). Because of our long standing interest in the enzymology of diphthamide biosynthesis, this report triggered us to ask two questions. Is YBR246W really required for the first step? If so, what is the molecular role of YBR246W in the first step? Thus, we set out to validate the reported functional assignment of YBR246W. Our results show that YBR246 is actually required for the third step of diphthamide biosynthesis. This corrected assignment for the function of YBR246W provides important information that will lead to the complete identification of the missing enzyme for the last step of diphthamide biosynthesis.

Results and discussion

YBR246W is required for diphthamide biosynthesis

To confirm the involvement of YBR246W in diphthamide biosynthesis, we first performed an in vitro ADP-ribosylation reaction. His_6-tagged eEF-2 was overexpressed and purified from wild-type (WT) and DPH gene deletion strains. A rhodamine-labeled NAD compound (Rh-NAD) was used in DT-catalyzed ADP-ribosylation reaction to visualize the product(*20*). Without DT, eEF-2 was not labeled (Figure 2). When 0.1 μM DT was used, the eEF-2 from WT yeast strain was clearly labeled. The eEF-2 from *Δdph2* or *Δybr246w* was not labeled (Figure 1). This result was consistent with the previous report that YBR246W is required for diphthamide biosynthesis(*19*). Without YBR246W, diphthamide modification is impaired and cannot be ADP-ribosylated efficiently.

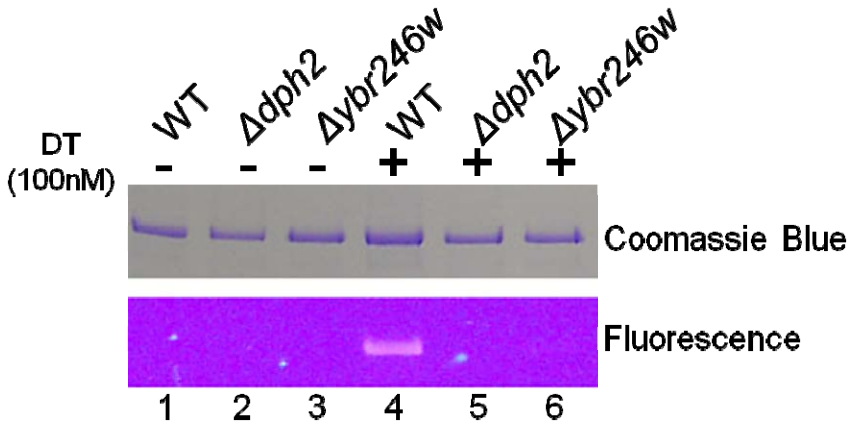

Figure 2.2 *In vitro* ADP-ribosylation using Rh-NAD. The upper panel was Coomassie blue-stained SDS-PAGE gel showing the eEF-2 proteins and the lower panel shows the corresponding fluorescence labeling. The source strains from which the eEF-2 proteins were purified were labeled above. No DT was added in lane 1-3 and 100 nM DT was added to lane 4-6. Reactions were carried out at 30°C for 20 min.

***In vivo* DT resistance assay revealed a different function of YBR246W**

We then tested the requirement of YBR246W in diphthamide biosynthesis using an in vivo DT resistance assay. This assay was similar to the one used to identify DPH1-DPH5 that are required for diphthamide biosynthesis(*8, 11*). WT, *Δdph1-Δdph5*, and *Δybr246w* strains were transformed with the pLMY101 plasmid(*11*), which contains the catalytic domain of the DT under the control of GAL1 promoter. When grown in glucose (Glc) medium, all strains were viable since DT expression was suppressed (Figure 2.3). The *Δdph3* strain showed minor growth defect due to the participation of DPH3 in other biological processes(*14, 21*). When 2% galactose (Gal) was used as the carbon source, the wild-type strain was killed due to the expression of the toxin, which ADP-ribosylates diphthamide on eEF-2. In contrast, DPH1-5 deletion strains were viable because they do not synthesize diphthamide. However, the Δybr246w strain failed to grow on medium with 2% Gal (Figure 2.4). The results showed that unlike other DPH gene deletions, the

YBR246W deletion does not confer DT resistance.

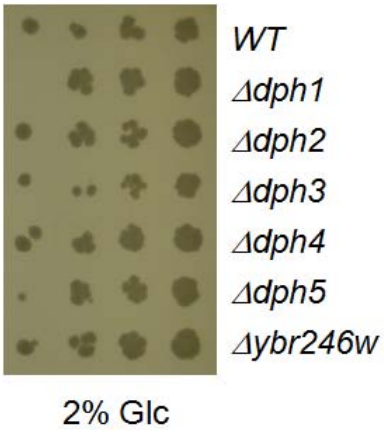

Figure 2.3 Growth assay of DPH gene deletion strains transformed with pLMY101. The strains were grown on 2% Glc medium.

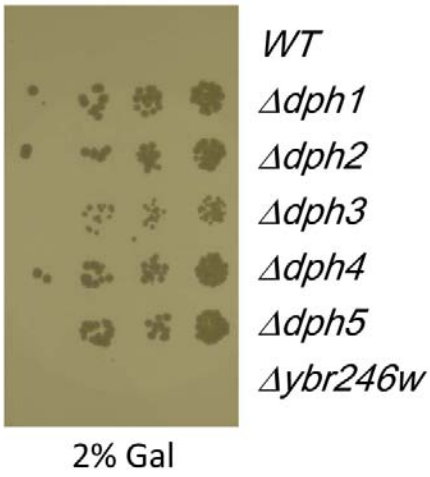

Figure 2.4 DT sensitivity assays of WT and deletion strains. The strains were transformed with pLMY101, which encodes the catalytic fragment of DT, and were grown on 2% Gal medium.

The DT sensitivity of *Δybr246w* was further examined by varying the Gal concentration in the medium to tune the expression level of DT. Raffinose (Raf) was used in combination with Gal to sustain the cell growth. Unlike Glc, which inhibits the GAL1 promoter transcription, Raf is a

neutral carbon source that does not promote nor inhibit GAL1-dependent expression. On plates with 2% Glc or 2% Raf, WT, *Δdph2*, and *Δybr246w* strains were all viable. When 0.001% Gal was added, WT strain showed severe growth defect and *Δybr246w* grew normally. When 0.01% Gal was added, the WT was completely killed and *Δybr246w* exhibited a significantly lowered viability. Neither the WT nor the *Δybr246w* strain was able to grow when 0.1% Gal was present in the medium (Figure 2.5). In contrast, the *Δdph2* strain was able to grow even in the presence of 2% Gal. This result shows that Δybr246w was only slightly more resistant to DT than WT.

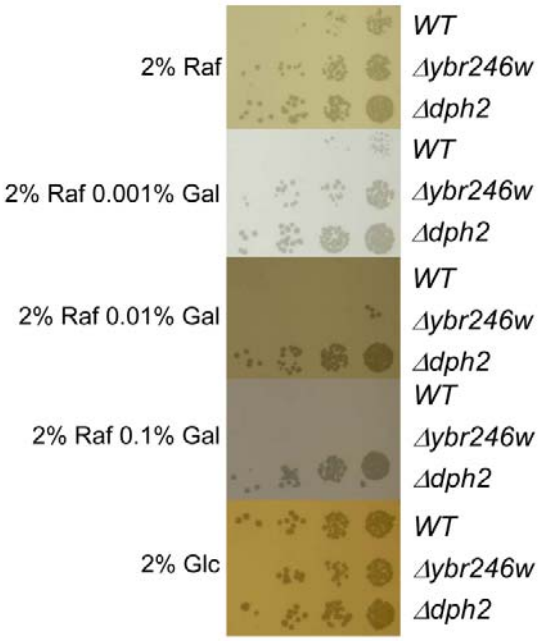

Figure 2.5 DT sensitivity assays of WT and deletion strains. (A) The strains were transformed with pLMY101, which encodes the catalytic fragment of DT, and were grown on 2% Gal medium. (B). WT, Δdph2 and Δybr246w were grown on 2% Raf plus varying concentrations of Gal. The growth on 2% Glc is shown as a control.

eEF-2 from *Δybr246w* shows lower ability to be ADP-ribosylated

The ADP-ribosylation results *in vitro* and the DT sensitivity results *in vivo* are seemingly in

conflict with each other. In other words, how can DT kill the *Δybr246w* yeast cells if the eEF-2 cannot be ADP-ribosylated? Two possibilities were considered. First, YBR246W is required for the first step and without YBR246W only a small fraction of eEF-2 is fully modified while the majority remains totally unmodified. The small fraction of diphthamide modification is enough to confer DT sensitivity. Second, the majority of eEF-2 is actually modified but to a form that is different from diphthamide. To test the two possibilities, the *in vitro* eEF-2 labeling experiment was repeated with a higher concentration of the toxin. If only a small fraction of eEF-2 is fully modified to diphthamide and can be ADP-ribosylated, then higher toxin concentrations would yield the same extent of labeling. However, the experimental result showed the opposite. The eEF-2 from the WT strain was labeled to similar levels at both low and high toxin concentrations. The eEF-2 from the *Δybr246w* was barely labeled when 0.1 μM DT was used, but was labeled clearly when 10 μM of DT was used (Figure 2.6). In contrast, the eEF-2 from *Δdph2* and *Δdph5* was not labeled even when high DT concentration was used (Figure 2.6 and 2.7). These results indicate that the eEF-2 from *Δybr246w* can be ADP-ribosylated by DT, but less efficiently. Similar results were obtained by labeling the endogenous eEF-2 (Figure 2.8). The difference in the ability to be ADP-ribosylated supports that eEF-2 from *Δybr246w* is different from the unmodified histidine (I in Figure 2.1), the intermediates (II in Figure 2.1) in the biosynthesis, or the fully modified diphthamide (IV in Figure 2.1). Thus the most logic possibility is that the eEF-2 from *Δybr246w* contains another intermediate such as diphthine.

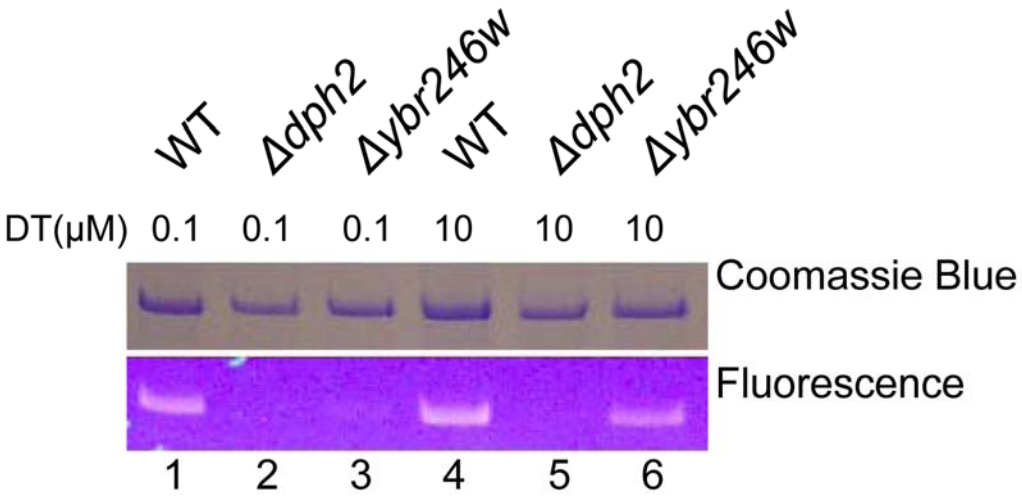

Figure 2.6 *In vitro* ADP-ribosylation assay with high concentration of DT. The upper panel shows a Coomassie blue-stained gel with the eEF-2 proteins and the lower panel shows the corresponding fluorescence labeling. The source strains from which the eEF-2 proteins were purified are labeled above. Reactions shown in lane 1-3 contained 0.1 μM of DT whereas those shown in lane 4-6 contained 10 μM of DT. Reactions were carried out at 30°C for 60 min.

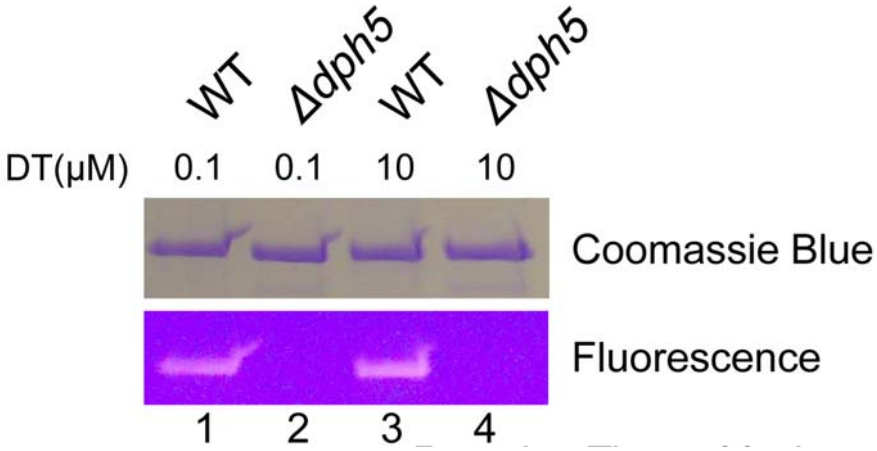

Figure 2.7 ADP-ribosylatability of eEF-2 from *Δdph5*. The upper panel was the Coomassie blue-stained gel showing the eEF-2 protein amount and the lower panel showed the corresponding fluorescence labeling. The source strains from which the eEF-2 were purified were shown above. Reactions shown in lane 1 and 2 contained 0.1 μM DT and reactions shown in lanes 3 and 4 contained 10 μM DT. Reactions were carried out at 30°C for 60 min.

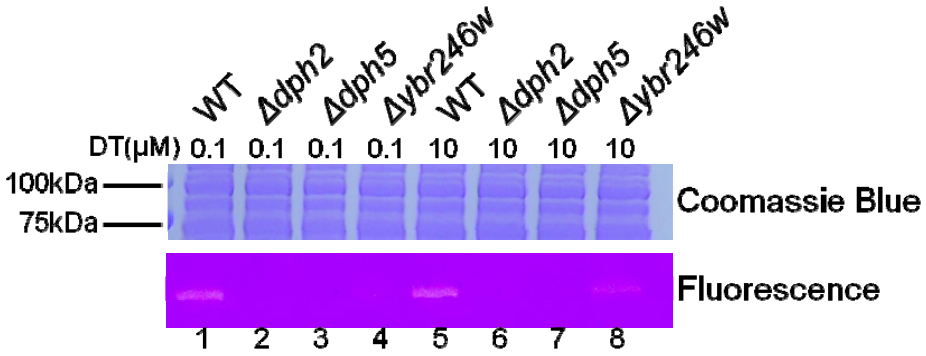

Figure 2.8 ADP-ribosylation assay using endogenous eEF-2. The yeast total protein extraction was performed as described in the Method. The upper panel shows a Coomassie blue-stained gel with the lysate proteins and the lower panel shows the corresponding fluorescence labeling. The source strains from which the lysates were obtained are labeled above. Reactions shown in lane 1-4 contained 0.1 μM of DT and those shown in lane 5-8 contained 10 μM of DT. The protein molecular weight marker positions are indicated on the left side. Reactions were carried out at 30°C for 60 min.

LC MS/MS confirmed diphthine on eEF-2 from *Δybr246w*

To confirm the presence of diphthine in the eEF-2 from *Δybr246w*, mass spectrometry (MS) studies were performed on eEF-2 purified from WT, *Δdph2* and *Δybr246w* yeast strains. The peptide (686-VNILDVTLHADAIHR-700) containing the unmodified histidine was found in all three eEF-2 samples (Figure 2.9 and 2.10). The diphthamide-containing peptide was only found in the eEF-2 from WT strain, and the diphthine-containing peptide was found only in the eEF-2 from *Δybr246w* (Figure 2.11). The identities of diphthamide and diphthine modifications on the peptides were supported by the MS/MS spectra (Figure 2.12). When singly charged, the peptide containing diphthamide is 0.984 Dalton smaller than the peptide containing diphthine. Both diphthamide and diphthine undergo a neutral loss of trimethylamino group during MS/MS, which was reported earlier(*22*). Because diphthine was present in *Δybr246w* yeast cells, we concluded that YBR246W is not required for the first step of diphthamide biosynthesis. The accumulation of

diphthine in *Δybr246w* but not in WT suggests that YBR246W is required for the last amidation step of diphthamide biosynthesis.

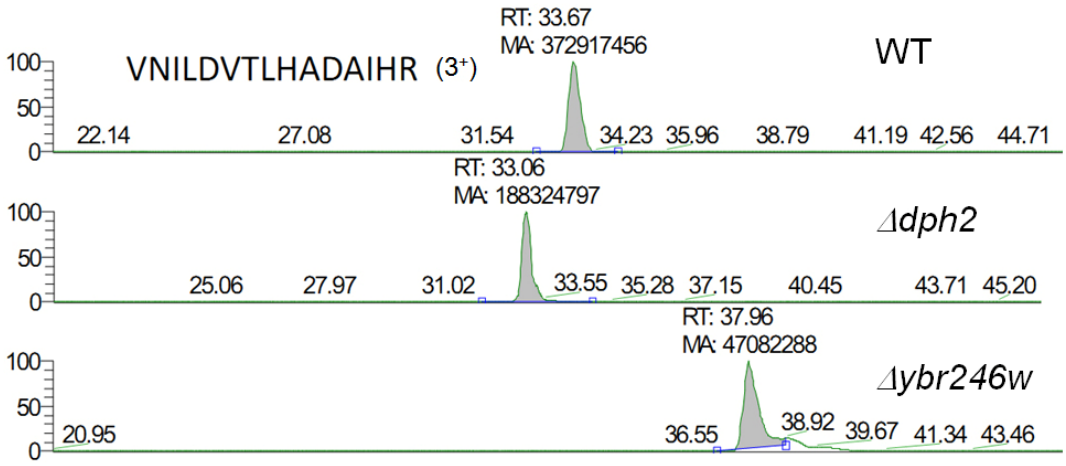

Figure 2.9 Extracted ion chromatograms of the unmodified peptides from WT, *Δdph2* and *Δybr246w*. The peaks corresponding to the unmodified peptide are highlighted in grey. The peptides carried 3 positive charges. The retention time (RT) and peak area by manual integration (MA) are marked. The identities of the peptides from different samples were confirmed by tandem MS/MS.

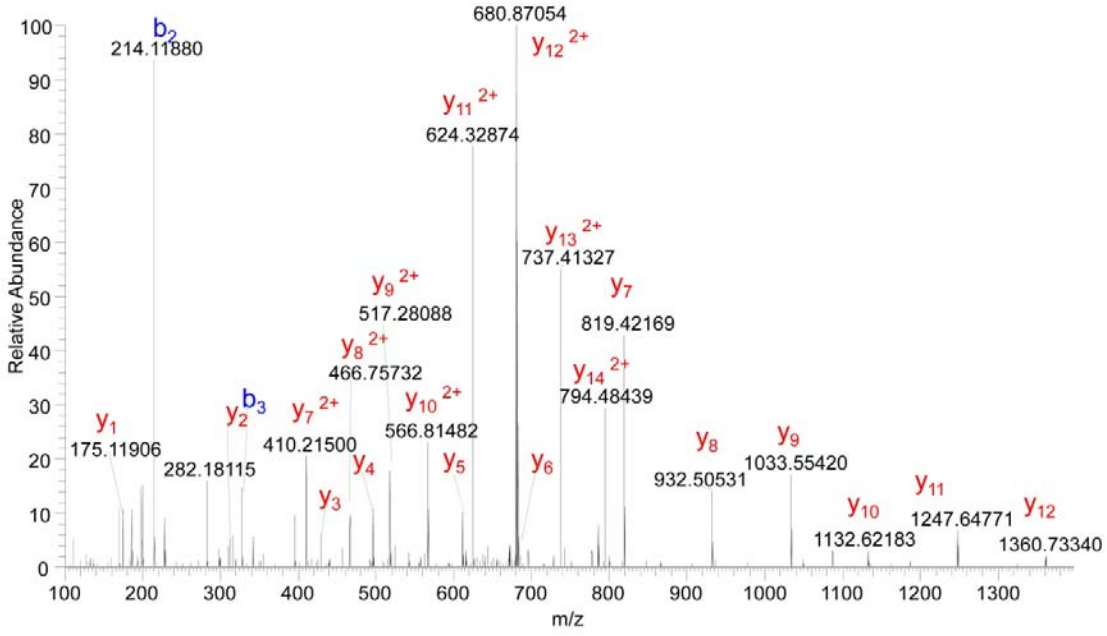

Figure 2.10 MS/MS spectra of the unmodified peptide (parental ion m/z 562.98114) from eEF-2 in WT strain.

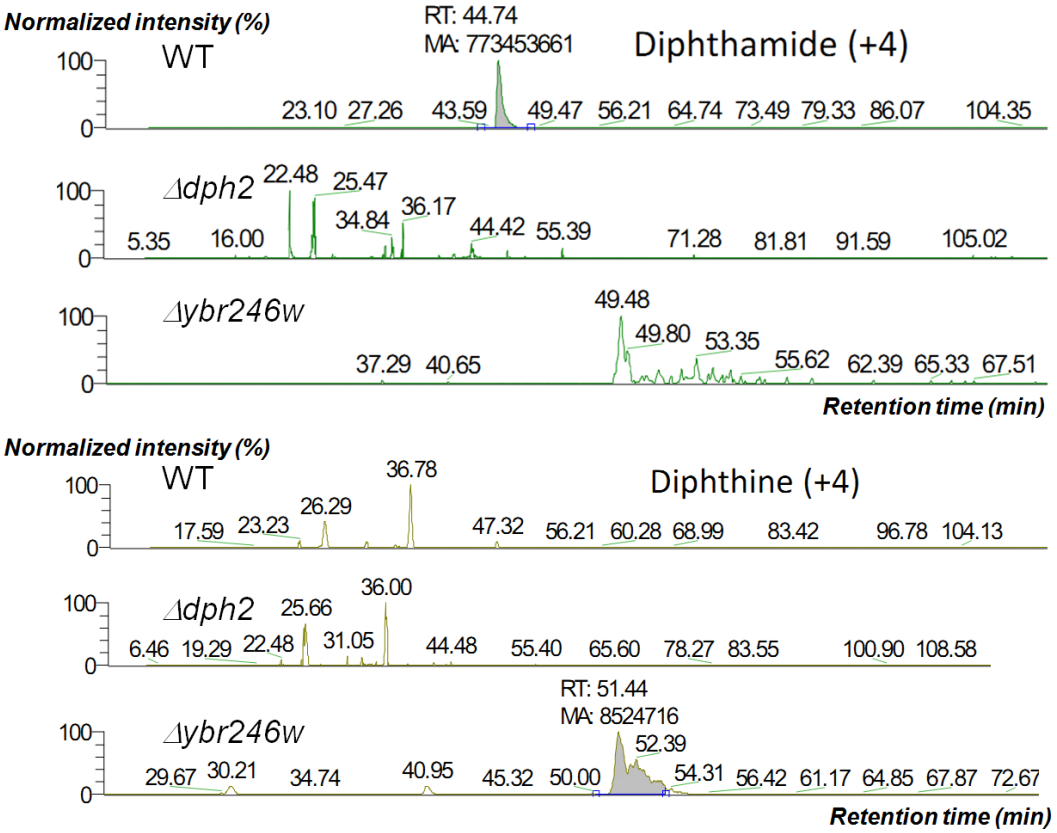

Figure 2.11 Extracted ion chromatograms of diphthamide and diphthine from different strains. The peaks corresponding to diphthamide and diphthine containing peptides are highlighted in grey. The peptides carried 4 positive charges. The retention time (RT) and peak area integration (MA) were shown above the highlighted peaks.

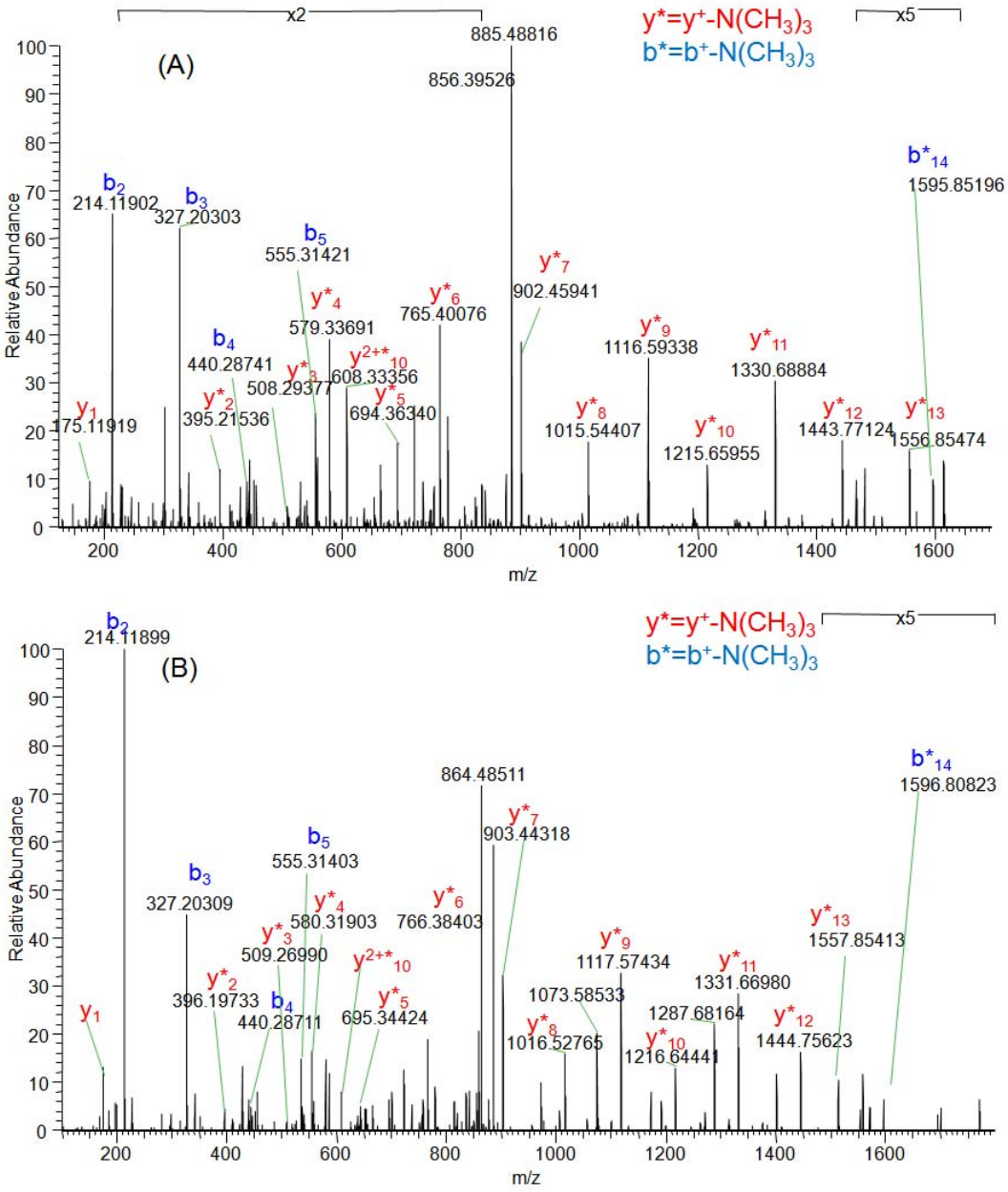

Figure 2.12 MS/MS spectra of diphthamide (A, parental ion m/z 915.02325) and diphthine (B, parental ion m/z 915.51520) containing peptides. A neutral loss of the trimethylamino group was observed in both spectra and labeled b* and y*.

We have previously reported that in *P. horikoshii* EF2 (PhEF-2), diphthine is not stable and readily eliminates the trimethylamino group and a proton in a reaction that is similar to

Hoffman/Cope elimination(*17*). This elimination is similar but different from the neutral loss of the trimethylamino group we observed for yeast diphthine during MS/MS. The elimination occurs before MS, while the neutral loss occurs during MS/MS. Two possible mechanisms for the elimination reaction of PhEF-2 diphthine were proposed(*17*). One mechanism uses an external base to attack the proton on the β-carbon and the other mechanism uses the carboxyl group as the intra-molecular base to deprotonate the β-carbon. Since the elimination reaction is species-dependent, it is possible that the actual base is a neighboring residue that is present in PhEF-2 but is not present in yeast eEF-2.

Previous genetics study provided crucial information that YBR246W is involved in diphthamide biosynthesis(*19*). However, our data presented here demonstrated that the biochemical function assignment was incorrect. The evidence used by Carette *et al.* to support that YBR246W was required for the first step was that eEF-2 from *Δybr246w* cannot be ADP-ribosylated and contained unmodified histidine residue. Our results demonstrated that although both observations can be repeated, they are only partially true. We have shown that eEF-2 from *Δybr246w* cannot be labeled when low concentration of DT was used, but can be labeled when higher concentration of DT was used. This labeling pattern is different from eEF-2 isolated from *Δdph2* strain, which cannot be labeled even when higher concentration of DT was used. Our study also showed that unmodified eEF-2 exists even in the WT strain, consistent with a previous report(*2*). So the presence of unmodified histidine in *Δybr246w* does not support that the first step modification is impaired. Instead, it may suggest that the first step of diphthamide biosynthesis is rate-limiting.

The accumulation of diphthine in *Δybr246w* strain but not in other DPH gene deletion strains or WT strain demonstrated that YBR246W is required for the third step of the diphthamide biosynthesis. Whether YBR246W alone is sufficient for the amidation step is unknown. It is possible that other proteins are also required. The protein that YBR246W encodes contains WD40 repeats which suggests that it may be a scaffold protein for the amidation step rather than a catalytic subunit(*23, 24*). Due to its scaffold role, YBR246W may be used to pull down other proteins required for the last step. Previous yeast genetic studies identified five DPH genes (DPH1-5), but YBR246W gene was not revealed. The reason is that under the selection condition previously used, *Δybr246w* was not viable to be selected, as we have shown in Figure 2.4. We observed that at a lower toxin induction level, the *Δybr246w* strain was able to grow while the WT strain was not. These findings may facilitate the identification of other genes involved in the amidation step. A recent report showed that YBR246W also functions in the retromer-mediated endosomal recycling pathway that is important for recycling amino acids transporters back to the plasma membrane(*24*). The fact that YBR246W functions in two apparently different biological pathways suggests an interesting possibility that YBR246W, as a possible scaffold protein, may coordinate nutrient availability (via recycling of amino acids transporters) and translation (via diphthamide biosynthesis). This may provide important clues to understand the function of diphthamide in protein biosynthesis, which has been almost completely unknown for more than three decades.

Methods

Expression and purification of yeast eEF-2.

The *Saccharomyces cerevisiae* eEF-2 with an added N/C-terminal His_6 tag was cloned into p423 MET25 vector (ATCC, Manassas, VA) as described before using the same restriction sites. The plasmid p423 MET25-eEF-2 (hosted by strain HL610E) was transformed into *S. cereisiae* strains with BY4741 background (OpenBiosystems, Huntsville, AL). The list of strains used in this study can be found in Table 2.1. To express the eEF-2 protein, the transformed cells were grown in synthetic complete media lacking histidine for 24 hours. Cells were harvested by centrifugation and resuspended in 20 mM Tris-HCl (pH 8.0), 500 mM NaCl, 10 mM $MgCl_2$, 5 mM imidazole, and 0.5 mM phenylmethylsulfonyl fluoride. Cells were lysed using the EmulsiFlex-C3 cell disruptor (Avestin, Inc., Canada), and purified on BioLogic DuoFlow 10 System (Bio-Rad, Hercules, CA). The purification was performed on HisTrap HP column (GE Healthcare, Piscataway, NJ) with a linear gradient from 30 mM imidazole to 500 mM imidazole in 30 min. The fractions were collected and dialyzed against 20 mM Tris-HCl buffer (pH 8.0) containing 50 mM NaCl. Protein concentration was determined by standard Bradford assay.

Yeast growth assay.

Cells were transformed with pLMY101 using the Frozen-EZ Yeast Transformation II Kit (Zymo Research, Irvine, CA). Transformed yeast cells (HL943Y – HL949Y, HL826Y – HL828Y) were grown on synthetic complete medium with uracil dropout. The carbon source was used as indicated. Colony formation was recorded 3 days after plating.

***In vitro* ADP-ribosylation using Rh-NAD.**

Rh-NAD was prepared as described previously. Purified yeast eEF-2 and Rh-NAD (50 μM) were incubated with DT at 30 °C in 25 mM Tris-HCl (pH 8.0), 50 mM NaCl, 30 mM dithiothreitol (DTT) and 2 mM ethylenediaminetetraacetic acid (EDTA). The DT concentration was 100 nM and the reaction time was 20 min if not specified otherwise. The reaction mixture was resolved by SDS PAGE. Rhodamine fluorescence signal from protein gel was visualized on a Fisher Scientific Ultraviolet Transilluminators.

Rh-NAD labeling of the endogenous eEF-2.

The yeast cell lysates were prepared as described previously. The concentration of the lysates were determined by Bradford assay. The labeling was performed as described above. The reaction mixture was resolved by SDS PAGE. Rhodamine fluorescence signal from protein gel was visualized on a Fisher Scientific Ultraviolet Transilluminators.

In-gel trypsin digestion of eEF-2

The eEF-2 bands were cut from a SDS-PAGE gel. The gel bands were washed in 100 μL water for 5 min, followed by 100 μL 100 mM ammonium bicarbonate (Ambic) : acetonitrile (1:1) for 10 min and finally 50 μL acetonitrile for 5 min. The acetonitrile was then discarded and the gel bands were allowed to dry in a ventilated fume hood for 10-20 min. The gel slices were then rehydrated with 20 μL of 10 mM DTT in 100 mM Ambic and incubated for 45 min at 56 °C. The samples were allowed to cool down to room temperature, then 20 μL of 55 mM iodoacetamide in 100 mM Ambic was added and the samples were incubated in the dark for 60 min. Following the incubation, the gel slices were again washed with water, Ambic / acetonitrile and acetonitrile as

described above. The gel slices were allowed to dry again.

Gel slices were rehydrated with trypsin solution (Promega, reconstituted at 100 µg/mL per protocol) on ice for 30 min. The trypsin solution was topped with 10 µL 50 mM Ambic with 10% acetonitrile. The digestion reactions were kept at 30°C for 16 h. The resulting solution was acidified with formic acid (FA, 1% in final). The trypsin digested peptides were extracted twice with 30 µl of 50% acetonitrile with 5% FA (45 min incubation at room temperature followed by 5 min sonication). The third extraction was done with 30 µl of 90% acetonitrile with 5% FA (5 min). All the extracts were combined and lyophilized.

Protein Identification with nano LC/MS/MS Analysis

The lyophilized in-gel tryptic digest samples were reconstituted in 20 µL of nanopure water with 0.5% FA for nanoLC-ESI-MS/MS analysis, which was carried out by a LTQ-Orbitrap Velos mass spectrometer (Thermo-Fisher Scientific, San Jose, CA) equipped with a"Plug and Play" nano ion source device (CorSolutions LLC, Ithaca, NY). The Orbitrap was interfaced with a nano HPLC carried out by Dionex UltiMate3000 RSLCnano system (Dionex, Sunnyvale, CA). The gel extracted peptide samples (2-4 µL) were injected onto a PepMap C18 trap column-nano Viper (5 µm, 100 µm id × 2 cm, Thermo Dionex) at 20 µL/min flow rate for on-line desalting and then separated on a PepMap C18 RP nano column (3 µm, 75 µm x 15 cm, Thermo Dionex) which was installed in the "Plug and Play" device with a 10-µm spray emitter (NewObjective, Woburn, MA). The peptides were then eluted with a 90 min gradient of 5% to 38% acetonitrile (ACN) in 0.1% formic acid at a flow rate of 300 nL/min. The Orbitrap Velos was operated in positive ion mode

with nano spray voltage set at 1.5 kV and source temperature at 275 °C. Internal calibration was performed with the background ion signal at m/z 445.120025 as the lock mass. The instrument was performed at data-dependent acquisition (DDA) mode by one precursor ion MS survey scan from m/z 350 to 1800 with a resolution of 60,000 at m/z 400 followed by up to 7 MS/MS scans at a resolution of 7,500 on top 7 most intensive peaks subjected to high energy collision dissociation (HCD). Dynamic exclusion parameters were set at repeat count 1 with a 15s repeat duration, exclusion list size of 500, 30 s exclusion duration, and ±10 *ppm* exclusion mass width. HCD parameters were set at the following values: isolation width 2.0 m/z, normalized collision energy 38%, activation Q at 0.25, and activation time 0.1 ms. All data are acquired under Xcalibur 2.1 operation software (Thermo-Fisher Scientific).

Data analysis.

Acquired MS and MS/MS raw spectra were processed using Proteome Discoverer 1.2 (PD1.2, Thermo) against Swissprot database with one missed cleavage site by trypsin allowed. Mass tolerances for precursor ions were set at 30 ppm and for MS/MS were set at 100 mmu. A fixed carbamidomethyl modification on cysteine, variable modifications on methionine oxidation, deamindation of asparagine and glutamine, and variable substitutions on histidine including diphthamide and diphthine as well as the possible elimination products were specified. All MS/MS spectra of identified peptides were manually inspected and verified using Xcalibur 2.1 software.

Table 2.1 Yeast strains used in Chapter 2

Strain	Genotype	Source
HL813Y	*MAT***a** *his3Δ1 leu2Δ0 met15Δ0 ura3Δ0*	Open Biosystems (YSC1048)
HL814Y	*MAT***a** *his3Δ1 leu2Δ0 met15Δ0 ura3Δ0 ybr246wΔ*	Open Biosystems (YSC1021-552106)
HL815Y	*MAT***a** *his3Δ1 leu2Δ0 met15Δ0 ura3Δ0 dph2Δ*	Open Biosystems (YSC1021-553846)
HL941Y	*MAT***a** *his3Δ1 leu2Δ0 met15Δ0 ura3Δ0 dph5Δ*	Open Biosystems (YSC1021-552709)
HL904Y	*MAT***α** *his3Δ1 leu2Δ0 lys2Δ0 ura3Δ0*	Open Biosystems (YSC1049)
HL905Y	*MAT***α** *his3Δ1 leu2Δ0 lys2Δ0 ura3Δ0 dph1Δ*	Open Biosystems (YSC1021-550206)
HL906Y	*MAT***α** *his3Δ1 leu2Δ0 lys2Δ0 ura3Δ0 dph2Δ*	Open Biosystems (YSC1021-548861)
HL907Y	*MAT***α** *his3Δ1 leu2Δ0 lys2Δ0 ura3Δ0 dph3Δ*	Open Biosystems (YSC1021-97228687)
HL908Y	*MAT***α** *his3Δ1 leu2Δ0 lys2Δ0 ura3Δ0 dph4Δ*	Open Biosystems (YSC1021-549671)
HL909Y	*MAT***α** *his3Δ1 leu2Δ0 lys2Δ0 ura3Δ0 dph5Δ*	Open Biosystems (YSC1021-547782)
HL940Y	*MAT***α** *his3Δ1 leu2Δ0 lys2Δ0 ura3Δ0 ybr246wΔ*	Open Biosystems (YSC1021-547231)
HL823Y	HL813Y [EFT1-p423MET25-HIS3]	This study
HL824Y	HL814Y [EFT1-p423MET25-HIS3]	This study
HL825Y	HL815Y [EFT1-p423MET25-HIS3]	This study
HL968Y	HL941Y [EFT1-p423MET25-HIS3]	This study
HL943Y	HL904Y [pLMY101]	This study
HL944Y	HL905Y [pLMY101]	This study
HL945Y	HL906Y [pLMY101]	This study
HL946Y	HL907Y [pLMY101]	This study
HL947Y	HL908Y [pLMY101]	This study
HL948Y	HL909Y [pLMY101]	This study
HL949Y	HL940Y [pLMY101]	This study
HL826Y	HL813Y [pLMY101]	This study
HL827Y	HL814Y [pLMY101]	This study
HL828Y	HL815Y [pLMY101]	This study

REFERENCES

1. Van Ness, B. G., Howard, J. B., and Bodley, J. W. (1980) ADP-ribosylation of elongation factor 2 by diphtheria toxin. NMR spectra and proposed structures of ribosyl-diphthamide and its hydrolysis products, *J Biol Chem 255*, 10710-10716.
2. Robinson, E. A., Henriksen, O., and Maxwell, E. S. (1974) Elongation factor 2. amino acid sequence at the site of adenosine diphosphate ribosylation, *J. Biol. Chem. 249*, 5088-5093.
3. Van Ness, B. G., Howard, J. B., and Bodley, J. W. (1980) ADP-ribosylation of elongation factor 2 by diphtheria toxin. Isolation and properties of the novel ribosyl-amino acid and its hydrolysis products, *J. Biol. Chem. 255*, 10717-10720.
4. Pappenheimer, A. M., Jr, Dunlop, P. C., Adolph, K. W., and Bodley, J. W. (1983) Occurrence of diphthamide in archaebacteria, *J. Bacteriol. 153*, 1342-1347.
5. Collier, R. J. (2001) Understanding the mode of action of diphtheria toxin: a perspective on progress during the 20th century, *Toxicon 39*, 1793-1803.
6. Ortiz, P. A., Ulloque, R., Kihara, G. K., Zheng, H., and Kinzy, T. G. (2006) Translation elongation factor 2 anticodon mimicry domain mutants affect fidelity and diphtheria toxin resistance, *J. Biol. Chem. 281*, 32639-32648.
7. Dunlop, P. C., and Bodley, J. W. (1983) Biosynthetic labeling of diphthamide in *Saccharomyces cerevisiae*, *J. Biol. Chem. 258*, 4754-4758.
8. Chen, J. Y., Bodley, J. W., and Livingston, D. M. (1985) Diphtheria toxin-resistant mutants of

Saccharomyces cerevisiae., *Mol. Cell. Biol. 5*, 3357-3360.

9. Moehring, J. M., and Moehring, T. J. (1984) Diphthamide: in vitro biosynthesis, *Methods Enzymol 106*, 388-395.

10. Moehring, J. M., and Moehring, T. J. (1988) The post-translational trimethylation of diphthamide studied in vitro, *J Biol Chem 263*, 3840-3844.

11. Mattheakis, L. C., Shen, W. H., and Collier, R. J. (1992) DPH5, a methyltransferase gene required for diphthamide biosynthesis in Saccharomyces cerevisiae, *Mol Cell Biol 12*, 4026-4037.

12. Mattheakis, L. C., Sor, F., and Collier, R. J. (1993) Diphthamide synthesis in *Saccharomyces cerevisiae*: structure of the DPH2 gene, *Gene 132*, 149.

13. Liu, S., and Leppla, S. H. (2003) Retroviral insertional mutagenesis identifies a small protein required for synthesis of diphthamide, the target of bacterial ADP-ribosylating toxins, *Mol Cell 12*, 603-613.

14. Liu, S., Milne, G. T., Kuremsky, J. G., Fink, G. R., and Leppla, S. H. (2004) Identification of the proteins required for biosynthesis of diphthamide, the target of bacterial ADP-ribosylating toxins on translation elongation factor 2, *Mol Cell Biol 24*, 9487-9497.

15. Schultz, D. C., Balasara, B. R., Testa, J. R., and Godwin, A. K. (1998) Cloning and localization of a human diphthamide biosynthesis-like protein-2 gene,DPH2L2, *Genomics 52*, 186.

16. Zhang, Y., Zhu, X., Torelli, A. T., Lee, M., Dzikovski, B., Koralewski, R. M., Wang, E., Freed, J., Krebs, C., Ealick, S. E., and Lin, H. (2010) Diphthamide biosynthesis requires an organic radical

generated by an iron-sulphur enzyme, *Nature 465*, 891-896.

17. Zhu, X., Kim, J., Su, X., and Lin, H. (2010) Reconstitution of diphthine synthase activity in vitro, *Biochemistry 49*, 9649-9657.

18. Zhu, X., Dzikovski, B., Su, X., Torelli, A. T., Zhang, Y., Ealick, S. E., Freed, J. H., and Lin, H. (2011) Mechanistic understanding of Pyrococcus horikoshii Dph2, a [4Fe-4S] enzyme required for diphthamide biosynthesis, *Mol. BioSystems 7*, 74-81.

19. Carette, J. E., Guimaraes, C. P., Varadarajan, M., Park, A. S., Wuethrich, I., Godarova, A., Kotecki, M., Cochran, B. H., Spooner, E., Ploegh, H. L., and Brummelkamp, T. R. (2009) Haploid genetic screens in human cells identify host factors used by pathogens, *Science 326*, 1231-1235.

20. Du, J., Jiang, H., and Lin, H. (2009) Investigating the ADP-ribosyltransferase activity of sirtuins with NAD analogues and 32P-NAD, *Biochemistry 48*, 2878-2890.

21. Huang, B. O., Johansson, M. J. O., and Bystrom, A. S. (2005) An early step in wobble uridine tRNA modification requires the Elongator complex, *RNA 11*, 424-436.

22. Zhang, Y., Liu, S., Lajoie, G., and Merrill, A. R. (2008) The role of the diphthamide-containing loop within eukaryotic elongation factor 2 in ADP-ribosylation by Pseudomonas aeruginosa exotoxin A, *Biochem J 413*, 163-174.

23. Finnigan, G. C., Ryan, M., and Stevens, T. H. (2011) A genome-wide enhancer screen implicates sphingolipid composition in vacuolar ATPase function in Saccharomyces cerevisiae, *Genetics*

187, 771-783.

24. Shi, Y., Stefan, C. J., Rue, S. M., Teis, D., and Emr, S. D. (2011) Two novel WD40 domain-containing proteins, Ere1 and Ere2, function in the retromer-mediated endosomal recycling pathway, *Mol Biol Cell 22*, 4093-4107.

CHAPTER 3

A CHEMOGENOMIC APPROACH IDENTIFIED YEAST YLR143W AS DIPHTHAMIDE SYNTHETASE

Abstract

Many genes are of unknown functions in any sequenced genome. A combination of chemical and genetic perturbations has been used to investigate gene functions. Here we present a case that such "chemogenomics" information can be effectively utilized to identify missing genes in a defined biological pathway. In particular, we identified the previously unknown enzyme, diphthamide synthetase, for the last step of diphthamide biosynthesis. We found yeast protein YLR143W is the diphthamide synthetase catalyzing the last amidation step using ammonium and ATP. Diphthamide synthetase is evolutionarily conserved in eukaryotes. The previously uncharacterized human gene ATPBD4 is the ortholog of yeast YLR143W and fully rescues the deletion of YLR143W in yeast.

Introduction

Diphthamide is a post-translationally modified histidine residue found on archaeal and eukaryotic translation elongation factor 2 (eEF-2)(*1-3*). Diphtheria toxin (DT) and Pseudomonas exotoxin A (ETA) recognize and ADP-ribosylate diphthamide, inhibiting eEF-2 and stopping ribosomal protein synthesis(*4*). Although diphthamide has been known for more than three decades, its biosynthesis and biological functions are still not completely understood. In eukaryotes, the diphthamide biosynthesis pathway consists of three steps (Figure 3.1)(*5-9*). The first step is the transfer of 3-amino-3-carboxypropyl (ACP) group from S-adenosyl methionine (SAM) to the histidine residue of eEF-2. Four proteins, DPH1-4, are required for this step in eukaryotes. The second step is a trimethylation reaction to form diphthine, catalyzed by a single methyltransferase DPH5. Both the first and the second steps have been reconstituted *in vitro* using purified proteins from a thermophilic archaea, *Pyrococcus horikoshii(10-12)*. The third step is the amidation of diphthine to form diphthamide. For a long time, no proteins for the last step were identified. Recently, yeast YBR246W (WDR85 in human) was reported to be another protein required for diphthamide biosynthesis(*13*). We demonstrated yeast cells lacking YBR246W accumulate diphthine, the intermediate that is one step away from the diphthamide modifications. Therefore, YBR246 is required for the last amidation step(*14*). However, we thought it is a scaffold or adaptor protein instead of the actual enzyme that catalyzes the amidation reaction because it lacks an ATP-dependent catalytic domain. Thus, the enzyme that catalyzes the amidation step remains unknown even three decades after the discovery of diphthamide.

In *Saccharomyces cerevisiae*, a systematic profiling of the growth fitness of ~5000 homozygous gene deletion strains has been performed and the data are publically available at Yeast Fitness Database (http://fitdb.stanford.edu/)(*15, 16*). The growth was scored in response to ~400 small molecules and environmental stresses. The similarity of growth fitness under various conditions between any two different deletion strains has been calculated as the co-fitness. Two genes that have similar biological functions are likely to have a high co-fitness value. In this study, we explored the possibility of using the co-fitness data to discover the missing diphthamide biosynthesis gene. We found that a previously uncharacterized yeast gene YLR143W is the diphthamide synthetase.

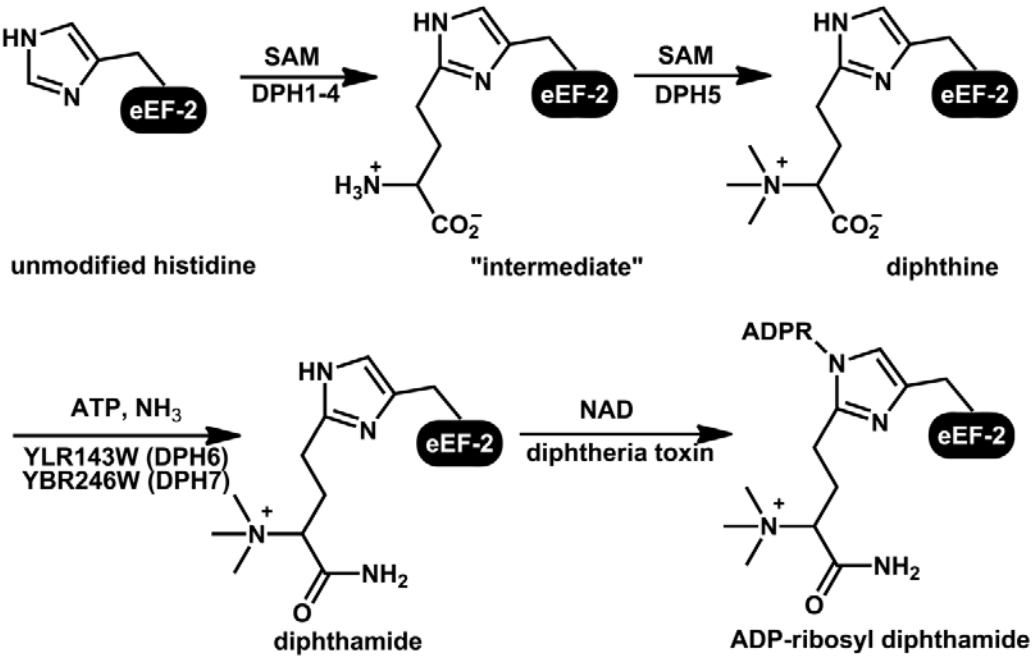

Figure 3.1 Biosynthetic pathway of diphthamide in eukaryotes.

Results

Co-fitness analysis revealed that YLR143W is closely related to diphthamide biosynthesis

We reasoned that the strain lacking the unknown diphthamide synthetase gene should have high co-fitness values with strains lacking other diphthamide biosynthesis genes. To validate this approach, we first analyzed the co-fitness data of *Δybr246w* strain. The *Δybr246w* strain has high co-fitness value with *Δdph2* (0.59624, ranked #3), *Δdph4* (0.55343, ranked #7), and *Δdph5* (0.57422, ranked #5) strains (Figure 3.2A). DPH3 is a fairly small ORF (249bp) and was not included in the original deletion strain collections. Based on the co-fitness data, it was clear that YBR246W has a close relation with diphthamide biosynthetic pathway. However, it was less clear which gene on the co-fitness list of *Δybr246w* could be the diphthamide synthetase.

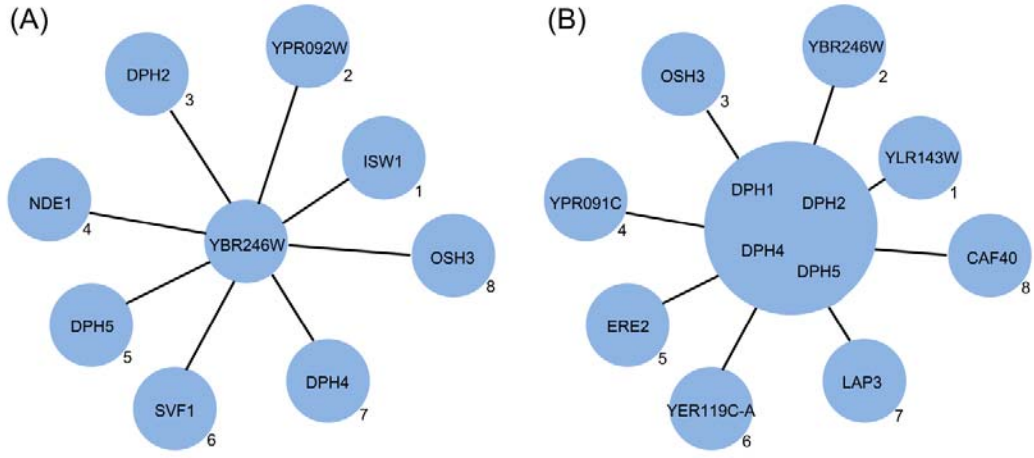

Figure 3.2 The top 8 co-fitness correlations to (A) YBR246W deletion strain (B) DPH1, 2, 4 and 5 deletion strains as a whole group. The rank of each correlation is labeled in the bottom-right corner.

To provide more accurate prediction of the diphthamide synthetase gene, we reasoned that instead of examining the co-fitness to any individual DPH gene deletion strain, looking at the co-fitness

to all the DPH gene deletion strains may lead to more reliable predictions. This was done by adding up the co-fitness values of all homozygous deletion strains to the four DPH gene (dph1, 2, 4 and 5) deletion strains. The grouped correlations were ranked from the highest to the lowest. Excluding the four DPH gene deletions strains, *Δybr246w* had the second highest sum co-fitness value, showing that the sum of the co-fitness values was effective in picking up genes in diphthamide biosynthesis. More interestingly, *Δylr143w* showed a higher co-fitness value than *Δybr246w* to other DPH deletion strains (Figure 3.2B). *Δylr143w* also has high co-fitness values with strains lacking known DPH genes (Figure 3.3). BLAST search indicated that YLR143W is conserved in both eukaryotes and archaea, but not in bacteria, similar to other proteins involved in diphthamide biosynthesis. The human ortholog is ATP-binding domain-containing protein 4 (ATPBD4), which is consistent with the report that the amidation step of diphthamide biosynthesis is ATP-dependent(*17*). The analysis of the co-fitness data thus pointed to the possibility that yeast YLR143W or human ATPBD4 is the diphthamide synthetase.

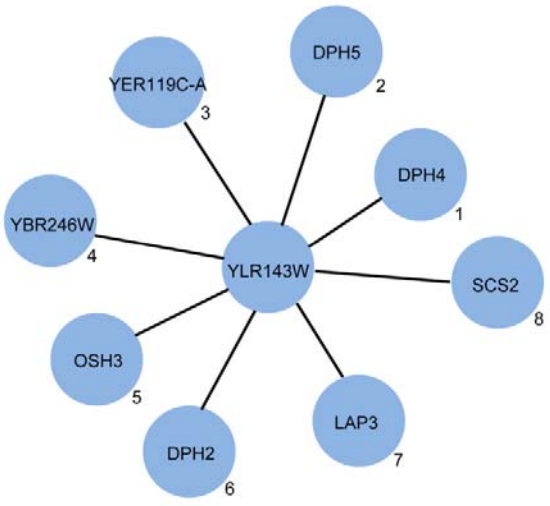

Figure 3.3 The top 8 co-fitness correlations to YLR143W deletion strain. The rank of each correlation is labeled in the bottom-right corner.

YLR143W is required for diphthine amidation in vivo

To test whether YLR143W is indeed required for the last step of diphthamide biosynthesis, we first showed that yeast strain lacking YLR143W did not make diphthamide. We obtained the *Δylr143w* strain and determined the modification on eEF-2 using DT and a fluorescent NAD analog, rhodamine-NAD (Rh-NAD). We have previously demonstrated that diphthamide can be labeled at both high (10 μM) and low (0.1 μM) DT concentrations, diphthine (from *Δybr246w* strain) can only be labeled at high (10 μM) DT concentration, while unmodified or ACP-modified eEF-2 (from *Δdph1*, *Δdph2*, *Δdph3*, *Δdph4*, or *Δdph5* strains) cannot be labeled even at high DT concentration(*14*). When labeling purified eEF-2 from WT and mutant strains with DT and Rh-NAD, eEF-2 from WT can be labeled at both high and low DT concentrations. In contrast, eEF-2 from *Δylr143w* strain can only be labeled at high DT concentration, just like the eEF-2 from *Δybr246w* strain (Figure 3.4). Similar results were obtained when labeling endogenous eEF-2 in the crude cell extract (Figure 3.5). The data suggested that eEF-2 from *Δylr143w* strain contains diphthine instead of diphthamide, similar to the eEF-2 from *Δybr246w*.

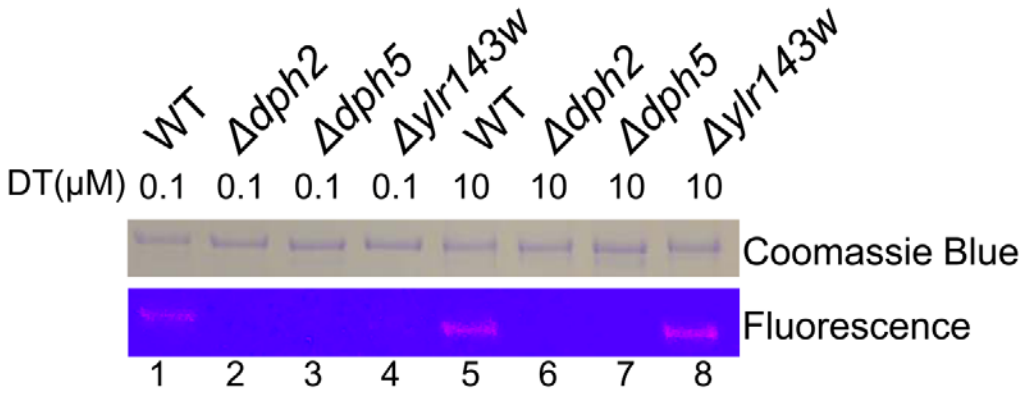

Figure 3.4 Diphthine accumulates in *Δylr143w* yeast strain. Labeling of eEF-2 purified from various strains using Rh-NAD and DT. The strains are specified on top. In lane 1-4, low DT concentration (0.1μM) was used. In lane 5-8, high DT concentration (10μM) was used.

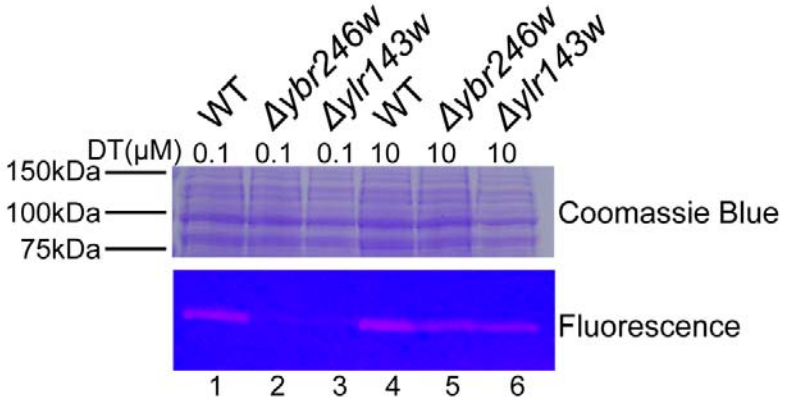

Figure 3.5 The Rh-NAD labeling of total lysates from various parental strains. The parental strains are specified on top. The upper panel displays the eEF2 band on Coomassie Blue stained SDS-PAGE gel. The lower panel displays the fluorescence labeling. In lane 1-3, low DT concentration (0.1μM)was used. In lane 4-6, high DT concentration (10 μM) was used.

We also confirmed the deficiency of diphthamide biosynthesis in *Δylr143w* strain using an *in vivo* assay. A truncated version of DT has been used to select strains with toxin resistance(*18*). This method allowed the identification of DPH1-5(*9*). However, this assay was not suitable for the identification of YBR246W because diphthine can be ADP-ribosylated at high DT

concentration(*14*). In order to detect yeast mutants defective in the last step of diphthamide biosynthesis, a better assay was in need. To develop such an assay, we need a diphtheria toxin (DT) mutant that can differentiate diphthamide from diphthine. The wild-type DT can ADP-ribosylate both diphthamide and diphthine and thus cannot be used in such an assay. In the reported structure of Exotoxin A (ETA), Asp461 forms hydrogen bond with diphthamide amide (Figure 3.6)(*19*). This is presumably the residue discriminating diphthamide and diphthine, as the negatively charged diphthine would be repelled by the negatively charged Asp461. In DT, this residue is replaced by an asparagine residue (Asn45), which may not differentiate diphthamide from diphthine (Figure 3.7)(*20*). Therefore, we thought an Asn45Asp (N45D) mutant of DT may be able to differentiate diphthamide from diphthine. The assay we developed also used a weaker GALS promoter (*21*) to drive the expression of the less active Asn45Asp (N45D) mutant of DT. The cells are transformed with plasmids containing DT mutant or wild type. The results showed that when strong promoter GAL1 was used, DT N55D was still too toxic (Figure 3.8A). But when a weaker promoter GALS was used, *Δybr246w* strain can grow but the WT strain cannot (Figure 3.8B). Therefore we have established a system using GALS-driven DT N45D mutant to discriminate diphthamide and diphthine-containing eEF-2. Similarly, *Δylr143w* strain was able to grow in this assay when DT(N45D) was present, but not when wild type DT was present (Figure 3.9 and 3.10). This *in vivo* assay data is consistent with the *in vitro* fluorescent labeling data and suggested that the eEF-2 from *Δylr143w* strain contained the same modification (diphthine) as the eEF-2 from *Δybr246w* strain.

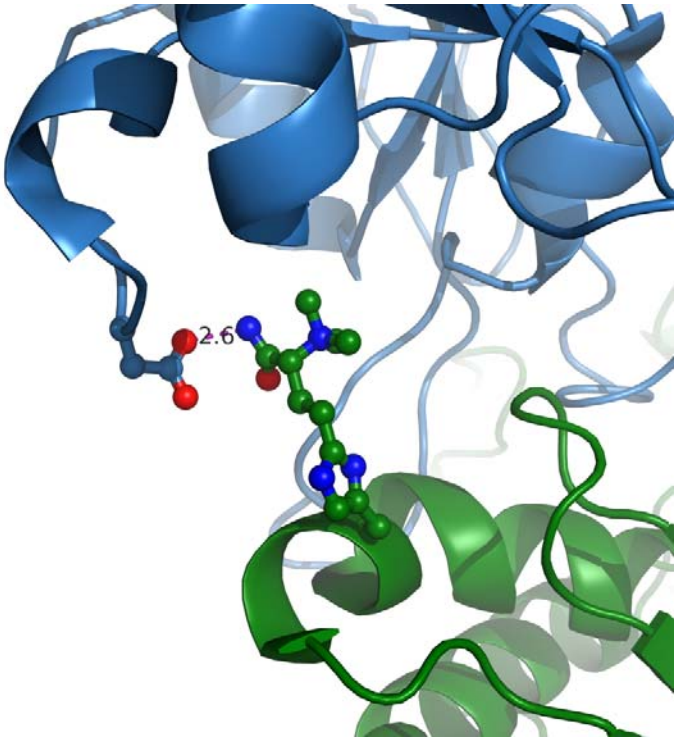

Figure 3.6 The structure of the eEF-2-Exotoxin A complex. The picture was rendered from Protein Data Bank (PDB) accession code 3B78. The diphthamide on eEF-2 (green) is closed to D461 on Exotoxin A (blue). The distance was measured to be 2.6 angstrom.

```
                                  ↓
Exotoxin_A          ----GGVRARSQDLDAIWRGFYIAGDPALAYGYAQDQEPDARGRIRNGALLRVYVPRSSL
Diphtheria_Toxin    KGIQKPKSGTQGNYDDDWKGFYSTDNKYDAAGYSVDNENPLSGKAG--GVVKVTY-----
                           . . : *  *:*** : :   * **: *:*    *:    .:::*

Exotoxin_A          PGFYRTGLTLAAPEAAGEVERLIGHPLPLRLDAITGPEE--------------------E
Diphtheria_Toxin    PGLTKV-LALK-VDNAETIKKELGLSLTEPLMEQVGTEEFIKRFGDGASRVVLSLPFAEG
                    **: :. *:*   : *  ::: :*  *   *   .* **

Exotoxin_A          GGRLETILGWPLAERTVVIPSAIPTDPRNVGGDLDPSSIPDKEQAISALPDYASQPGKPP
Diphtheria_Toxin    SSSVEYINNWEQAKALSV-ELEINFETRGKR-------------GQDAMYEYMAQACAGN
                    .. :* *  *  *:   *    *  : *               . .*: :* :*

Exotoxin_A          REDLK
Diphtheria_Toxin    RVRR-
                    *
```

Figure 3.7 The sequence alignment of Exotoxin A and Diphtheira toxin. The diphthine recongnizing site is arrow-pointed.

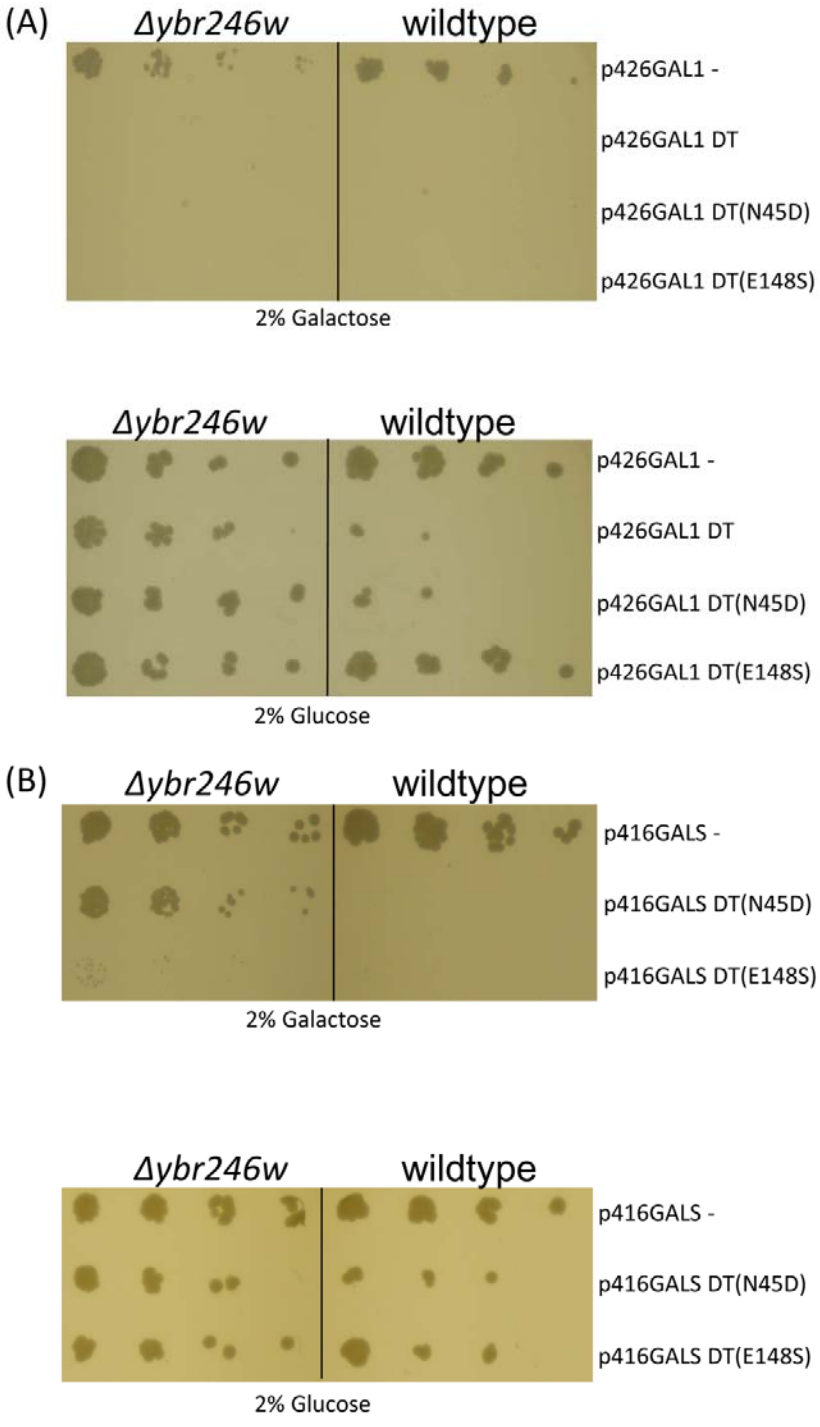

Figure 3.8 Growth assay using DT mutants. (A) DT (N45D) in p426GAL1 gave no phenotypic difference between the wildtype (BY4741) and *Δybr246w*. (B) DT (N45D) in p416GALS gave phenotypic difference between the wildtype and *Δybr246w*. The parental strains used are specified on top. The control and toxin encoding plasmids used are specified on the right. The

cells were grown on 2% galactose (upper panel) or 2% glucose (lower panel).

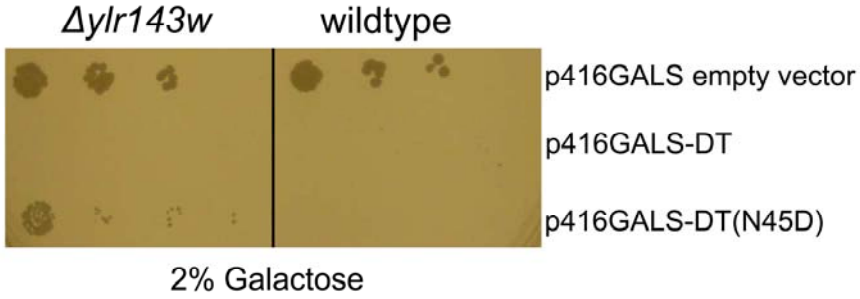

Figure 3.9 Diphtheria toxin sensitivity assay. The strains used are specified on top. Plasmids used in the transformation are listed on the right. The cells were grown on 2% galactose. Each row represents a serial dilution from left to the right.

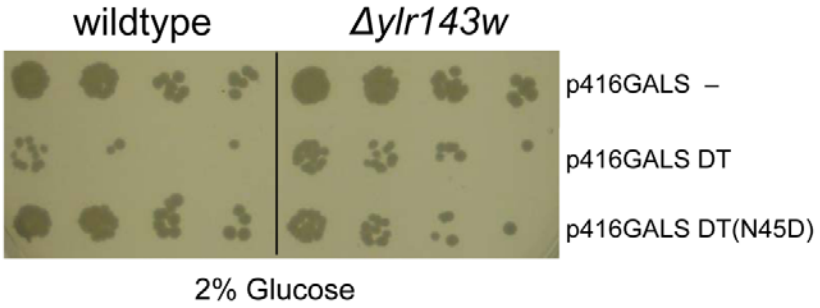

Figure 3.10 Control plates of diphtheria toxin sensitivity assay. The parental strains used are specified on top. The control and toxin encoding plasmids used are specified on the right. The cells were grown on 2% glucose.

We further confirmed that the modification in eEF-2 from *Δylr143w* strain is diphthine using mass spectrometry (MS). The peptide (686-VNILDVTLHADAIH*R-700) containing the modified His residue (indicated by *) from *Δylr143w* strain has an observed *m/z* of 915.51245 (doubly charged, Figure 3.11 The calculated *m/z* is 915.51580), while the corresponding diphthamide containing peptide has an *m/z* of 915.02351 (doubly charged)(*14*). The observed *m/z* value is consistent with the modification in *Δylr143w* being diphthine. Tandem MS further

confirmed the modification and sequence of the peptide (Figure 3.12). Thus, all data suggested that eEF-2 from *Δylr143w* strain contains diphthine.

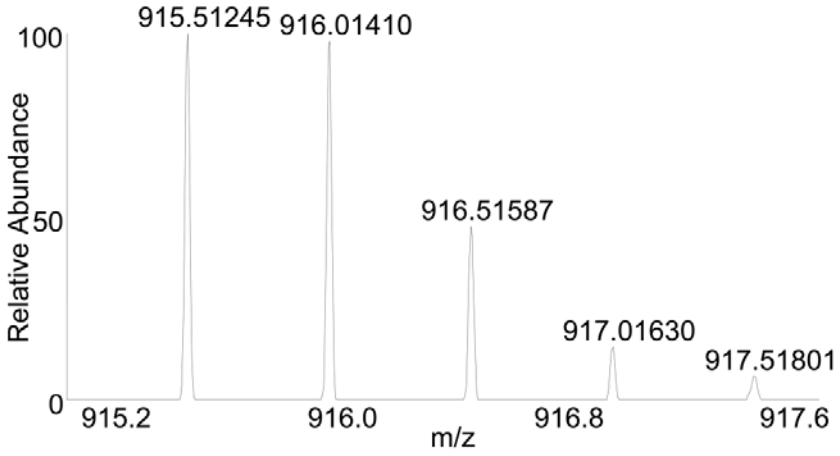

Figure 3.11 The mass spectrum of the eEF-2 peptide containing diphthine from the *Δylr143w* strain.

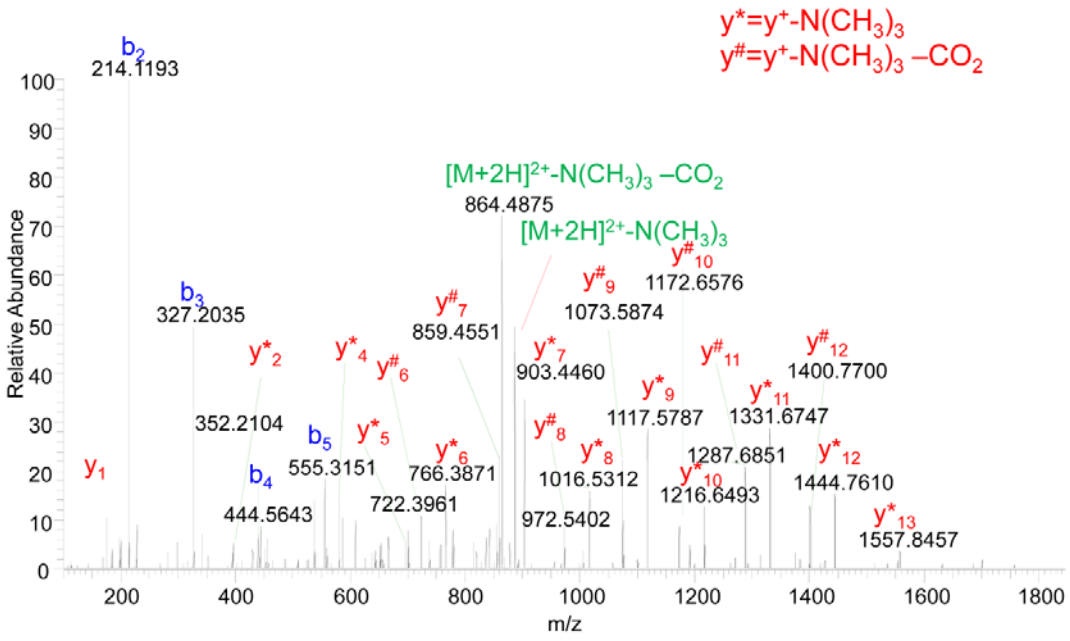

Figure 3.12 The MS/MS spectrum of the diphthine containing peptide derived from the eEF2 purified from *Δylr143w*. Two neutral loss patterns were observed in the spectrum and labeled y* and y#.

YLR143W and human ortholog ATPBD4 restores diphthamide biosynthesis in *Δylr143w* strain

To confirm that the lack of diphthamide in *Δylr143w* is indeed due to the lack of YLR143W, we tested whether diphthamide biosynthesis can be restored in *Δylr143w* strain by introducing YLR143W back to the cells. When *Δylr143w* was transformed with YLR143W, diphthamide can be detected by the labeling with low concentration of DT and Rh-NAD (Figure 3.13). Transformation with an empty vector failed to restore diphthamide biosynthesis. These results demonstrated that the lack of YLR143W was the direct cause for the lack of diphthamide biosynthesis in *Δylr143w* and provided further support that YLR143W is required for the last step of diphthamide biosynthesis. Furthermore, human ATPBD4 can also fully restore diphthamide biosynthesis in *Δylr143w*, demonstrating that human ATPBD4 is also a diphthamide synthetase (Figure 3.14). It is noteworthy that YLR143W is almost three times larger than human ATPBD4. The two proteins are similar at N-termini but YLR143W has a long C-terminal extension. The C-terminal extension appears to be important for the proper function of YLR143W, as the truncated version of YLR143W failed to restore diphthamide biosynthesis (Figure 3.14). This could be due to poor solubility or misfolding of truncated YLR143W. The *P. horikoshii* ATPBD4 (PH1257) also failed to restore the diphthamide biosynthesis in *Δylr143w*. We think this is likely because of its inability to recognize yeast eEF-2.

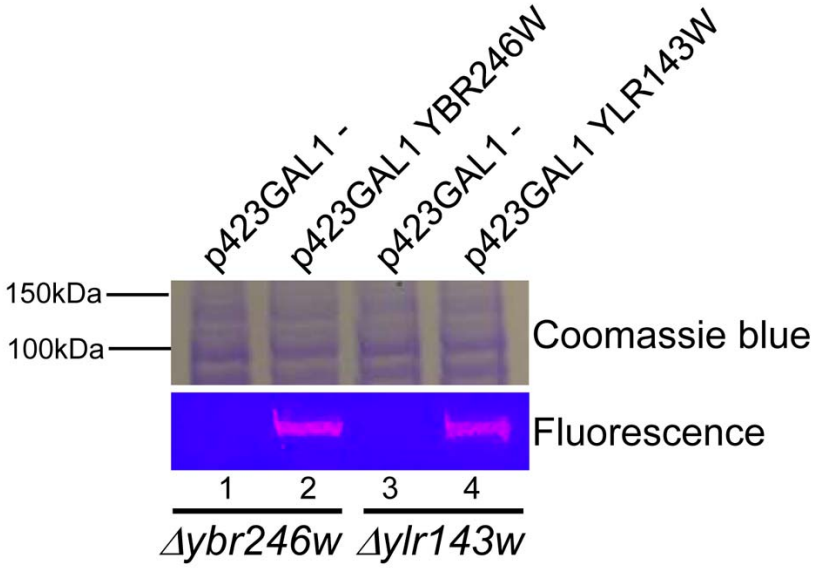

Figure 3.13 YBR246W and YLR143W restore diphthamide biosynthesis in their deletion strains. The deletion strains used are specified on bottom. The plasmids used are specified on top. The upper panel displays the lysates on Coomassie Blue stained SDS-PAGE gel. The lower panel displays the fluorescence labeling. In all lanes, low DT concentration (0.1 μM) was used.

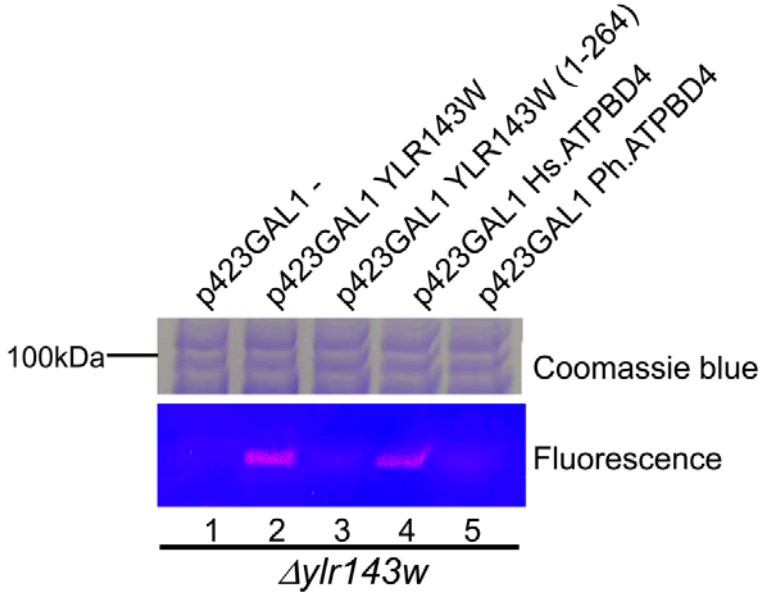

Figure 3.14 Ectopic expression of YLR143W or human ATPBD4 restores diphthamide biosynthesis in the *Δylr143w* strain. The plasmids used are specified on top. HsATPBD4 is the human ATPBD4. PhATPBD4 is the ortholog from *P. Horikoshii* (PH1257). Low DT

concentration (0.1 μM) was used in all lanes.

YLR143W amidates diphthine in vitro

To provide direct evidence that YLR143W is the enzyme catalyzing the last step of diphthamide biosynthesis, we reconstituted the diphthine amidation *in vitro* using purified proteins. The reconstitution reaction was carried out by incubating diphthine-containing eEF-2 with YLR143W, ATP, and either glutamine or ammonium chloride as the nitrogen sources. The formation of diphthamide was detected with Rh-NAD and low concentration of DT. As shown in Figure 3.15, diphthamide was formed when ammonium was used as the nitrogen source in the presence of both ATP and YLR143W. When glutamine was used as the nitrogen source, no diphthamide formation was detected.

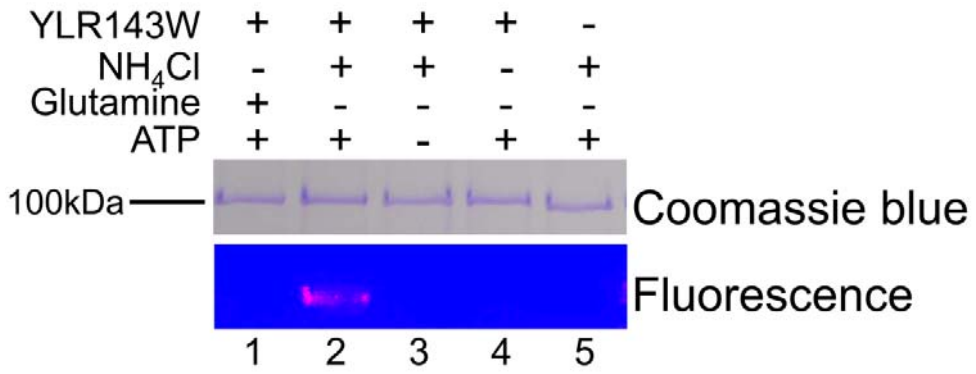

Figure 3.15 YLR143W uses ATP and NH_4^+ for the amidation reaction. YLR143W *in vitro* reconstitution detected using DT (0.1 μM) and Rh-NAD. All reactions contain eEF-2 purified from the *Δylr143w* strain. Purified YLR143W and small molecule substrates used are indicated on top.

Sequence analysis of ATP-binding domain of YLR143W revealed that it belongs to adenine nucleotide alpha hydrolases superfamily. The members of this superfamily include GMP

synthetases, argininosuccinate synthetases, and asparagine synthetases. All of these enzymes catalyze the cleavage of the bond between that α and β phosphates of ATP to form AMP as the end product. The P-loop-like motif SGGXD(S/T) is the signature of the ATP pyrophosphatase domains(*22*). The SGGKDS motif is strictly conserved among all the YLR143W orthologs (Figure 3.16). Therefore we speculated that YLR143W should form AMP in the reaction. To gain further insights into the catalytic mechanism of YLR143W, we determined the reaction product generated from ATP. α-^{32}P ATP was used to allow the detection of reaction product by autoradiography. Standard spots of AMP and ADP were generated by acyl-CoA synthetase and glutamine synthetase, respectively. We detected the formation of AMP only when YLR143W and eEF-2 were both present, showing that AMP is the enzymatic product (Figure 3.17). eEF-2 by itself generated ADP spot, probably due to its GTPase/ATPase activity(*23*). It is less clear why ADP was generated by YLR143W in the absence of eEF-2. Nevertheless, AMP was found to be the major product of the diphthine amidation reaction. Based on the dependence on ATP and NH_4^+ and the formation of AMP, we propose the reaction pathway for YLR143W as shown in Figure 3.18.

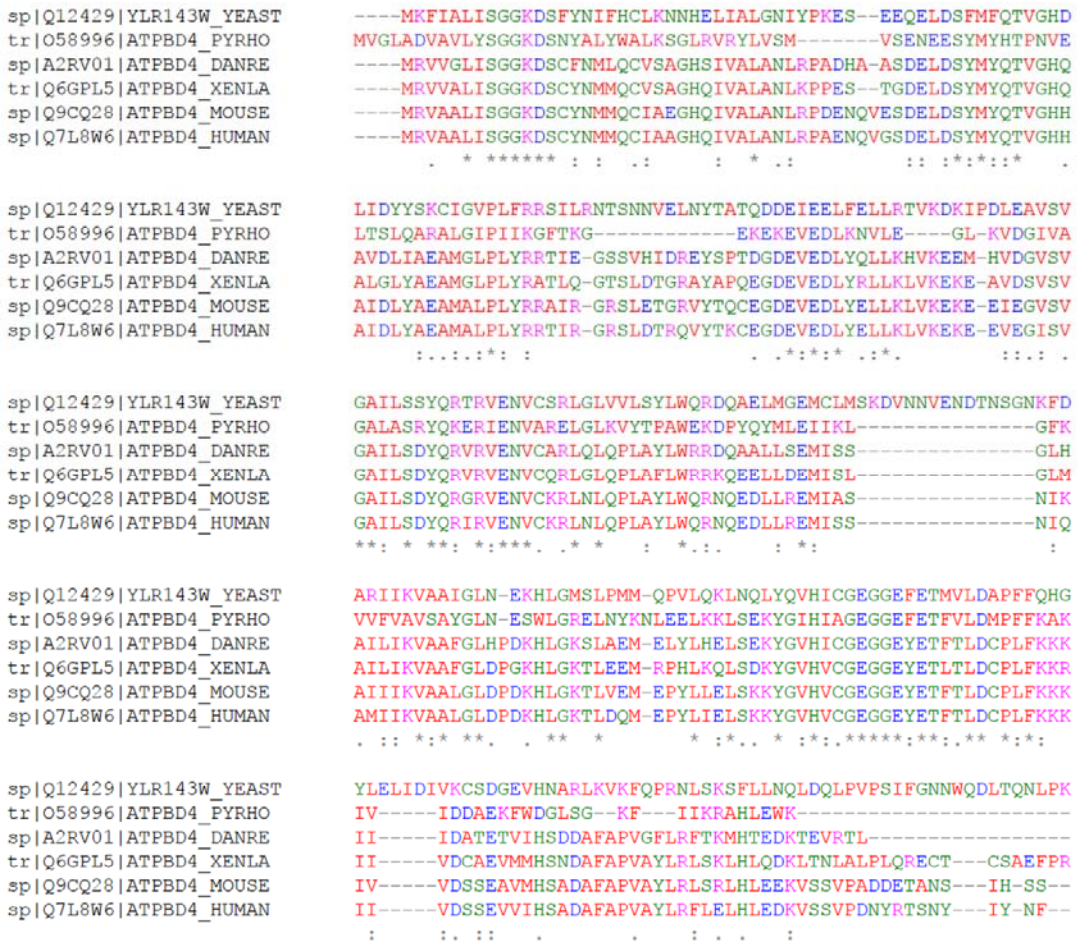

Figure 3.16 Clustal Omega protein sequence alignment result. The compared sequences are from *Saccharomyces cerevisiae*, *Pyrococcus Horikoshii*, *Danio rerio*, *Xenopus laevis*, *Mus musculus* and *Homo sapiens*.

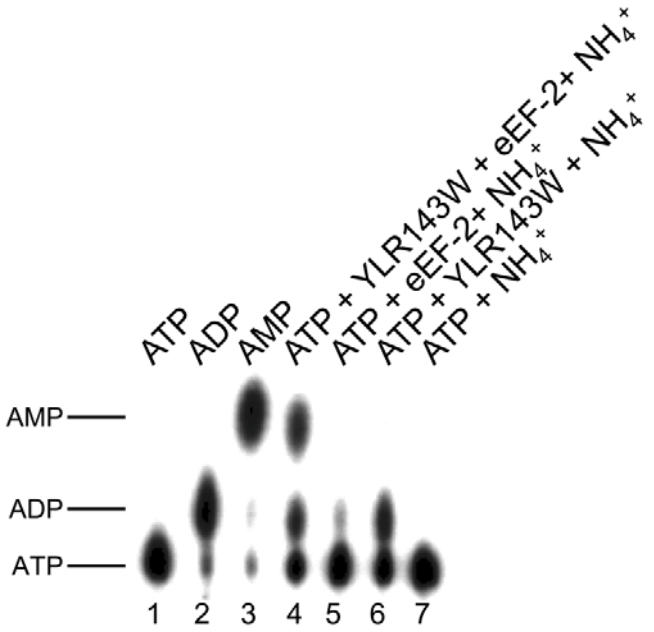

Figure 3.17 AMP is formed in the diphthine amidation reaction. All lanes contained [α-^{32}P]-ATP. ADP and AMP standards in lane 2 and 3 were generated enzymatically from ATP.

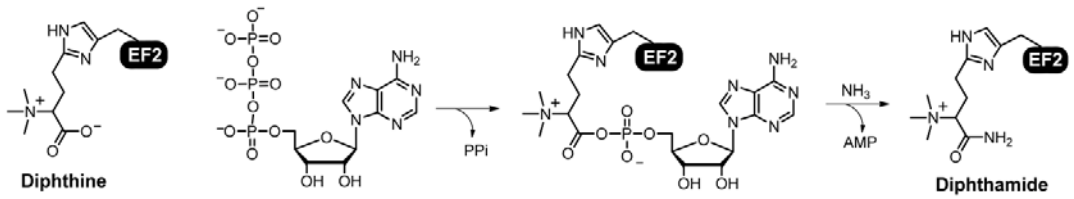

Figure 3.18 Proposed reaction pathway for YLR143W-catalyzed diphthine amidation reaction.

Discussion

We have shown that the co-fitness data are powerful in discovering missing members in a biosynthetic pathway. Moreover, our method takes advantages of existing knowledge of the diphthamide biosynthetic pathway by combining the co-fitness to known DPH genes. This is an easy-to-perform yet reliable method as it eliminates correlations not due to functional relations. For example, for YBR246W, the highest correlation is to ISW1, which is the ATPase subunit of imitation-switch class chromatin remodelers. ISW1 has no function in diphthamide biosynthesis.

The reason ISW1 is showing close relation to YBR246W in the co-fitness data is that ISW1, which is the ORF YBR245C, is the neighboring ORF of YBR246W. Therefore the disruption of ISW1 may affect the integrity of YBR246W or vice versa. Such non-functional relation may give high pair-wise co-fitness and may lower the rank of true functional partner. In fact, YLR143W only ranks #13 in the correlation list of YBR246W. Fortunately, it seems that by combining the correlations to all the known pathway members, the missing member will stand out. We think this is a useful method to guide the discovery of missing pathway members.

The physiological function of diphthamide is still not well understood. Yeast strains that lack diphthamide modification show no phenotype other than insensitivity to diphtheria toxin. However, DPH1, DPH3 and DPH4 do show important roles in mammal development(*24-26*). It has been suggested that diphthamide modification ensures translation fidelity(*27, 28*). Our correlation analysis shows that there may be a connection between diphthamide modification and phosphoinositide metabolism. OSH3, SCS2 and SLM1 are all on top of the correlation list. It would be interesting to find out whether diphthamide modification is connected to phosphoinositide metabolism, which may provide further insights into the function of diphthamide.

The discovery of missing diphthamide synthetase may have practical implications. Exotoxin A, which is an ADP-ribosylating toxin like diphtheria toxin, has been used in cancer chemotherapy. Recent research revealed a survival strategy of cancer cells treated with exotoxin A(*29*). In some patient samples, it was found that the DPH4 promoter region can be methylated and it leads to the

missing of diphthamide and renders the chemotherapy inefficient(*29*). This was an important research report that helps to make better evaluation of the efficacy of the exotoxin A based chemotherapy. This report showed that DPH1, 2, 3 and 5 are not silenced by DNA methylation. However, because the knowledge of diphthamide biosynthesis pathway was not complete, we do not know if the epigenetic silencing happens to other diphthamide biosynthesis genes. The discovery of YBR246W and YLR143W as proteins required for the last step of the biosynthesis will be helpful to complete such studies.

YLR143W is conserved in eukaryotes. The ortholog in humans is ATPBD4. We have shown that ATPBD4 can complement the loss of YLR143W in yeast, demonstrating that ATPBD4 has diphthamide synthetase activity. Interestingly, in a human cancer genetic study, ATPBD4 is found to be significantly focally deleted in all epithelial cancers. ATPBD4 is deleted in 38% of all lung cancer samples BD4(*30*). Another interesting observation was that ATPBD4 was found to be ubiquitylated in two independent studies(*31, 32*). These facts may provide crucial information to further understand the physiological role of ATPBD4 and diphthamide.

In summary, we discovered the diphthamide synthetase, the enzyme that has remained unknown for more than 30 years after the diphthamide structure was determined. This was achieved by grouping the co-fitness values to all known diphthamide biosynthetic genes. Compared with the co-fitness analysis to an individual gene, this method provides more reliable results and is a powerful method to discover missing genes in defined pathways. During the preparation of the manuscript, we found that the alias DPH6 has been reserved on Saccharomyces Genome

Database, but no detail regarding the biochemical function of YLR143W was revealed. We agree with this naming suggestion and propose the alias DPH7 to YBR246W.

Method

Co-fitness analysis.

The homozygous co-fitness data of DPH1, DPH2, DPH4, DPH5, YBR246W and YLR143W deletion strains were acquired from Yeast Fitness Database (http://fitdb.stanford.edu/fitdb.cgi). The co-fitness values were added and sorted using Microsoft Excel. The full calculation spreadsheet is in http://www.pnas.org/content/suppl/2012/11/15/1214346109.DCSupplemental/sd01.xlsx. The top 40 lines of the added cofitness are also listed in the spreadsheet with the gene name and function annotations from the Saccharomyces genome database (www.yeastgenome.org).

***In vitro* ADP-ribosylation using Rh-NAD.**

Rh-NAD was prepared as described previously(*33*). Purified yeast eEF-2 and Rh-NAD (25 μM) were incubated with DT at 30 °C in 25 mM Tris-HCl (pH 8.0), 50 mM NaCl, 30 mM dithiothreitol (DTT) and 2 mM ethylenediaminetetraacetic acid (EDTA). The DT concentration was 100 nM and the reaction time was 15 min if not specified otherwise. The reaction mixture was resolved by SDS-PAGE. The rhodamine fluorescence signal from the protein gel was visualized on a Fisher Scientific Ultraviolet transilluminator.

***In vitro* diphthine amidation**

Purified eEF-2 from YLR143W deletion strain was used for the amidation reaction. The eEF-2 concentration was 0.5μM and the purified YLR143W concentration was 3 nM. The reaction buffer contained 80 mM Tris-HCl (pH 8.0), 15 mM KCl, 5mM $MgCl_2$, 5mM β-mercaptoethanol, 1mM ATP, 10mM NH_4Cl and 0.1mg/ml BSA. Glutamine was used at 10 mM concentration as the potential alternative nitrogen source. The reaction was carried out at 30°C for 30min. The formation of diphthamide was visualized by Rh-NAD labeling as described above.

Expression and purification of yeast eEF-2.

The plasmid p423 MET25-eEF-2 (hosted by strain HL610E) was transformed into *S. cerevisiae* strains with BY4741 background (OpenBiosystems, Huntsville, AL). The list of strains used in this study can be found in Table 3.1. The expression and purification of eEF-2 was the same as previously reported(*14*).

Rh-NAD labeling of the endogenous eEF-2.

The yeast cell lysates were prepared as described previously(*33*). The concentrations of the lysates were determined using absorbance at 280nm. For each labeling reaction, the lysate was diluted to 10μl with the final A_{280} of 0.16. Then the lysate and Rh-NAD (25 μM) were incubated with DT at 30 °C in 25 mM Tris-HCl (pH 8.0), 50 mM NaCl, 30 mM dithiothreitol (DTT) and 2 mM ethylenediaminetetraacetic acid (EDTA). The DT concentration was 100 nM and the reaction time was 15 min if not specified otherwise. The reaction mixture was resolved by SDS-PAGE. Rhodamine fluorescence signal from protein gel was visualized on a Fisher Scientific Ultraviolet transilluminator.

Cloning and mutagenesis of diphtheria toxin

The truncated diphtheria toxin was cloned from pLMY101into p426 GAL1 plasmid or others using primers XS182 (5'-agtcagGGATCCatgagcagaaaactgtttgcg-3') and XS183 (5'-agtcagCTCGAGTTAcggagaatacgcgggacga-3'). The DT mutants were made by overlap extension PCR(*34*). The primers for N45D were XS180 (5'-gccaaaatctggtacacaaggaGATtatgacgatgattggaaaggg-3') and XS181 (5'-tccttgtgtaccagattttggc-3'). The primers for E148S were XS178 (5'- ctgaggggagttctagcgttTCAtatattaataactgggaacaggc-3') and XS179 (5'- aacgctagaactcccctcag-3').

Yeast growth assay.

Cells were transformed using the Frozen-EZ Yeast Transformation II Kit (Zymo Research, Irvine, CA). Transformed yeast cells were grown on synthetic complete medium with uracil dropout. The carbon sources were used as indicated. Colony formation was recorded 3 days after plating.

Cloning, expression and purification of YLR143W

Yeast YLR143W was amplified from yeast genomic DNA, which was extracted from BY4741 using Pierce Yeast DNA Extraction Kit. The primers used were XS198 (5'-agtcagGGATCCATGAAGTTTATAGCATTAATATCAGG-3') and XS199 (5'-agtcagGTCGACttaGGAACGAATATGCAACCCAAA -3'). The amplified gene was inserted into pET28a vector for protein production. The pET28a YLR143W plasmid was transformed into BL21(DE3) pRARE2 strain. Cells were grown in 2 liters LB medium at 37°C and 200 rpm. It took 4-5 hours for the OD600 to reach 0.5 after inoculation with the overnight culture. Then the

culturing temperature was changed to 15°C, and the protein expression was induced by 0.1 mM isopropyl-D-thiogalac-toside (IPTG). Cells were harvested after incubation at 15°C for 20 h. The protein was purified using a HisTrap column (GE Healthcare). Protein concentrations were determined by Bradford assay.

^{32}P-ATP autoradiography detecting reaction products

To detect the product formed from ATP, the diphthine amidation reaction was performed in 10 μl solutions with 2 μCi [α-^{32}P]-ATP (PerkinElmer, 800Ci/mmol, 2mCi/ml), 80 mM Tris-HCl (pH 8.0), 15 mM KCl, 5 mM $MgCl_2$, 5 mM β-mercaptoethanol and 10 mM NH_4Cl. The eEF-2 concentration was 0.5 μM and the purified YLR143W concentration was 0.75 μM. The reactions were incubated at room temperature for 5 min. The ADP standard spot was generated with L-glutamine synthetase (Sigma, G3144). The reaction contained 2 μCi [α-^{32}P]-ATP (PerkinElmer, 800Ci/mmol, 2mCi/ml), 80 mM Tris-HCl (pH 8.0), 15 mM KCl, 5 mM $MgCl_2$, 5 mM β-mercaptoethanol, 10 mM NH_4Cl and 1 mM L-glutamate. The AMP spot was generated with acyl-coenzyme A synthetase (Sigma, A3352). The reaction contained 2μCi [α-^{32}P]-ATP (PerkinElmer, 800Ci/mmol, 2mCi/ml), 80 mM Tris-HCl (pH 8.0), 15 mM KCl, 5 mM $MgCl_2$, 5 mM β-mercaptoethanol, 1 mM coenzyme A and 1 mM sodium myristate. The reactions were incubated at room temperature for 45 min. A total of 0.5 μl of each reaction were spotted onto cellulose PEI-F TLC plates (Baker-flex) and developed with 2 M lithium chloride in water. After development, the plates were air-dried and exposed to a PhosphorImaging screen (GE Healthcare, Piscataway, NJ). The signal was detected using a STORM860 phosphorimager (GE Healthcare,

Piscataway, NJ).

In-gel trypsin digestion of eEF-2 and nano LC/MS/MS analysis

The in-gel digestion of eEF-2, the nano LC/MSMS analysis and associated data analysis was same as previously used.

Table 3.1 Yeast strains used in Chapter 3

Strain	Genotype	Source
HL813Y	*MAT***a** *his3Δ1 leu2Δ0 met15Δ0 ura3Δ0*	Open Biosystems (YSC1048)
HL814Y	*MAT***a** *his3Δ1 leu2Δ0 met15Δ0 ura3Δ0 ybr246wΔ*	Open Biosystems (YSC1021-552106)
HL904Y	*MAT***α** *his3Δ1 leu2Δ0 lys2Δ0 ura3Δ0*	Open Biosystems (YSC1049)
HL940Y	*MAT***α** *his3Δ1 leu2Δ0 lys2Δ0 ura3Δ0 ybr246wΔ*	Open Biosystems (YSC1021-547231)
HL1025Y	*MAT***a** *his3Δ1 leu2Δ0 met15Δ0 ura3Δ0 ylr143wΔ*	Open Biosystems (YSC1021-552695)
HL823Y	HL813Y [p423MET25 EFT1-Histag]	[1]
HL824Y	HL814Y [p423MET25 EFT1-Histag]	[1]
HL825Y	HL815Y [p423MET25 EFT1-Histag]	[1]
HL968Y	HL941Y [p423MET25 EFT1-Histag]	[1]
HL1026Y	HL1025Y [p423MET25 EFT1-Histag]	This study
HL958Y	HL904Y [p426GAL1 DT-F2]	This study
HL959Y	HL904Y [p426GAL1 DT-F2 (N45D)]	This study
HL960Y	HL904Y [p426GAL1 DT-F2 (E148S)]	This study
HL962Y	HL904Y [p426GAL1 -]	This study
HL963Y	HL940Y [p426GAL1 DT-F2]	This study
HL964Y	HL940Y [p426GAL1 DT-F2 (N45D)]	This study
HL965Y	HL940Y [p426GAL1 DT-F2 (E148S)]	This study
HL967Y	HL940Y [p426GAL1 -]	This study
HL1008Y	HL813Y [p416GALS DT-F2]	This study
HL1013Y	HL814Y [p416GALS DT-F2]	This study

Table 3.1 Yeast strains used in Chapter 3 (continued)

Strain	Genotype	Source
HL1058Y	HL813Y [p416GALS DT-F2 (N45D)]	This study
HL1059Y	HL813Y [p416GALS DT-F2 (E148S)]	This study
HL1060Y	HL813Y [p416GALS -]	This study
HL1061Y	HL814Y [p416GALS DT-F2 (N45D)]	This study
HL1062Y	HL814Y [p416GALS DT-F2 (E148S)]	This study
HL1063Y	HL814Y [p416GALS -]	This study
HL1064Y	HL1025Y [p416GALS DT-F2]	This study
HL1065Y	HL1025Y [p416GALS DT-F2 (N45D)]	This study
HL1066Y	HL1025Y [p416GALS DT-F2 (E148S)]	This study
HL1067Y	HL1025Y [p416GALS -]	This study
HL1039Y	HL814Y [p423GAL1 YBR246W]	This study
HL1040Y	HL1025Y [p423GAL1 YLR143W]	This study
HL1068Y	HL814Y [p423GAL1 -]	This study
HL1069Y	HL1025Y [p423GAL1 -]	This study
HL1054Y	HL1025Y [p423GAL1 YLR143W-Histag]	This study
HL1055Y	HL1025Y [p423GAL1 YLR143W(1-264)-Histag]	This study
HL1056Y	HL1025Y [p423GAL1 ph ATPBD4-Histag]	This study
HL1057Y	HL1025Y [p423GAL1 Human ATPBD4-Histag]	This study

REFERENCES

1. Robinson, E. A., Henriksen, O., and Maxwell, E. S. (1974) Elongation factor 2. amino acid sequence at the site of adenosine diphosphate ribosylation, *J. Biol. Chem. 249*, 5088-5093.

2. Van Ness, B. G., Howard, J. B., and Bodley, J. W. (1980) ADP-ribosylation of elongation factor 2 by diphtheria toxin. NMR spectra and proposed structures of ribosyl-diphthamide and its hydrolysis products, *J. Biol. Chem. 255*, 10710-10716.

3. Van Ness, B. G., Howard, J. B., and Bodley, J. W. (1980) ADP-ribosylation of elongation factor 2 by diphtheria toxin. Isolation and properties of the novel ribosyl-amino acid and its hydrolysis products, *J. Biol. Chem. 255*, 10717-10720.

4. Collier, R. J. (2001) Understanding the mode of action of diphtheria toxin: a perspective on progress during the 20th century, *Toxicon 39*, 1793-1803.

5. Moehring, J. M., and Moehring, T. J. (1988) The post-translational trimethylation of diphthamide studied in vitro, *J. Biol. Chem. 263*, 3840-3844.

6. Moehring, J. M., Moehring, T. J., and Danley, D. E. (1980) Posttranslational modification of elongation factor 2 in diphtheriatoxin-resistant mutants of CHO-K1 cells, *Proc. Natl. Acad. Sci. USA 77*, 1010-1014.

7. Moehring, J. M., and Moehring, T. J. (1984) Diphthamide: in vitro biosynthesis, *Methods Enzymol 106*, 388-395.

8. Liu, S., and Leppla, S. H. (2003) Retroviral insertional mutagenesis identifies a small

protein required for synthesis of diphthamide, the target of bacterial ADP-ribosylating toxins, *Mol. Cell 12*, 603.

9. Liu, S., Milne, G. T., Kuremsky, J. G., Fink, G. R., and Leppla, S. H. (2004) Identification of the proteins required for biosynthesis of diphthamide, the target of bacterial ADP-ribosylating toxins on translation elongation factor 2, *Mol. Cell. Biol. 24*, 9487-9497.

10. Zhang, Y., Zhu, X., Torelli, A. T., Lee, M., Dzikovski, B., Koralewski, R. M., Wang, E., Freed, J., Krebs, C., Ealick, S. E., and Lin, H. (2010) Diphthamide biosynthesis requires an organic radical generated by an iron-sulphur enzyme, *Nature 465*, 891-896.

11. Zhu, X., Dzikovski, B., Su, X., Torelli, A. T., Zhang, Y., Ealick, S. E., Freed, J. H., and Lin, H. (2011) Mechanistic understanding of Pyrococcus horikoshii Dph2, a [4Fe-4S] enzyme required for diphthamide biosynthesis, *Mol. BioSystems 7*, 74-81.

12. Zhu, X., Kim, J., Su, X., and Lin, H. (2010) Reconstitution of diphthine synthase activity in vitro, *Biochemistry 49*, 9649-9657.

13. Carette, J. E., Guimaraes, C. P., Varadarajan, M., Park, A. S., Wuethrich, I., Godarova, A., Kotecki, M., Cochran, B. H., Spooner, E., Ploegh, H. L., and Brummelkamp, T. R. (2009) Haploid genetic screens in human cells identify host factors used by pathogens, *Science 326*, 1231-1235.

14. Su, X., Chen, W., Lee, W., Jiang, H., Zhang, S., and Lin, H. (2012) YBR246W is required for the third step of diphthamide biosynthesis, *J Am Chem Soc 134*, 773-776.

15. Hillenmeyer, M. E., Fung, E., Wildenhain, J., Pierce, S. E., Hoon, S., Lee, W., Proctor,

M., St Onge, R. P., Tyers, M., Koller, D., Altman, R. B., Davis, R. W., Nislow, C., and Giaever, G. (2008) The chemical genomic portrait of yeast: uncovering a phenotype for all genes, *Science 320*, 362-365.

16. Hillenmeyer, M. E., Ericson, E., Davis, R. W., Nislow, C., Koller, D., and Giaever, G. (2010) Systematic analysis of genome-wide fitness data in yeast reveals novel gene function and drug action, *Genome Biol 11*, R30.

17. Moehring, T. J., Danley, D. E., and Moehring, J. M. (1984) In vitro biosynthesis of diphthamide, studied with mutant Chinese hamster ovary cells resistant to diphtheria toxin, *Mol Cell Biol 4*, 642-650.

18. Mattheakis, L., Shen, W., and Collier, R. (1992) DPH5, a methyltransferase gene required for diphthamide biosynthesis in *Saccharomyces cerevisiae*., *Mol. Cell. Biol. 12*, 4026-4037.

19. Jorgensen, R., Wang, Y., Visschedyk, D., and Merrill, A. R. (2008) The nature and character of the transition state for the ADP-ribosyltransferase reaction, *EMBO Rep 9*, 802-809.

20. Carroll, S. F., and Collier, R. J. (1988) Amino acid sequence homology between the enzymic domains of diphtheria toxin and Pseudomonas aeruginosa exotoxin A, *Mol Microbiol 2*, 293-296.

21. Mumberg, D., Muller, R., and Funk, M. (1994) Regulatable promoters of Saccharomyces cerevisiae: comparison of transcriptional activity and their use for heterologous expression, *Nucleic Acids Res 22*, 5767-5768.

22. Bork, P., and Koonin, E. V. (1994) A P-loop-like motif in a widespread ATP pyrophosphatase domain: implications for the evolution of sequence motifs and enzyme activity, *Proteins 20*, 347-355.

23. Demeshkina, N., Hirokawa, G., Kaji, A., and Kaji, H. (2007) Novel activity of eukaryotic translocase, eEF2: dissociation of the 80S ribosome into subunits with ATP but not with GTP, *Nucleic Acids Res 35*, 4597-4607.

24. Webb, T. R., Cross, S. H., McKie, L., Edgar, R., Vizor, L., Harrison, J., Peters, J., and Jackson, I. J. (2008) Diphthamide modification of eEF2 requires a J-domain protein and is essential for normal development, *J Cell Sci 121*, 3140-3145.

25. Chen, C.-M., and Behringer, R. R. (2004) Ovca1 regulates cell proliferation, embryonic development, and tumorigenesis, *Genes Dev. 18*, 320-332.

26. Liu, S., Wiggins, J. F., Sreenath, T., Kulkarni, A. B., Ward, J. M., and Leppla, S. H. (2006) Dph3, a small protein required for diphthamide biosynthesis, is essential in mouse development, *Mol Cell Biol 26*, 3835-3841.

27. Ortiz, P. A., Ulloque, R., Kihara, G. K., Zheng, H., and Kinzy, T. G. (2006) Translation elongation factor 2 anticodon mimicry domain mutants affect fidelity and diphtheria toxin resistance, *J. Biol. Chem. 281*, 32639-32648.

28. Liu, S., Bachran, C., Gupta, P., Miller-Randolph, S., Wang, H., Crown, D., Zhang, Y., Wein, A. N., Singh, R., Fattah, R., and Leppla, S. H. (2012) Diphthamide modification on eukaryotic elongation factor 2 is needed to assure fidelity of mRNA translation and mouse development, *Proc Natl Acad Sci U S A*.

29. Wei, H., Xiang, L., Wayne, A. S., Chertov, O., FitzGerald, D. J., Bera, T. K., and Pastan, I. (2012) Immunotoxin resistance via reversible methylation of the DPH4 promoter is a unique survival strategy, *Proc Natl Acad Sci U S A 109*, 6898-6903.

30. Beroukhim, R., Mermel, C. H., Porter, D., Wei, G., Raychaudhuri, S., Donovan, J., Barretina, J., Boehm, J. S., Dobson, J., Urashima, M., Mc Henry, K. T., Pinchback, R. M., Ligon, A. H., Cho, Y. J., Haery, L., Greulich, H., Reich, M., Winckler, W., Lawrence, M. S., Weir, B. A., Tanaka, K. E., Chiang, D. Y., Bass, A. J., Loo, A., Hoffman, C., Prensner, J., Liefeld, T., Gao, Q., Yecies, D., Signoretti, S., Maher, E., Kaye, F. J., Sasaki, H., Tepper, J. E., Fletcher, J. A., Tabernero, J., Baselga, J., Tsao, M. S., Demichelis, F., Rubin, M. A., Janne, P. A., Daly, M. J., Nucera, C., Levine, R. L., Ebert, B. L., Gabriel, S., Rustgi, A. K., Antonescu, C. R., Ladanyi, M., Letai, A., Garraway, L. A., Loda, M., Beer, D. G., True, L. D., Okamoto, A., Pomeroy, S. L., Singer, S., Golub, T. R., Lander, E. S., Getz, G., Sellers, W. R., and Meyerson, M. (2010) The landscape of somatic copy-number alteration across human cancers, *Nature 463*, 899-905.

31. Kim, W., Bennett, E. J., Huttlin, E. L., Guo, A., Li, J., Possemato, A., Sowa, M. E., Rad, R., Rush, J., Comb, M. J., Harper, J. W., and Gygi, S. P. (2011) Systematic and quantitative assessment of the ubiquitin-modified proteome, *Mol Cell 44*, 325-340.

32. Wagner, S. A., Beli, P., Weinert, B. T., Nielsen, M. L., Cox, J., Mann, M., and Choudhary, C. (2011) A proteome-wide, quantitative survey of in vivo ubiquitylation sites reveals widespread regulatory roles, *Mol Cell Proteomics 10*, M111 013284.

33. Du, J., Jiang, H., and Lin, H. (2009) Investigating the ADP-ribosyltransferase activity of

sirtuins with NAD analogues and 32P-NAD, *Biochemistry 48*, 2878-2890.

34. Ho, S. N., Hunt, H. D., Horton, R. M., Pullen, J. K., and Pease, L. R. (1989) Site-directed mutagenesis by overlap extension using the polymerase chain reaction, *Gene 77*, 51-59.

CHAPTER 4

A REVISIT OF THE FUNCTION OF DPH7

Abstract

Diphthamide biosynthesis is a stepwise process. The current model is that three steps are involved. We found that although both *Δdph6* and *Δdph7* accumulate diphthine intermediate, the two diphthine-containing intermediates are not the same. The eEF-2 from *Δdph6* can be amidated by purified Dph6 but eEF-2 from *Δdph7* cannot be amidated by purified Dph6, although both types of eEF2 contain the diphthine modification. Therefore, there must be one more step in diphthamide biosynthesis that requires Dph7. Dph7 catalyzes or helps catalyze the reaction between Dph5 and Dph6. The exact nature of the distinction of the two diphthine-containing eEF-2 is not clear. A few possibilities are discussed in the end of this chapter.

Introduction

Diphthamide is a post-translationally modified histidine residue found in eukaryotic and archael elongation factor 2(*1-4*). It is the target of diphtheria toxin produced by *Corynebacterium diphtheriae(5)*. Diphtheria toxin (DT) catalyzes the ADP-ribosylation reaction on the diphthamide residue of EF-2 using NAD as the ADP-ribose donor. The ADP-ribosylated EF-2 is inactive and unable to catalyze the translocation step in the ribosomal protein synthesis. diphthamide is one of the most complicated post-translational modifications. It has been thought to involve three enzymatic steps in and seven proteins(*6-17*). Dph1-4 are required for the first step, which is the transfer of the 3-amino-3-carboxypropyl (ACP) group. The second step requires Dph5 which is a methyltransferase that produces diphthine intermediate. Dph6 is the diphthamide synthetase that uses ATP and amidates diphthine to give diphthamide.

In the previous chapters, we have been able to show that Dph6 is the diphthamide synthetase, which catalyzes the amidation step converting diphthine into diphthamide. However, little was explored on the biochemical function of Dph7. Dph7 was identified in a genetic screening in which human WDR85, which is homolog of yeast Dph7, and was shown to be required for the first step of diphthamide biosynthesis*(15)*. Later discovered that Dph7 is required for diphthine amidation, since *Δdph7* accumulates diphthine intermediate*(16)*. This result suggests that Dph7's function is a prerequisite for the diphthine amidation reaction. So there are several possibilities about Dph7's function. One of them is that Dph7 may enhance the activity of Dph6. Dph7 has a WD40-repeat domain, which is thought to mediate protein-protein interaction(*18*). Dph7 may

work as a Dph6 binding partner and promotes its activity. Interestingly, our work shows that this model is not correct. Our data suggest that Dph7 is responsible for one more enzymatic step in the diphthamide biosynthesis pathway. The exact nature of this conversion is not yet clear. Nevertheless, our results suggest that diphthamide biosynthesis has a minimum of four steps.

Results

eEF-2 from *Δdph7* cannot be amidated by Dph6.

In the previous chapter, we have shown that the diphthine-containing eEF-2 can be *in vitro* amidated by purified Dph6. However, in that experiment, the eEF-2 was purified from *Δdph6*. To determine if there is any difference on the eEF-2 purified from *Δdph6* and *Δdph7*, we used both of them in the amidation reaction as substrates. DT was used at low concentration to detect the formation of diphthamide after the amidation step. To our surprise, only the eEF-2 from *Δdph6* was amidated but not the one from *Δdph7* (Figure 4.1). This result means that there are actually two diphthine-containing eEF-2 species, one can be amidated but not the other one. This was a surprising result. The eEF-2 proteins from *Δdph6* and *Δdph7* are quite similar. They have been shown to have diphthine by mass spectrometry and they have similar activity working as DT's substrate. The ability to serve as Dph6's substrate is their only distinction that we know.

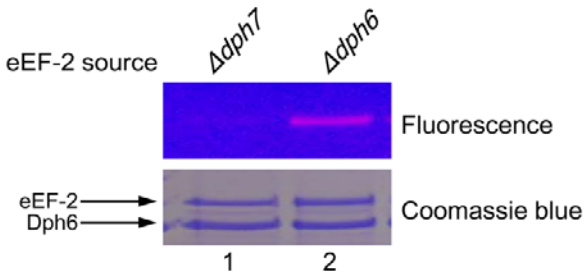

Figure 4.1 eEF-2 from *Δdph7* cannot be amidated by purified Dph6. Purified eEF-2 was used in this experiment and the sources from which the eEF-2 was purified is specified on top. The lower panel displays the eEF-2 band on Coomassie Blue stained SDS-PAGE gel. The upper panel displays the fluorescence labeling. Low DT concentration (0.1μM) was used in this assay.

***In vitro* preparation of diphthine-containing eEF-2 using Dph5.**

In the originally proposed diphthamide biosynthetic pathway, there is no room for two diphthine-containing eEF-2 species. Therefore, this pathway needs to be revised. To determine at which step the Dph7 activity is required, we took a step back to carry out the methylation step *in vitro* to make diphthine-containing eEF-2.

Dph5 was cloned into pET28a vector and was expressed and purified from *E. coli* (Figure 4.2). The activity of Dph5 was first tested using eEF-2 purified from *Δdph5*, which is ACP-modified (Figure 4.3). When provided with Dph5 and SAM, diphthine was generated as it can be labeled with high concentration of DT. There was no sign of the elimination of the trimethylamino group even when high concentration of SAM was used. The elimination reaction has been reported to happen on PhEF-2(*19*). As we have discussed in the previous chapter, it seems that diphthine on yeast eEF-2 is much more stable. The stability of diphthine on yeast eEF-2 allows the detection of diphthine as an intermediate in the diphthamide biosynthesis. Here we show again that excess of SAM does not lead to the elimination of the trimethylamino group.

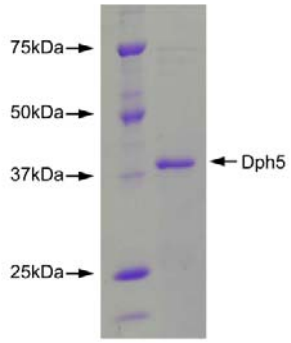

Figure 4.2 Dph5 purified from *E. coli*. The calculated mass of His_6-tagged Dph5 is 38kDa.

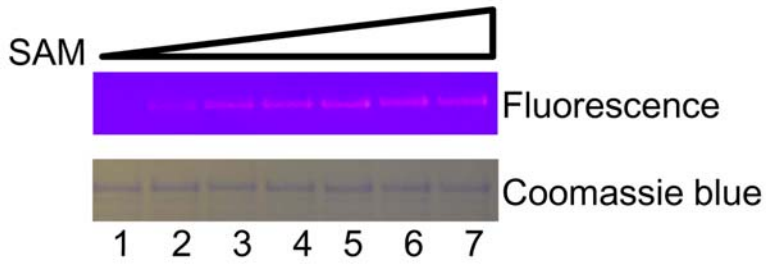

Figure 4.3 Activity assay of purified Dph5. eEF-2 purified from *Δdph5* was used as the substrate. The lower panel displays the eEF-2 band on Coomassie Blue stained SDS-PAGE gel. The upper panel displays the fluorescence labeling. High DT concentration (10μM) was used in this assay to detect the formation of diphthine. The SAM concentration in the reaction was 30 μM (lane 1), 50 μM (lane 2), 100 μM (lane 3), 300 μM (lane 4), 500 μM (lane 5), 1 mM (lane 6), 3 mM (lane 7).

Diphthine generated from Dph5 cannot be amidated

The next step was to determine as which point the Dph7 activity is needed. It is obvious that Dph6 is the last step of diphthamide biosynthesis as the product from this step is diphthamide. Dph7, however, may work before or after Dph5. We are not clear about the nature of Dph7 catalyzed reaction. We may assume that Dph7 catalyzes a phosphorylation reaction on eEF-2. And Dph6's recognition of eEF-2 as a substrate depends on this phosphorylation, while the non-phosphorylated eEF-2 is acceptable by Dph1-5, then without Dph7 the eEF-2 could only be

diphthine-modified. The Dph7 catalyzed phosphorylation may work upstream of Dph5 or even Dph1-4. Therefore, to determine the reaction order, we tried to use Dph5 generated diphthine as a substrate for Dph6 amidation. In this experiment, the eEF-2 was isolated from *Δdph5*, so that Dph7 was in that strain. If there is a reaction that can be done by Dph7 upstream of Dph5, it must have been done. In that case, the *in vitro* trimethylated eEF-2 should be able to work as Dph6's substrate. Our experimental results showed the opposite. When provided Dph5, Dph6 and other small molecule co-substrates, the eEF-2 can only be labeled by high concentration of DT. It means that only diphthine was formed. Diphthamide was not generated from this reaction, suggesting that Dph7's activity is required after the action of Dph5.

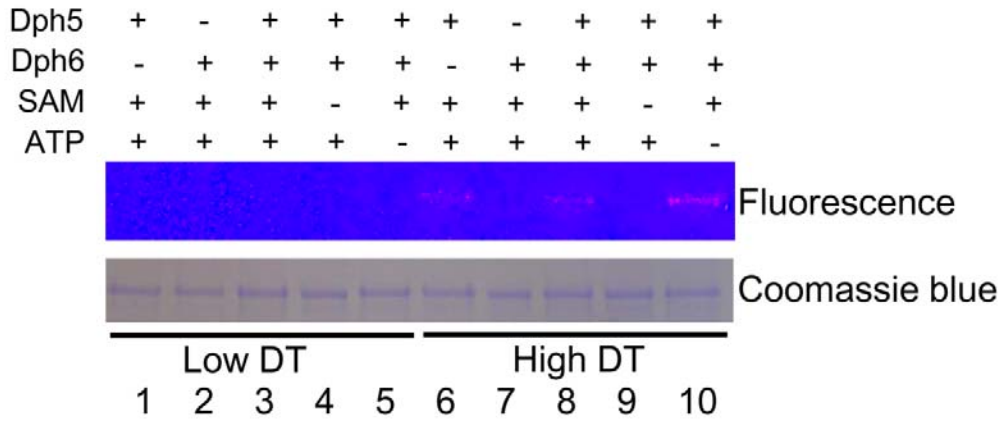

Figure 4.4 Amidation assay of diphthine produced by Dph5. eEF-2 purified from *Δdph5* was used as the substrate. The lower panel displays the eEF-2 band on Coomassie Blue stained SDS-PAGE gel. The upper panel displays the fluorescence labeling. Low (0.1μM) and high DT concentration (10μM) was used in this assay to detect the formation of diphthamide and diphthine. The components used in the reactions are indicated on top of the gel.

Discussion

Previous study only identified three steps in diphthamide biosynthetic pathway. We have identified yeast ORF YLR143W (Dph6) as the diphthamide synthetase. In this chapter, we showed that there are actually two diphthine-containing eEF-2 species, one can be converted to diphthamide by Dph6 and the other one cannot. Dph7 works after Dph5, converting the non-amidatable diphthine to the amidatable form. We are trying to reconstitute this step *in vitro* using purified Dph7, which may provide more information regarding this reaction and the biochemical function of Dph7.

There are two possibilities about the two diphthine-containing eEF-2 species. One is that their distinction is post-translational modification on a different site on eEF-2. The other possibility is the two diphthine are structurally not the same. There has been no sufficient evidence to support either one. We do notice one report though, in which the configuration of diphthamide is thought to be different from previously reported(*20*). The ACP group of diphthamide comes from methionine(*6*). Therefore the chiral carbon on the side chain of diphthamide has been assigned S configuration. However, crystallography study suggested the R configuration on the third carbon of diphthamide side chain (Figure 4.5)(*21*). If this result is true, there may be an isomerization step to convert S-diphthine to R-diphthine, then the R-diphthine is amidated to give R-diphthamide. In this case, the function of Dph7 is to catalyze this isomerization reaction (Figure 4.6).

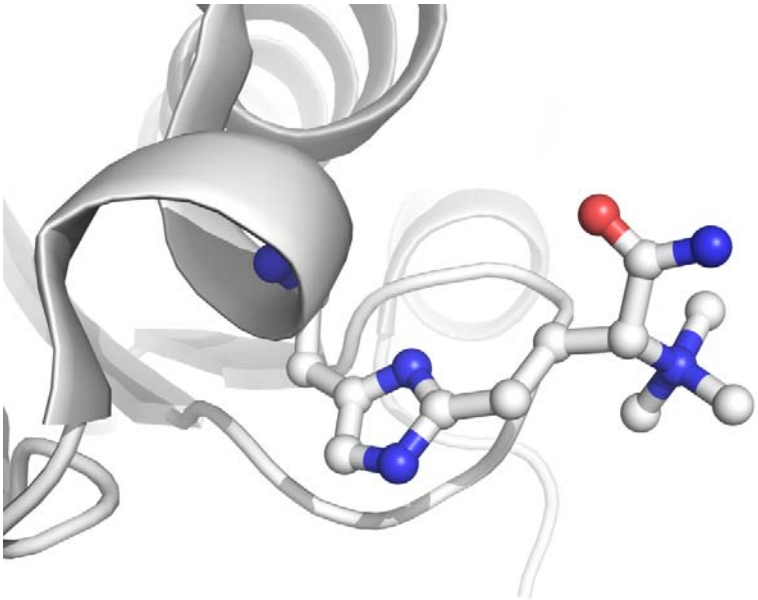

Figure 4.5 Structure of diphthamide on eEF-2 (Rendered from PDB 3B82) may be in R-configuration.

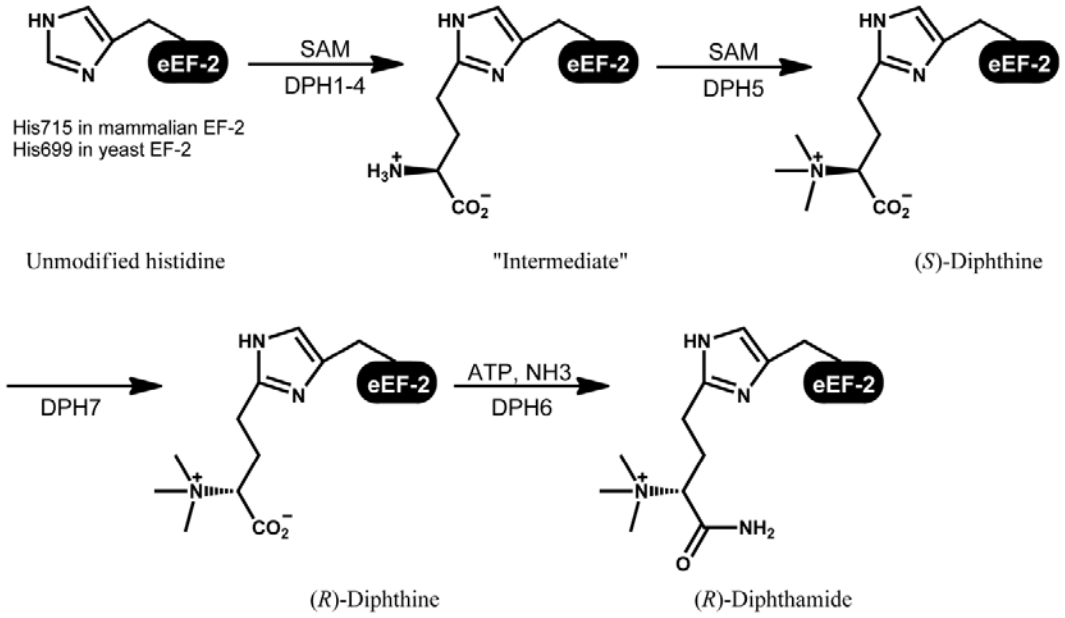

Figure 4.6 Proposed diphthamide biosynthetic pathway.

Other possibilities exist regarding the identity of two diphthine-containing eEF-2 species. For example, the addition or removal of a post-translational modification on a different residue of eEF-2. Again, the reconstitution of the Dph7-catalyzed step may help to elucidate this. If a phosphorylation or acetylation is involved, ATP or acetyl-CoA would be required as the co-substrate. And MS study on eEF-2 would reveal the site of this modification.

Methods

***In vitro* ADP-ribosylation using Rh-NAD.**

Rh-NAD was prepared as described previously(*22*). Purified yeast eEF-2 and Rh-NAD (25 μM) were incubated with DT at 30 °C in 25 mM Tris-HCl (pH 8.0), 50 mM NaCl, 30 mM dithiothreitol (DTT) and 2 mM ethylenediaminetetraacetic acid (EDTA). The DT concentration was 10 μM and the reaction time was 60 min if not specified otherwise. The reaction mixture was resolved by SDS-PAGE. The rhodamine fluorescence signal from the protein gel was visualized on a Fisher Scientific Ultraviolet transilluminator.

Cloning, expression and purification of Dph5

Yeast Dph5 was amplified from yeast genomic DNA, which was extracted from BY4741 using Pierce Yeast DNA Extraction Kit. The primers used were XS221 (5'-agtcagGGATCCatgctttatttgatcggacttg-3') and XS220 (5'-agtcagGTCGACttactcgtcgctgtcgtcttct-3'). The amplified gene was inserted into pET28a

vector for protein production. The pET28a Dph5 plasmid was transformed into BL21 pRARE2 strain. Cells were grown in 2 liters LB medium at 37°C and 200 rpm. It took 4-5 hours for the OD600 to reach 0.5 after inoculation with the overnight culture. Then the culturing temperature was changed to 15°C, and the protein expression was induced by 0.1 mM isopropyl-D-thiogalac-toside (IPTG). Cells were harvested after incubation at 15°C for 20 h. The purification using HisTrap column (GE Healthcare) is the same as eEF-2 protein. Protein concentrations were determined by Bradford assay.

***In vitro* eEF-2 methylation**

Purified eEF-2 from DPH5 deletion strain was used for the methylation reaction. The eEF-2 concentration was 0.5μM and the purified Dph5 was used at a concentration of 1μM. The reaction buffer contained 80 mM Tris-HCl (pH 8.0), 15 mM KCl, 5mM $MgCl_2$, 5mM β-mercaptoethanol and various concentration of SAM as indicated. The reaction was carried out at 30°C for 40min. The formation of diphthine was visualized by Rh-NAD labeling as described above.

***In vitro* eEF-2 methylation and amidation**

Purified eEF-2 from DPH5 deletion strain was used for the methylation and amidation reaction. The eEF-2 concentration was 0.5μM and the purified Dph5 and Dph6 were used at a concentration of 1μM. The reaction buffer contained 80 mM Tris-HCl (pH 8.0), 15 mM KCl, 5mM $MgCl_2$, 5mM β-mercaptoethanol, 1mM ATP, 10mM NH_4Cl and 300μM SAM. The

reaction was carried out at 30°C for 40min. The formation of diphthine/diphthamide was visualized by Rh-NAD labeling as described above.

REFERENCES

1. Van Ness, B. G., Howard, J. B., and Bodley, J. W. (1980) ADP-ribosylation of elongation factor 2 by diphtheria toxin. NMR spectra and proposed structures of ribosyl-diphthamide and its hydrolysis products, *J. Biol. Chem. 255*, 10710-10716.

2. Robinson, E. A., Henriksen, O., and Maxwell, E. S. (1974) Elongation factor 2. amino acid sequence at the site of adenosine diphosphate ribosylation, *J. Biol. Chem. 249*, 5088-5093.

3. Van Ness, B. G., Howard, J. B., and Bodley, J. W. (1980) ADP-ribosylation of elongation factor 2 by diphtheria toxin. Isolation and properties of the novel ribosyl-amino acid and its hydrolysis products, *J. Biol. Chem. 255*, 10717-10720.

4. Pappenheimer, A. M., Jr, Dunlop, P. C., Adolph, K. W., and Bodley, J. W. (1983) Occurrence of diphthamide in archaebacteria, *J. Bacteriol. 153*, 1342-1347.

5. Collier, R. J. (2001) Understanding the mode of action of diphtheria toxin: a perspective on progress during the 20th century, *Toxicon 39*, 1793-1803.

6. Dunlop, P. C., and Bodley, J. W. (1983) Biosynthetic labeling of diphthamide in *Saccharomyces cerevisiae*, *J. Biol. Chem. 258*, 4754-4758.

7. Chen, J. Y., Bodley, J. W., and Livingston, D. M. (1985) Diphtheria toxin-resistant mutants of *Saccharomyces cerevisiae.*, *Mol. Cell. Biol. 5*, 3357-3360.

8. Moehring, J. M., and Moehring, T. J. (1984) Diphthamide: in vitro biosynthesis, *Methods Enzymol 106*, 388-395.

9. Moehring, J. M., and Moehring, T. J. (1988) The post-translational trimethylation of

diphthamide studied in vitro, *J. Biol. Chem. 263*, 3840-3844.

10. Mattheakis, L., Shen, W., and Collier, R. (1992) DPH5, a methyltransferase gene required for diphthamide biosynthesis in *Saccharomyces cerevisiae*., *Mol. Cell. Biol. 12*, 4026-4037.

11. Mattheakis, L. C., Sor, F., and Collier, R. J. (1993) Diphthamide synthesis in *Saccharomyces cerevisiae*: structure of the DPH2 gene, *Gene 132*, 149.

12. Liu, S., and Leppla, S. H. (2003) Retroviral insertional mutagenesis identifies a small protein required for synthesis of diphthamide, the target of bacterial ADP-ribosylating toxins, *Mol. Cell 12*, 603.

13. Liu, S., Milne, G. T., Kuremsky, J. G., Fink, G. R., and Leppla, S. H. (2004) Identification of the proteins required for biosynthesis of diphthamide, the target of bacterial ADP-ribosylating toxins on translation elongation factor 2, *Mol. Cell. Biol. 24*, 9487-9497.

14. Schultz, D. C., Balasara, B. R., Testa, J. R., and Godwin, A. K. (1998) Cloning and localization of a human diphthamide biosynthesis-like protein-2 gene,DPH2L2, *Genomics 52*, 186.

15. Carette, J. E., Guimaraes, C. P., Varadarajan, M., Park, A. S., Wuethrich, I., Godarova, A., Kotecki, M., Cochran, B. H., Spooner, E., Ploegh, H. L., and Brummelkamp, T. R. (2009) Haploid genetic screens in human cells identify host factors used by pathogens, *Science 326*, 1231-1235.

16. Su, X., Chen, W., Lee, W., Jiang, H., Zhang, S., and Lin, H. (2012) YBR246W is

required for the third step of diphthamide biosynthesis, *J Am Chem Soc 134*, 773-776.

17. Su, X., Lin, Z., Chen, W., Jiang, H., Zhang, S., and Lin, H. (2012) Chemogenomic approach identified yeast YLR143W as diphthamide synthetase, *Proc Natl Acad Sci U S A 109*, 19983-19987.

18. Shi, Y., Stefan, C. J., Rue, S. M., Teis, D., and Emr, S. D. (2011) Two novel WD40 domain-containing proteins, Ere1 and Ere2, function in the retromer-mediated endosomal recycling pathway, *Mol Biol Cell 22*, 4093-4107.

19. Zhu, X., Kim, J., Su, X., and Lin, H. (2010) Reconstitution of diphthine synthase activity in vitro, *Biochemistry 49*, 9649-9657.

20. Jorgensen, R., Merrill, A. R., and Andersen, G. R. (2006) The life and death of translation elongation factor 2, *Biochem Soc Trans 34*, 1-6.

21. Jorgensen, R., Wang, Y., Visschedyk, D., and Merrill, A. R. (2008) The nature and character of the transition state for the ADP-ribosyltransferase reaction, *EMBO Rep 9*, 802-809.

22. Du, J., Jiang, H., and Lin, H. (2009) Investigating the ADP-ribosyltransferase activity of sirtuins with NAD analogues and 32P-NAD, *Biochemistry 48*, 2878-2890.

CHAPTER 5

FUNCTIONAL STUDIES OF YEAST DPH1-4

Abstract

The most complicated step of diphthamide biosynthesis in eukaryotes is the first step, which is the transfer of 3-amino-3-carboxylpropyl (ACP) group onto the histidine residue on eEF-2. Several approaches were taken to study the reaction mechanism in greater details. By using an *in vivo* activity assay of Dph1 and Dph2, we have discovered 3 and 2 catalytically important cysteine residues in Dph1 and Dph2 respectively. Dph1 and Dph2 were co-expressed and purified. The resulting Dph1/Dph2 complex is active in SAM cleavage and generates 5'-deoxy-5'-methylthioadenosine. Dph3 has also been expressed and purified. It can bind iron and is redox-active. Unfortunately, the reconstitution of the first step reaction using purified proteins has not been successful, making it challenging to study the function of each protein in detail.

Introduction

In the previous chapters, we have been focusing on later steps of diphthamide biosynthetic pathway. In eukaryotes, the most complicated step is probably the first step, which is the transfer of the 3-amino-3-carboxylpropyl (ACP) group onto the histidine residue on eEF-2(*1-8*). The mechanism of this step has been extensively studied in an archaeal system(*9, 10*). The archaeal species *Pyrococcus horikoshii*, unlike yeast, has only one identifiable gene to catalyze this step. The *Pyrococcus horikoshii* Dph2 (PhDph2) is homologous to eukaryotic Dph1 and Dph2. Crystal structure of PhDhp2 revealed a homodimeric organization and the coordination of one [4Fe-4S] cluster per monomer. PhDph2 lacks the CX3CX2C motif which is the signature of canonical radical SAM enzymes, but contains three conserved cysteine residues Cys59, Cys163 and Cys287 that are spatially close and coordinate the [4Fe-4S] cluster. PhDph2 cleaves the $C_{\gamma,Met}$–S bond of SAM to form 5'-deoxy-5'-methylthioadenosine (MTA) and ACP radical. The ACP radical performs hydrogen abstraction on the C-2 position of the imidazole ring to give the final product(*9, 10*).

The yeast system, however, is more complicated than the archaeal system. There are four gene Dph1-4 that are found to be required for the first step(*7, 8*). Dph1 and Dph2 are homologous to PhDph2(*11*). There is no homolog of yeast Dph3 and Dph4 in *Pyrococcus horikoshii*. Based on the fact that PhDph2 alone is sufficient to catalyze the first step of diphthamide biosynthesis in *Pyrococcus horikoshii*, we assume that Dph1/Dph2 are the catalytic components for the first step diphthamide biosynthesis in eukaryotes. Dph3 and Dph4 may have some auxiliary roles. In this

chapter, we present data showing that Dph1 and Dph2 complex is active in generating MTA and ACP radical, but failed to perform the transfer of the ACP group to eEF-2. Dph3 was found to bind iron. *E. coli.* riboflavin reductase NorW is able to reduce the iron on Dph3 in a NADH-dependent manner.

Results

Sequence alignment of Dph1/Dph2 and PhDph2

Yeast Dph1 and Dph2 are homologous to PhDph2. The sequence alignment shows that eukaryotic Dph1 has higher similarity to PhDph2 (Figure 5.1). There are three cysteine residues in PhDph2 that coordinate the [4Fe-4S] cluster, Cys59, Cys163 and Cys287. The corresponding residues are Cys133, Cys239 and Cys368 in yeast Dph1. In yeast Dph2, Cys106 and Cys362 correspond to PhDph2 Cys59 and Cys287. There is no cysteine in yeast Dph2 that corresponds to PhDph2 Cys163. The conserved cysteine pattern implies an asymmetry of the Dph1/Dph2 heterodimer. In PhDph2, it has been shown that only one of the two monomers is required for the full activity. Yeast Dph1 has the three conserved cysteine residues to bind the [4Fe-4S] cluster and has higher homology to PhDph2, therefore Dph1 maybe more important for the catalysis. Yeast Dph2 has only two out of the three conserved cysteine residues. So the function of Dph2 may not be the same as the Dph1.

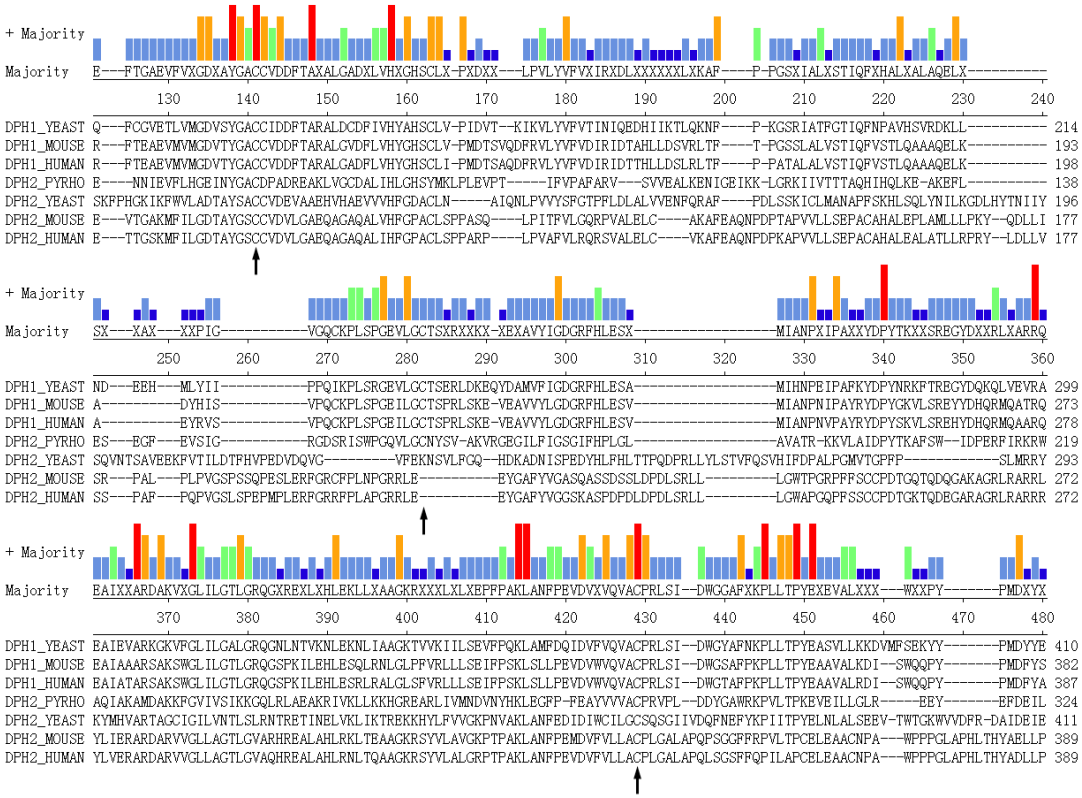

Figure 5.1 Sequence alignment of Dph1 and Dph2 proteins from different species. Black arrows indicate the cysteine residues that bound the [4Fe-4S] cluster in PhDph2.

Mutagenesis of Dph1/Dph2 revealed important cysteine residues

To study the function of Dph1 and Dph2 in greater detail, we first did the mutagenesis study on Dph1/Dph2. Various Dph1 or Dph2 mutants were constructed and introduced back into the Dph1 or Dph2 deletion background, respectively. If the mutated residue is not important, the mutant would retain activity and restore the generation of diphthamide in the Dph1 or Dph2 deletion background. The restoration of diphthamide biosynthesis can be detected by diphtheria toxin (DT) sensitivity assay. Dph2 mutants were studied first (Figure 5.2). The results showed that Dph2 C362A mutants failed to restore DT sensitivity while C106A mutant succeeded. Therefore Cys362 is required for Dph2's activity but not the Cys106. We noticed the presence of Cys107 in

Dph2 so we tried C107A mutant too. The results showed that Cys107 is indeed required for Dph2's activity (Figure 5.2). The Dph1 mutants have also been studied. Cys133, Cys239 and Cys362 in yeast Dph1 are shown to be required for activity. These are the residues conserved from PhDph2 to yeast Dph1.

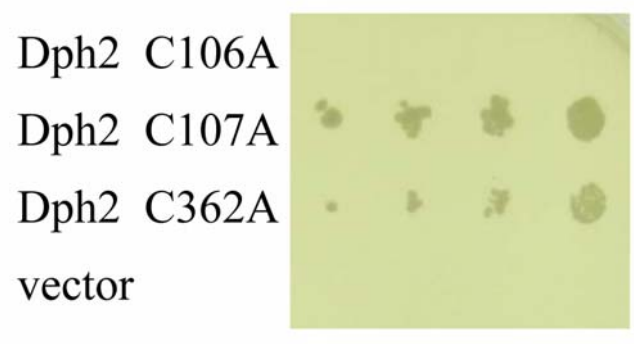

Figure 5.2 Mutagenesis study of Dph2. Mutants or wt DPH2 gene were inserted into p413Gal1 plasmid which was used to transform the *Δdph2* strain together with the pLMY101 plasmid encoding DT. The DT sensitivity was evaluated on 2% Galactose medium. The plasmids used are specified on the left side. The spots from right to left represent a serial dilution.

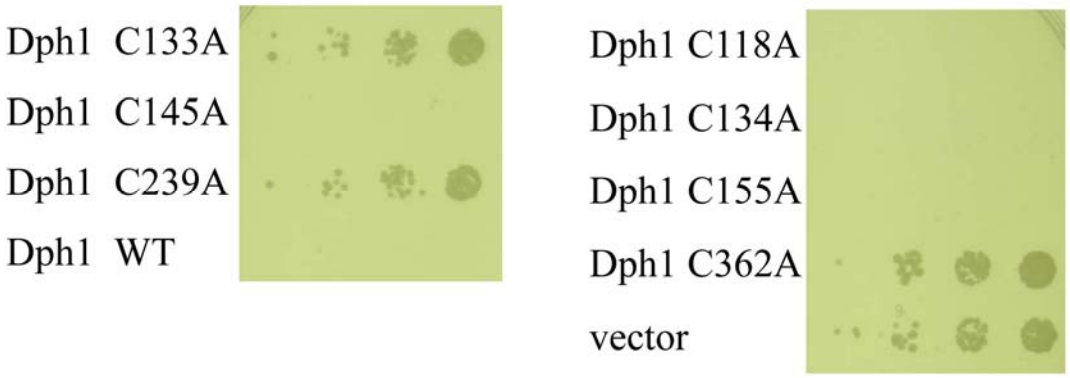

Figure 5.3 Mutagenesis study of Dph1. Mutants or wt DPH1 gene were inserted into p413Gal1 plasmid which was used to transform the *Δdph1* strain together with the pLMY101 plasmid encoding DT. The DT sensitivity was evaluated on 2% Galactose medium. The plasmids used are specified on the left side. The spots from right to left represent a serial dilution.

The mutagenesis study not only revealed the important cysteine residues but also show that both

Dph1 and Dph2 are required for the first step reaction of diphthamide biosynthesis. In PhDph2, a chimeric heterodimer which has one active monomer and one inactive monomer is functional. But in yeast Dph1/Dph2, a point mutation in Dph2 makes the heterodimer inactive. Therefore, the catalytic mechanism of yeast Dph1/Dph2 must be different from PhDph2.

Expression and purification of yeast Dph1/Dph2

To study how Dph1/Dph2 catalyze the first step biosynthesis, we aimed to express the proteins and reconstitute the activity *in vitro*. We first cloned Dph1/Dph2 genes into pDEST expression vectors with either N-His_6 or N-His_6-MBP (maltose-binding protein) fusions using Gateway technologies (Invitrogen). From the *E. coli* expression, Dph1 and Dph2 cannot give soluble protein when singly expressed. Considering that the complex they form may have better stability and solubility, we also tried to co-express these two proteins using the Duet vectors (Novagen). The Dph1/Dph2 can be expressed from the pET duet vector but the level was not high. Later, we moved the multiple cloning site region of pET duet-1 containing Dph1 and Dph2 to pET28b and the expression was greatly improved (Figure 5.4). In order to make Dph1/Dph2 active, Fe and cysteine were supplemented to the growth medium when culturing cells. Dph1/Dph2 was also purified under anaerobic condition.

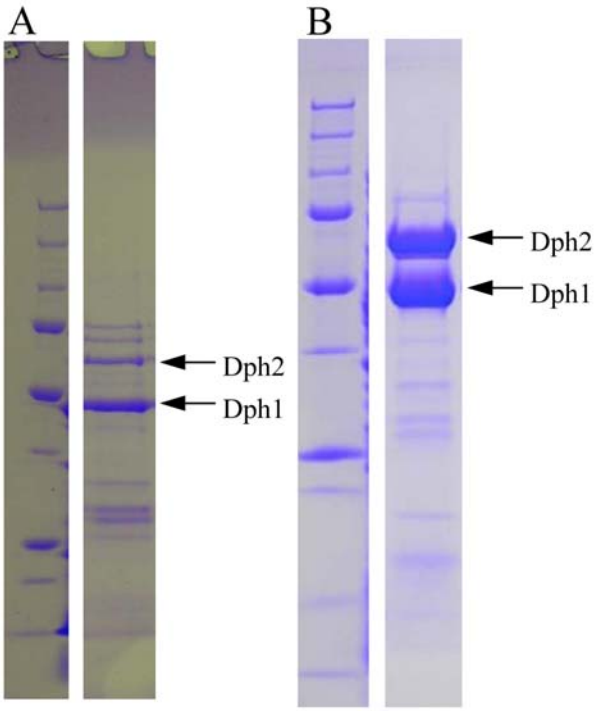

Figure 5.4 Expression and purification of yeast Dph1-Dph2 in pET duet-1 **(A)** and pET28b **(B).** A higher expression level was achieved in pET28b vector. Proteins were purified by Ni-affinity purification. For each panel, the left lane shows the protein ladder and the right shows the purified Dph1/Dph2.

Characterization of Dph1/Dph2 and the activity assay

Before testing the enzymatic activity of Dph1/Dph2, the iron-sulfur cluster was characterized first. The iron content was measured to be 1.2 per monomer and the sulfur content was measured to be 0.6 per monomer. To better characterize the iron-sulfur cluster on Dph1/Dph2, the UV spectra were taken. The oxidized form of [4Fe-4S] cluster shows absorbance at 410nm. Our result showed that Dph1/Dph2 indeed has absorbance at 410nm. When reduced with dithionite, the 410nm absorbance decreased.

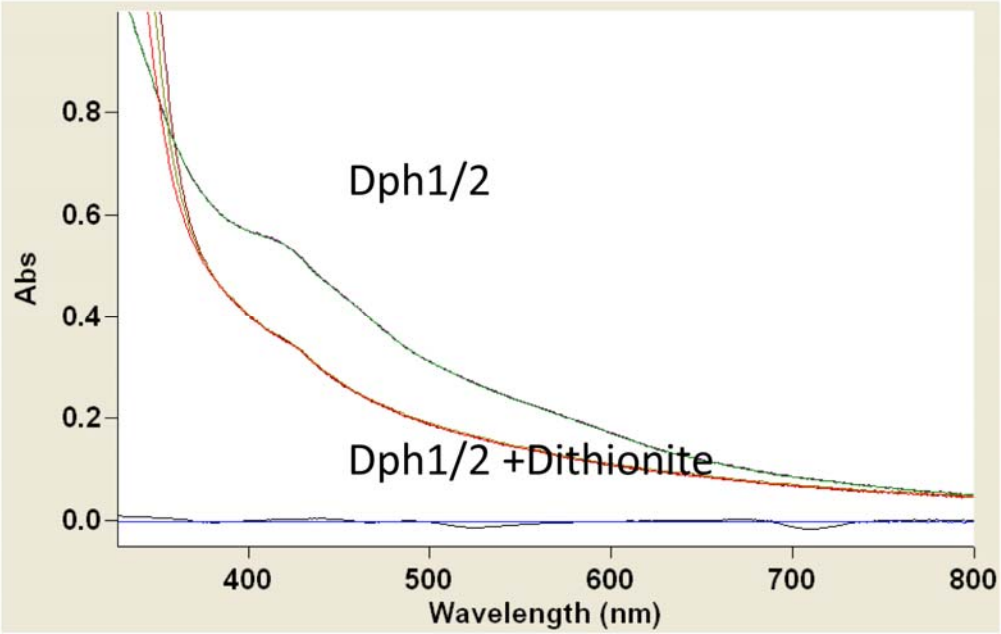

Figure 5.5 The UV spectra of Dph1/Dph2. The blue and black lines are showing the background. The green line is showing the absorbance of Dph1/Dph2, and the red line is showing the Dph1/Dph2 after the dithionite reduction.

The first step of PhDph2 catalyzed reaction is the cleavage of SAM to generate MTA. We were able to show that the Dph1/Dph2 is capable of catalyzing the same reaction. Dph1/Dph2's activity depends on the presence of dithionite. 5'-deoxyadenosine is not a product from Dph1/Dph2 catalyzed SAM cleavage.

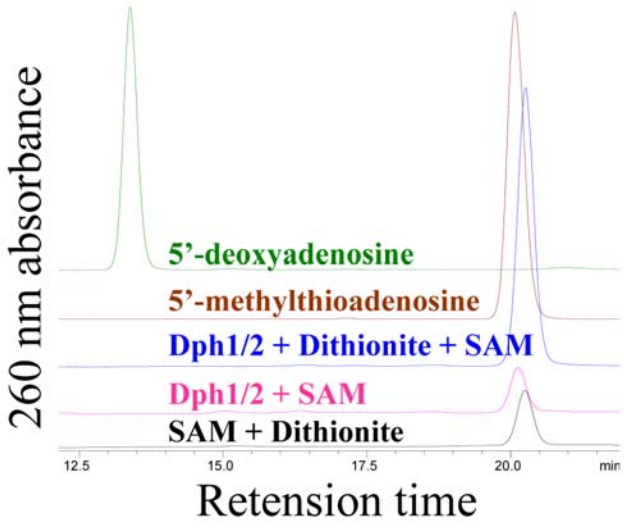

Figure 5.6 Purified yeast Dph1-Dph2 can cleave SAM. The reaction products were analyzed on HPLC to detect the formation of MTA. MTA production is dependent on Dph1-Dph2 and dithionite.

Expression, purification and characterization of Dph3 and Dph4

We assume that Dph1/Dph2 *in vitro* are sufficient to catalyze the transfer of the ACP group. However, we also cloned, expressed and purified yeast Dph3 and Dph4 to study their function. The Dph3/Dph4 genes were cloned into pDEST expression vectors with either N-His_6 or N-His_6-MBP (maltose-binding protein) fusions using Gateway technologies (Invitrogen). The MBP tag was removed by using TEV protease. Dph3 and Dph4 were expressed in BL21R2 cells and purified (Figure 5.7).

Dph3 showed purple color after the purification, implying the coordination with iron. To confirm it, we took the UV spectra of Dph3. Dph3 showed absorbance at 495nm. When reduced with dithionite, the 495nm absorbance decreased and the color was gone. The reduced Dph3 can be slowly re-oxidized in air (Figure 5.8). Dph4 has no color after purification.

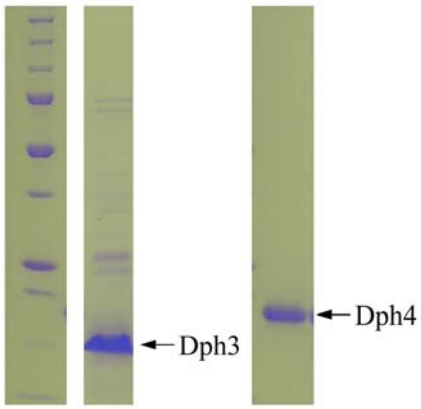

Figure 5.7 Expression and purification of yeast Dph3 and Dph4. Proteins were purified by Ni-affinity purification. The left lane shows the protein ladder and the right lanes show the purified Dph3 and Dph4.

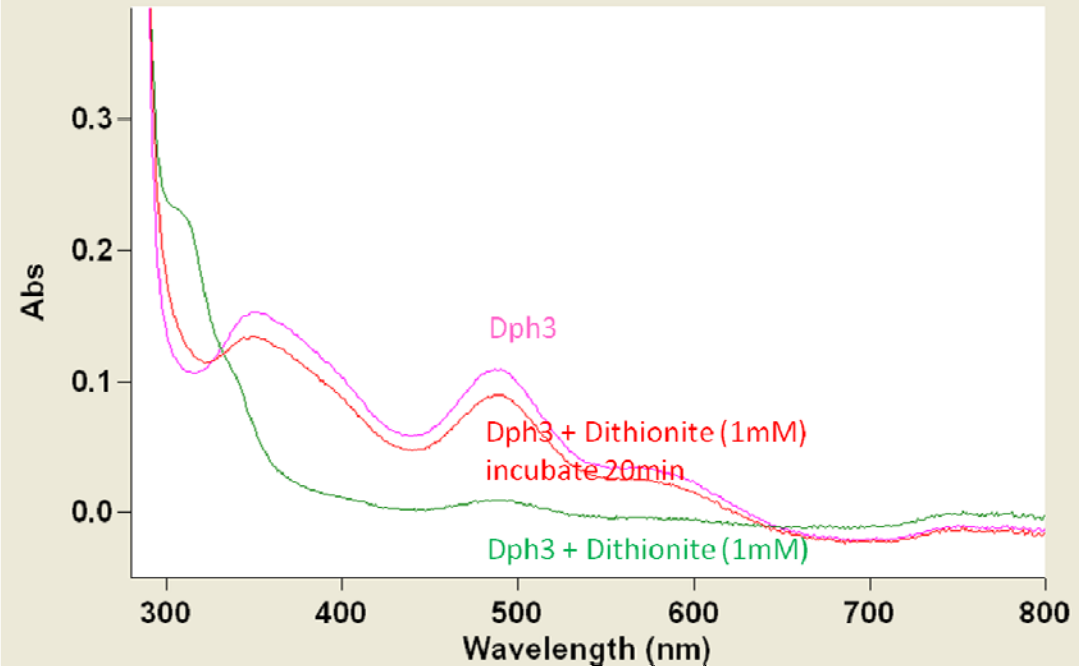

Figure 5.8 The UV spectra of Dph3. The pink trace is showing the absorbance of Dph3. The green trace is showing the Dph3 after dithionite reduction. The red trace is showing the Dph3 re-oxidized in air.

We have also confirmed that Dph3 can be reduced by riboflavin reductase NorW. NorW was cloned and expressed in *E. coli*. NorW showed bright yellow color, indicating the presence of

flavin adenine dinucleotide (FAD). When incubated with NorW and NADH, Dph3 can be quickly reduced (Figure 5.9).

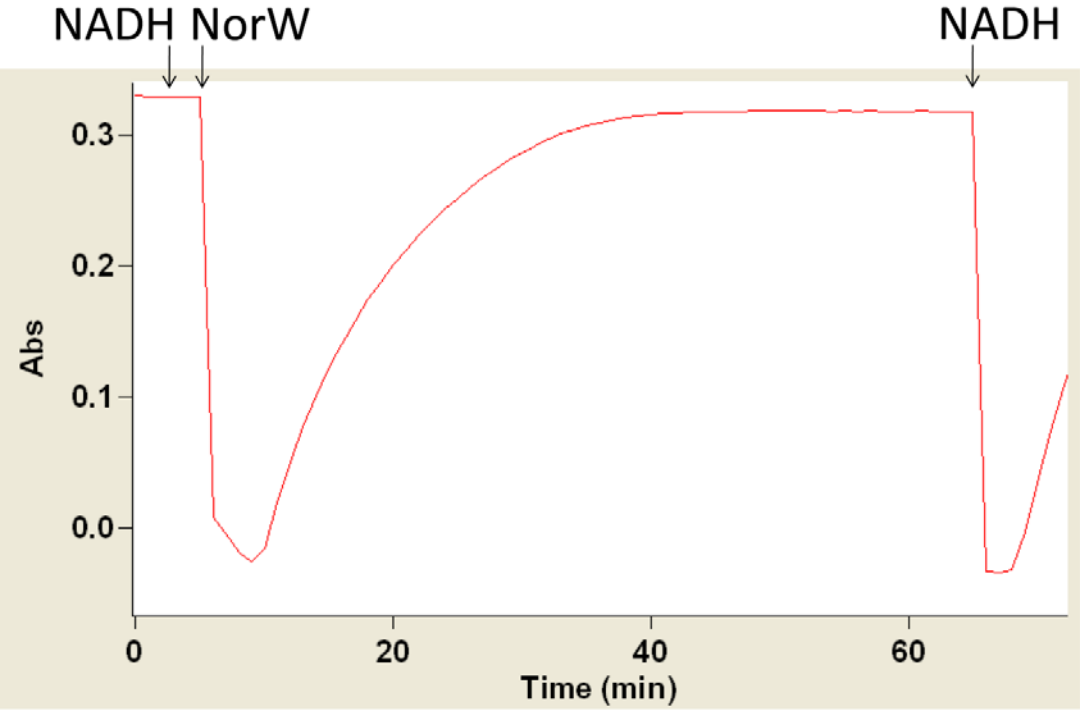

Figure 5.9 Dph3 characterized by UV-Vis spectroscopy. The pink trace was Dph3 and the green trace was Dph3 reduced by 1mM dithionite. The reaction was then open to air for 20 minutes. The red trace shows the absorbance after the incubation.

Reconstitution of the ACP transfer reaction

Attempts were made to reconstitute the ACP transfer reaction. To monitor this reaction, carboxyl-^{14}C-SAM was used as the co-substrate. Purified Dph1-4 and eEF-2 was used. All proteins were desalted using anaerobic buffer. Unfortunately, no ^{14}C labeling on eEF-2 was detected (Figure 5.10). There may be many reasons for it. The primary concern was the concentration and/or quality of eEF-2.

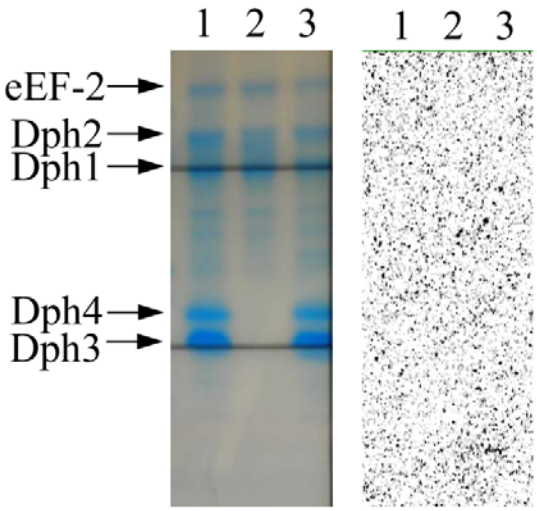

Figure 5.10 The ^{14}C labeling assay of eEF-2. The left panel displays the protein bands on Coomassie Blue stained SDS-PAGE gel. The right panel displays the autoradiography from ^{14}C. Lane 1 contained Dph1-4 and eEF-2. Lane 2 contained Dph1-2 and eEF-2. Lane 3 contained another batch of Dph1/Dph2 as well as Dph3/4 and eEF-2.

Discussion

Our hypothesis is that Dph1 and Dph2 form a heterodimer (Dph1-Dph2) that is equivalent to the homodimer of PhDph2. Dph1 and Dph2 are homologous to each other and has been reported to form a complex(*8*). The function of Dph3 and Dph4 is probably involved in assembly of the Fe-S cluster or transferring electron to the Fe-S cluster in Dph1-Dph2. However, exactly what they do and how they do it is unknown. Our preliminary data suggest that the enzymology of Dph1-Dph2 is different and much more complicated than that of PhDph2. For the PhDph2 homodimer, we found that only one of the subunits is required to have a [4Fe-4S] cluster. A PhDph2 heterodimer with one wt subunit and one C59A/C287A double mutant (cannot bind Fe-S cluster) is still able to catalyze the reaction *in vitro* with efficiency undistinguishable from that of wt PhDph2

homodimer. In contrast, in our *in vivo* studies with yeast Dph1 and Dph2, we found that each of them have three Cys residues that are required for activity. In Dph1, the three Cys residues (C133, C239, C368) are equivalent to the three Cys residues in PhDph2 (C59, C163, C287) that bind the Fe-S cluster. The required Cys residues in Dph2 are C107 and C362. C362 in yeast Dph2 is equivalent to C287 in PhDph2, but C107 in yeast Dph2 is only conserved in eukaryotic Dph1 and Dph2 proteins but not in archaeal Dph2. Thus it seems that Dph1-Dph2 is different from the PhDph2 homodimer. We suspect that the electron transfer chemistry in eukaryotic Dph1-Dph2 may be different from that in PhDph2. It should be pointed out that conserved and/or catalytically important Cys residues should never be overlooked, as recent work by Dr. Squire Booker and coworkers on the ribosomal RNA methylating enzymes RlmN and Cfr discovered an extremely interesting methylation mechanism by radical SAM enzymes(*12, 13*). Therefore, we think eukaryotic Dph1-Dph2 is worth studying in great details. The Dph1/Dph2 we prepared has been shown to be active in SAM cleavage, therefore it is most likely that the Fe-S cluster was in an active form. However, the Dph1/Dph2 failed to show activity in catalyzing the ACP transfer. There could be many reasons to it, and the primary concern is the concentration/quality of the yeast eEF-2. We have tried to express and purify yeast eEF-2 from *E. coli* but failed.

Our hypothesis about Dph3 is that it is an electron carrier that mediates the reduction of the Fe-S clusters in Dph1-Dph2. This is supported by our and others' finding that it can bind iron with four conserved Cys residues and is redox active(*14*). This can also explain why Dph3 is required for certain tRNA modifications that require another radical SAM enzyme Elp3, because Dph3 could

also be responsible for reducing the Fe-S cluster in Elp3(*15*).

Dph4 contains four conserved Cys residues similar to Dph3. In addition, it has a J domain that is found in many co-chaperon proteins(*16, 17*). We hypothesized that the function of Dph4 is to help assemble the Fe-S clusters in Dph1-Dph2. This hypothesis is based on the similarity of Dph4 with human HscB. Human HscB has an N-terminal tetra-Cys motif, and a C-terminal J domain(*18, 19*). In contrast, Dph4 has an N-terminaI J domain and a C-terminal tetra-Cys motif. HscB is conserved in most species, including bacteria. However, the bacterial HscB and the yeast homolog Jac1 both lack the tetra-Cys motif. In bacteria, it is known that HscB is a co-chaperon that interacts with the chaperon protein HscA, and the two together help to transfer the Fe-S cluster assembled on IscU to apo Fe-S cluster proteins. Thus, the function of Dph4 is probably similar to bacterial HscB, functioning with a chaperon protein to transfer Fe-S clusters to apo Fe-S proteins in the cytosol, either non-specifically to multiple proteins or specifically to Dph1-Dph2. In contrast, human HscB or yeast Jac1 is the mitochondrial co-chaperon for transferring Fe-S clusters to apo Fe-S proteins in the mitochondria.

Methods

Cloning, expression of Dph1 and Dph2

Yeast Dph1 and Dph2 was amplified from yeast genomic DNA, which was extracted from BY4741 using Pierce Yeast DNA Extraction Kit. The primers used for Dph1 were XS022 (5'-**agtcag**gaattcTATGAGTGGCTCTACAGAATC-3') and HL002 (5'-agtcaggtcgacCTATTCAATCGCATGTTTCGG -3') and the primers used for Dph2 were XS035

(5'-**agtcag**CATATGATGcaccatcaccaccatcatcaccatGAAGTTGCACCGGCCTT-3') and XS004 (5'- agtcagGGTACCtcatttgttttccttttcatagc-3'). Dph2 was inserted into pETduet-1 vector first, followed by the insertion of Dph1. The Dph1/Dph2 part from pETduet-1 was also amplified using primers XS022 and XS004 and transferred to the pET28b vector. The plasmids pET28duet-1 Dph1/Dph2 and pET28b Dph1/Dph2 were used to transform BL21(DE3) pRARE2 strain respectively. Cells were grown in 2 liters LB medium at 37°C and 200 rpm. It took 4-5 hours for the OD600 to reach 0.5 after inoculation with the overnight culture. The cultures were supplemented with $FeCl_3$, $Fe(NH_4)_2(SO_4)_2$ and L-cysteine to final concentrations of 50 μM, 50 μM and 400 μM, respectively. Then the culturing temperature was changed to 15°C, and the protein expression was induced by 0.1 mM isopropyl-D-thiogalac-toside (IPTG). Cells were harvested after incubation at 15°C for 20 h.

Anaerobic purification of Dph1 and Dph2

Purification of Dph1/Dph2 was performed in an anaerobic chamber (Coy Laboratory Products). Cell pellet from 2 liter culture was resuspended in 30 mL lysis buffer (500 mM NaCl, 10 mM $MgCl_2$, 5 mM imidazole, 1 mM DTT, 0.3% (w/v) lysozyme and 20 mM Tris-HCl at pH 7.4). Cells were incubated at 25 °C for 1 h, followed by liquid nitrogen freezing and then thawed at 25 °C. Cell debris was removed by centrifugation at 48,000g (Beckman Coulter Avanti J-E) for 30 min. The supernatant was incubated for 1 h with 1.2 ml Ni-NTA resin (Qiagen) pre-equilibrated with the lysis buffer (without lysozyme). The resin after incubation was loaded onto a polypropylene column and washed with 20 ml lysis buffer (without lysozyme). Dph1/Dph2 was

eluted from the column with elution buffers (100 mM or 150 mM imidazole in the lysis buffer, 1.5 ml each). The brown-coloured elution fractions were buffer-exchanged to 150 mM NaCl, 1 mM DTT and 200 mM Tris-HCl at pH 7.4 using a Bio-Rad 10-DG desalting column. Protein concentrations were determined by Bradford assay.

Mutagenesis of Dph1 and Dph2

Yeast Dph1/Dph2 were cloned into p413GAL1 vector for the *in vivo* activity assay. Dph1 gene was amplified from pETduet-1 Dph1/Dph2 vector using primers MVG003 (5'-acgtcgACTAGTATGAGTGGCTCTACAGAATCTA-3') and MVG004 (5'-acgtcgCTCGAGCTATTCAATCGCATGTTTCGGA-3'). Dph2 gene was amplified from pETduet-1 Dph1/Dph2 vector using primers HL004 (5'-agtcagctcgagTCATTTGTTTTCCTTTTTCATAGC-3') and HL008 (5'-agtcagactagtATGGAAGTTGCACCGGCCTT-3'). The mutations were made by overlap extension PCR. The primers for Dph1 C133A were XS005 (5'-ggatgtgtcttatggtgcaGCCtgtattgatgattttactgctag-3') and XS006 (5'- tgcaccataagacacatccc-3'). The primers for Dph1 C239A were XS007 (5'- gaggggtgaagtattggggGCTacttctgaaagattagataaaga-3') and XS008 (5'-ccccaatacttcacccctc-3'). The primers for Dph1 C368A were XS009 (5'-gatgtttttgttcaggtcgcaGCTcctagactgtccatcgattg

-3') and XS010 (5'- tgcgacctgaacaaaaacatc -3'). The primers for Dph2 C107A were XS011 (5'-cacagcgtacagtgcatgcGCTgtagacgaggtcgctgctg-3') and XS012 (5'-gcatgcactgtacgctgtg-3').

The primers for Dph1 C118A were XS015 (5'- cattttggaacagttcGCTggtgttgaaactctag-3') and

XS016 (5'- ctagagtttcaacaccAGCgaactgttccaaaatg -3'). The primers for Dph1 C134A were XS013 (5'-gatgtgtcttatggtgcatgcGCTattgatgattttactgctagg-3') and XS014 (5'-ctagcagtaaaatcatcaatAGCgcatgcaccataagacacatcc -3'). The primers for Dph1 C145A were XS017 (5'-gctagggcattggatGCCgattttattgtgcattacg-3') and XS018 (5'-cgtaatgcacaataaaatcGGCatccaatgccctagc -3'). The primers for Dph1 C155A were XS019 (5'-gcattacgctcattcgGCTttagttcctattgacg-3') and XS020 (5'-cgtcaataggaactaaAGCcgaatgagcgtaatgc -3').

Yeast growth assay.

Cells were transformed with the Dph1 or Dph2 encoding plasmid together with the pLMY101 plasmid which encodes the diphtheria toxin using the Frozen-EZ Yeast Transformation II Kit (Zymo Research, Irvine, CA). Transformed yeast cells were grown on synthetic complete medium with histidine and uracil dropout with 2% glucose as the carbon source. For the survival assay 2% galactose was used as the carbon source. Colony formation was recorded 3 days after plating.

Analyzing reaction product from Dph1/2 with high-performance liquid chromatography

Under anaerobic conditions, reactions were assembled with 30 μM Dph1/Dph2, 30 μM SAM, 10 mM dithionite, 150 mM NaCl, 1 mM DTT and 200 mM Tris-HCl at pH 7.4 in a final volume of 60 μl. The mixture was incubated at 25 °C for 60 min. Then the reaction was quenched with 60 μl 10% TFA. And this was followed by centrifugation to separate the precipitated proteins and the supernatant. The supernatant was analysed by high-performance liquid chromatography (Shimadzu) on a C18 column (HαSprite) monitored at 260-nm absorbance, using a linear gradient

from 0 to 40% buffer B over 20 min at a flow rate of 0.3 ml min^{-1} (buffer A: 50 mM ammonium acetate, pH 5.4; buffer B, 50% (v/v) methanol/water).

UV-Vis spectroscopy of Dph1/Dph2

Dph1/Dph2 (50 μM) was prepared anaerobically in 150 mM NaCl and 200 mM Tris-HCl at pH 7.4. The dithionite treated sample was allowed to incubate for 30 min after adding the reducing agent at a final concentration of 0.5 mM. The samples were sealed in a quartz cell (100 μl each) before being taken out of the anaerobic chamber. The UV-Vis spectra were obtained on a Cary 50 Bio UV-Vis spectrophotometer (Varian), scanning from 200 nm to 800 nm. The baseline was corrected with the buffer used to prepare the samples.

Cloning, expression and purification of Dph3 and Dph4

Yeast Dph3 and Dph4 was amplified from yeast genomic DNA, which was extracted from BY4741 using Pierce Yeast DNA Extraction Kit. The primers used for Dph3 were XS024 (5'-agtcagGATATCgatgtcaacatatgacgaaatc-3') and JT008 (5'-AGTCAGCTCGAGTTAatggtgatgatggtggtgatggtgGGCAGCAGCGGCAATAGG-3') and the primers used for Dph4 were XS023 (5'-agtcagGGATCCcatgtcattggtgaattcgttaa-3') and XS003 (5'-agtcagGTCGACttattgtccttcttgctcttcc-3'). Dph3 and Dph4 were inserted into pCDFduet vector respectively. The plasmid was used to transform BL21(DE3) pRARE2 strain. Cells were grown in 2 liters LB medium at 37°C and 200 rpm. It took 4-5 hours for the OD600 to reach 0.5 after inoculation with the overnight culture. Then the culturing temperature was changed to 15°C, and the protein expression was induced by 0.1 mM isopropyl-

D-thiogalac-toside (IPTG). Cells were harvested after incubation at 15°C for 20 h. The protein was purified using a HisTrap column (GE Healthcare). Protein concentrations were determined by Bradford assay.

UV-Vis spectroscopy of Dph3

The UV-Vis spectra of Dph3 (87 μM) were obtained on a Cary 50 Bio UV-Vis spectrophotometer (Varian), scanning from 200 nm to 800 nm. The baseline was corrected with the buffer used to prepare the samples. The dithionite was added to the sample at a final concentration of 0.5 mM. The sample was then exposed to air to re-oxidize Dph3.

Cloning, expression and purification of NorW

NorW gene was amplified from the genomic DNA of *E.coli.* strain TOP10. The primers used were XS055 (5'-agtcagCATATGagtaacggcattgtgatcatc-3') and XS056 (5'-agtcagCTCGAGctacatcggcaatgttttcaac-3'). NorW gene was inserted into pET28a vector. The plasmid was used to transform BL21(DE3) pRARE2 strain. Cells were grown in 2 liters LB medium at 37°C and 200 rpm. It took 4-5 hours for the OD600 to reach 0.5 after inoculation with the overnight culture. Then the culturing temperature was changed to 15°C, and the protein expression was induced by 0.1 mM isopropyl-D-thiogalac-toside (IPTG). Cells were harvested after incubation at 15°C for 20 h. The protein was purified using a HisTrap column (GE Healthcare). Protein concentrations were determined by Bradford assay.

Reduction of Dph3 with NorW and NADH

The reaction was monitored on a Cary 50 Bio UV-Vis spectrophotometer (Varian), at the wavelength of 488 nm. Dph3 was used at the concentration of 87μM. NorW was added to a final concentration of 1 μM. NADH was used at a final concentration of 2mM.

Expression and purification of yeast eEF-2.

The plasmid p423 MET25-eEF-2 (hosted by strain HL610E) was used to transforme the *S. cerevisiae* cells with BY4741 background and the deletion of DPH2 gene (OpenBiosystems, Huntsville, AL). The expression and purification of eEF-2 was the same as previously reported.

Anaerobic reconstitution of Dph1-4 activity

The reaction mixture contained 4 μM Dph1, 4 μM Dph2, 20 μM Dph3, 20 μM Dph4, 2 μM eEF-2 and 10 mM dithionite in the buffer of 150 mM NaCl, 1 mM DTT and 200 mM Tris-HCl at pH 7.4. The reaction mixture was assembled in the anaerobic chamber under strictly anaerobic conditions. The reaction vials were sealed before being taken out of the anaerobic chamber. 14C-SAM (2 μl, final concentration of 267 μM) was injected into each reaction vial to start the reaction. The reaction mixtures were vortexed briefly to mix and incubated at 30 °C for 60 min. The reaction was stopped by adding protein loading dye to the reaction mixture and subsequently heating at 100 °C for 5 min, followed by 12% SDS–polyacrylamide gel electrophoresis. The dried gel was exposed to a PhosphorImaging screen (GE Healthcare) and the radioactivity was detected using a STORM 860 PhosphorImager (GE Healthcare).

REFERENCES

1. Van Ness, B. G., Howard, J. B., and Bodley, J. W. (1980) ADP-ribosylation of elongation factor 2 by diphtheria toxin. NMR spectra and proposed structures of ribosyl-diphthamide and its hydrolysis products, *J. Biol. Chem. 255*, 10710-10716.

2. Van Ness, B. G., Howard, J. B., and Bodley, J. W. (1980) ADP-ribosylation of elongation factor 2 by diphtheria toxin. Isolation and properties of the novel ribosyl-amino acid and its hydrolysis products, *J. Biol. Chem. 255*, 10717-10720.

3. Dunlop, P. C., and Bodley, J. W. (1983) Biosynthetic labeling of diphthamide in *Saccharomyces cerevisiae*, *J. Biol. Chem. 258*, 4754-4758.

4. Moehring, J. M., Moehring, T. J., and Danley, D. E. (1980) Posttranslational modification of elongation factor 2 in diphtheriatoxin-resistant mutants of CHO-K1 cells, *Proc. Natl. Acad. Sci. USA 77*, 1010-1014.

5. Moehring, J. M., and Moehring, T. J. (1984) Diphthamide: in vitro biosynthesis, *Methods Enzymol 106*, 388-395.

6. Moehring, J. M., and Moehring, T. J. (1988) The post-translational trimethylation of diphthamide studied in vitro, *J. Biol. Chem. 263*, 3840-3844.

7. Liu, S., and Leppla, S. H. (2003) Retroviral insertional mutagenesis identifies a small protein required for synthesis of diphthamide, the target of bacterial ADP-ribosylating toxins, *Mol. Cell 12*, 603.

8. Liu, S., Milne, G. T., Kuremsky, J. G., Fink, G. R., and Leppla, S. H. (2004)

Identification of the proteins required for biosynthesis of diphthamide, the target of bacterial ADP-ribosylating toxins on translation elongation factor 2, *Mol. Cell. Biol. 24*, 9487-9497.

9. Zhang, Y., Zhu, X., Torelli, A. T., Lee, M., Dzikovski, B., Koralewski, R. M., Wang, E., Freed, J., Krebs, C., Ealick, S. E., and Lin, H. (2010) Diphthamide biosynthesis requires an organic radical generated by an iron-sulphur enzyme, *Nature 465*, 891-896.

10. Zhu, X., Dzikovski, B., Su, X., Torelli, A. T., Zhang, Y., Ealick, S. E., Freed, J. H., and Lin, H. (2011) Mechanistic understanding of Pyrococcus horikoshii Dph2, a [4Fe-4S] enzyme required for diphthamide biosynthesis, *Mol. BioSystems 7*, 74-81.

11. Mattheakis, L. C., Sor, F., and Collier, R. J. (1993) Diphthamide synthesis in *Saccharomyces cerevisiae*: structure of the DPH2 gene, *Gene 132*, 149.

12. Yan, F., LaMarre, J. M., Roì^hrich, R., Wiesner, J., Jomaa, H., Mankin, A. S., and Fujimori, D. G. (2010) RlmN and Cfr are radical SAM enzymes involved in methylation of ribosomal RNA, *J. Am. Chem. Soc. 132*, 3953-3964.

13. Yan, F., and Fujimori, D. G. (2011) RNA methylation by radical SAM enzymes RlmN and Cfr proceeds via methylene transfer and hydride shift, *Proc. Natl. Acad. Sci. USA 108*, 3930-3934.

14. Proudfoot, M., Sanders, S. A., Singer, A., Zhang, R., Brown, G., Binkowski, A., Xu, L., Lukin, J. A., Murzin, A. G., Joachimiak, A., Arrowsmith, C. H., Edwards, A. M., Savchenko, A. V., and Yakunin, A. F. (2008) Biochemical and structural characterization of a novel family of cystathionine [beta]-synthase domain proteins fused to a Zn ribbon-

like domain, *J. Mol. Biol. 375*, 301-315.

15. Paraskevopoulou, C., Fairhurst, S. A., Lowe, D. J., Brick, P., and Onesti, S. (2006) The Elongator subunit Elp3 contains a Fe_4S_4 cluster and binds S-adenosylmethionine, *Molecular Microbiology 59*, 795-806.

16. Kelley, W. L. (1998) The J-domain family and the recruitment of chaperone power, *Trends Biochem. Sci. 23*, 222-227.

17. Sahi, C., and Craig, E. A. (2007) Network of general and specialty J protein chaperones of the yeast cytosol, *Proc Natl Acad Sci U S A 104*, 7163-7168.

18. Fuzery, A. K., Tonelli, M., Ta, D. T., Cornilescu, G., Vickery, L. E., and Markley, J. L. (2008) Solution structure of the iron-sulfur cluster cochaperone HscB and its binding surface for the iron-sulfur assembly scaffold protein IscU, *Biochemistry 47*, 9394-9404.

19. Bitto, E., Bingman, C. A., Bittova, L., Kondrashov, D. A., Bannen, R. M., Fox, B. G., Markley, J. L., and Phillips, G. N., Jr. (2008) Structure of human J-type co-chaperone HscB reveals a tetracysteine metal binding domain, *J. Biol. Chem. 10.1074/jbc.M804746200*, M804746200.

CHAPTER 6

SIRT5 IS AN NAD-DEPENDENT PROTEIN LYSINE DEMALONYLASE AND DESUCCINYLASE

Abstract

Sirtuins are NAD-dependent deacetylases that regulate important biological processes. Mammals have seven sirtuins, Sirt1-7. Four of them (Sirt4-7) have no detectable or very weak deacetylase activity. Here we found that Sirt5 is an efficient protein lysine desuccinylase and demalonylase in vitro. The preference for succinyl and malonyl groups was explained by the presence of an arginine residue (Arg105) and tyrosine residue (Tyr102) in the acyl pocket of Sirt5. Several mammalian proteins were identified to have succinyl or malonyl lysine modifications by mass spectrometry. Deletion of Sirt5 in mice appeared to increases the level of succinylation on carbamoyl phosphate synthase 1, a known target of Sirt5. Thus protein lysine succinylation may represent a posttranslational modification that can be reversed by Sirt5 *in vivo*.

Introduction

Silent Information Regulator 2 (Sir2) proteins, or sirtuins, are a family of evolutionally conserved enzymes with nicotinamide adenine dinucleotide (NAD)-dependent deacetylase activity (Figure 6.1)(*1-3*). Since the initial discovery of the deacetylase activity(*4, 5*), many important biological functions of sirtuins have been revealed(*2, 3*). Based on sequence similarity, sirtuins can be grouped into different classes(*6*). Mammals have seven sirtuins, Sirt1-7. Among them, only Class I sirtuins (Sirt1-3) have robust deacetylase activity. Sirt4-7 have either no detectable or very weak deacetylase activity(*7-11*).

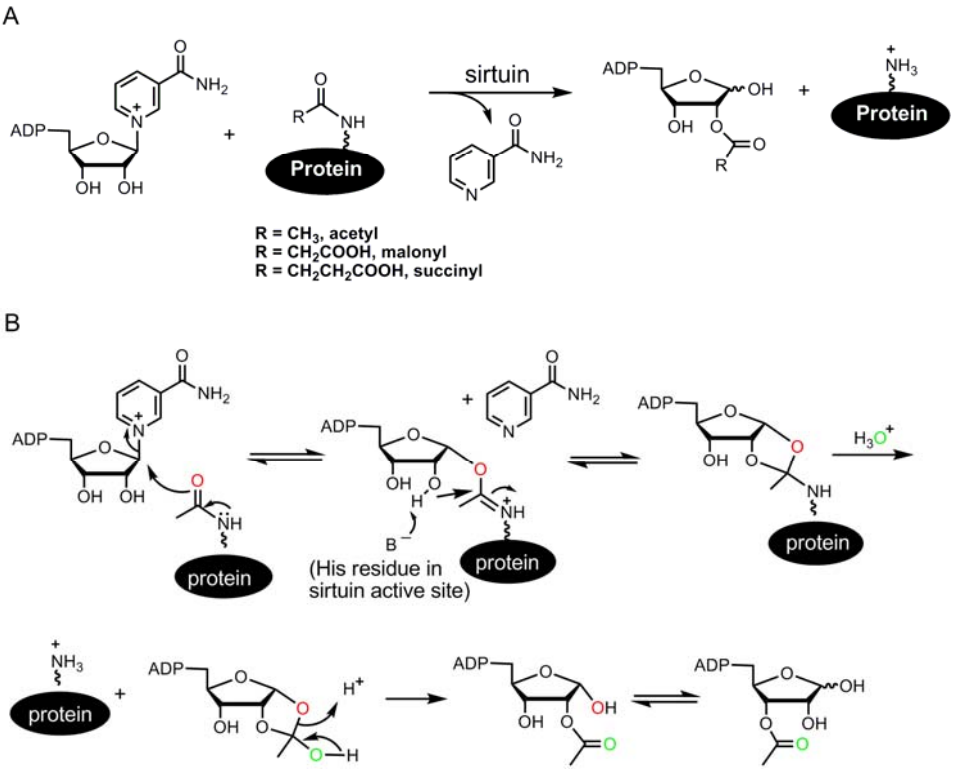

Figure 6.1 The sirtuins catalyzed NAD-dependent deacylation reaction (A) Deacetylation reaction and the resulting *O*-acetyl-ADP-ribose. (B) Mechanism of sirtuin-catalyzed NAD-dependent deacetylation. Some of the oxygen atoms were colored differently to indicate where they come from.

Results and discussion

To check whether the lack of robust deacetylase activity for Sirt4-7 is due to strict requirement for the peptide sequence, the activities of six human sirtuins (all except Sirt4, which could not be expressed in soluble forms in *E. coli*) were monitored using 16 different acetyl peptides (Table 6.1). Under the experimental conditions used, Sirt1-3 and 5 showed deacetylase activity, but Sirt6 and Sirt7 did not. All 16 peptides could be deacetylated by Sirt1-3, while only eight could be deacetylated slowly by Sirt5 (data not shown). A histone H3K9 acetyl peptide was one of the best substrates for Sirt1-3 and Sirt5. With this peptide, the k_{cat} and K_m of different sirtuins were determined (Table 6.2). The catalytic efficiency (k_{cat}/K_m) of Sirt5 was about 500-fold lower than that of Sirt1.

Table 6.1 Acetyl peptides used to assay the deacetylase activity of sirtuins.

Protein/lysine residue	Peptide sequence	Predicted mass (m/z)	Observed mass (m/z)
Histone H3 K9 (1-17)	ARTKQTAR**(AcK)**STGGKAPR	928.6 $[M+2H]^{2+}$	928.5 $[M+2H]^{2+}$
Histone H3 K9 (4-15)	KQTAR**(AcK)** STGGKA	1274.7 $[M+H]^{+}$	1273.8 $[M+H]^{+}$
Histone H3 K14 (6-22)	TARKSTGG**(AcK)**APRKQLAT	907.0 $[M+2H]^{2+}$	906.7 $[M+2H]^{2+}$
Histone H4 K5 (1-16)	SGRG**(AcK)**GGKGLGKGGAK	728.9 $[M+2H]^{2+}$	728.8 $[M+2H]^{2+}$
Histone H4 K8 (1-16)	SGRGKGG**(AcK)**GLGKGGAK	728.9 $[M+2H]^{2+}$	728.8 $[M+2H]^{2+}$
Histone H4 K12 (1-16)	SGRGKGGKGLG**(AcK)**GGAK	728.9 $[M+2H]^{2+}$	728.6 $[M+2H]^{2+}$
Histone H4 K16 (8-24)	KGLGKGGA**(AcK)**RHRKVLRD	959.6 $[M+2H]^{2+}$	958.9 $[M+2H]^{2+}$
Histone H4 K91 (80-99)	TVTAMDVVYAL**(AcK)**RQGRTLYG	1142.6 $[M+2H]^{2+}$	1142.2 $M+2H]^{2+}$
Histone H2A K5 (1-17)	SGRG**(AcK)**QGGKARAKAKTR	900.0 $[M+2H]^{2+}$	899.3 $[M+2H]^{2+}$
Histone H2A K13 (1-17)	SGRGKQGGKARA**(AcK)**AKTR	900.0 $[M+2H]^{2+}$	899.8 $[M+2H]^{2+}$
Histone H2B K5 (1-18)	PEPA**(AcK)**SAPAPKKGSKKAV	917.1 $[M+2H]^{2+}$	916.7 $[M+2H]^{2+}$
Histone H2B K12 (1-18)	PEPAKSAPAPK**(AcK)**GSKKAV	917.1 $[M+2H]^{2+}$	916.8 $[M+2H]^{2+}$
Histone H2B K15 (1-18)	PEPAKSAPAPKKGS**(AcK)**KAV	917.1 $[M+2H]^{2+}$	916.4 $[M+2H]^{2+}$
α-tubulin K40 (32-48)	PDGQMPSD**(AcK)**TIGGGDDS	859.9 $[M+2H]^{2+}$	859.4 $[M+2H]^{2+}$
p53 K382 (374-389)	GQSTSRHK**(AcK)**LMFKTEG	939.0 $[M+2H]^{2+}$	938.5 $[M+2H]^{2+}$
Acetyl-CoA synthetase 2 K642 (620-636)	RLPKTRSG**(AcK)**VMRRLLRK	1069.2 $[M+2H]^{2+}$	1068.6 $[M+2H]^{2+}$

Table 6.2 The kinetic parameters of four human sirtuins on H3 K9 acetyl peptide

Sirtuins	k_{cat} (s^{-1})	K_m **for acetyl peptide** (μM)	k_{cat}/K_m ($s^{-1}M^{-1}$)
Sirt1	0.039 ± 0.001	38 ± 4	1.0×10^3
Sirt2	0.030 ± 0.001	190 ± 14	1.6×10^2
Sirt3	0.012 ± 0.001	50 ± 9	2.4×10^2
Sirt5	ND*	ND (>750)*	2.0

* The k_{cat} and K_m values for Sirt5 could not be determined because the V versus [S] plot was linear (Km was greater than the highest substrate concentration tested). Thus only kcat/Km value can be obtained.

The k_{cat} and K_m values were obtained by curve-fitting the $V_{initial}/[E]$ versus [S] plot using KaleidaGraph.

To understand why the deacetylase activity of Sirt5 is weak, a crystal structure of Sirt5 in complex with a thioacetyl peptide was obtained (the corresponding acetyl peptide could not be crystallized with Sirt5). A buffer molecule, CHES (*N*-cyclohexyl-2-aminoethanesulfonic acid), was also bound to Sirt5 (Figure 6.2A and 6.3A). The interactions between the thioacetyl peptide and Sirt5 involved mostly backbone hydrogen bonding (Figure 6.3B), similar to what was observed for *Thermotoga maritime* Sir2 (Sir2Tm), a sirtuin with robust deacetylase activity(*12*). Thus, the selectivity for peptide sequences is unlikely to be the major reason for the lack of robust deacetylase activity for Sirt5.

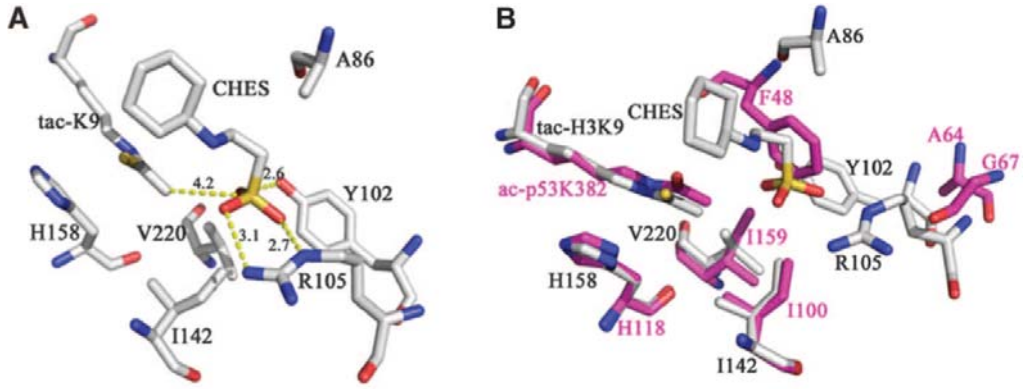

Figure 6.2 The structure of Sirt5 revealed an unusual acyl pocket. (A) The acyl pocket of Sirt5 was partially occupied by the sulfate from the CHES molecule via interactions with Arg105 and Tyr102. The sulfur was 4.2 Å away from the thioacetyl group. (B) Alignment of Sirt5-thioacetyl peptide structure (grey) and Sir2Tm-acetyl peptide structure (PDB 2h4f, magenta).

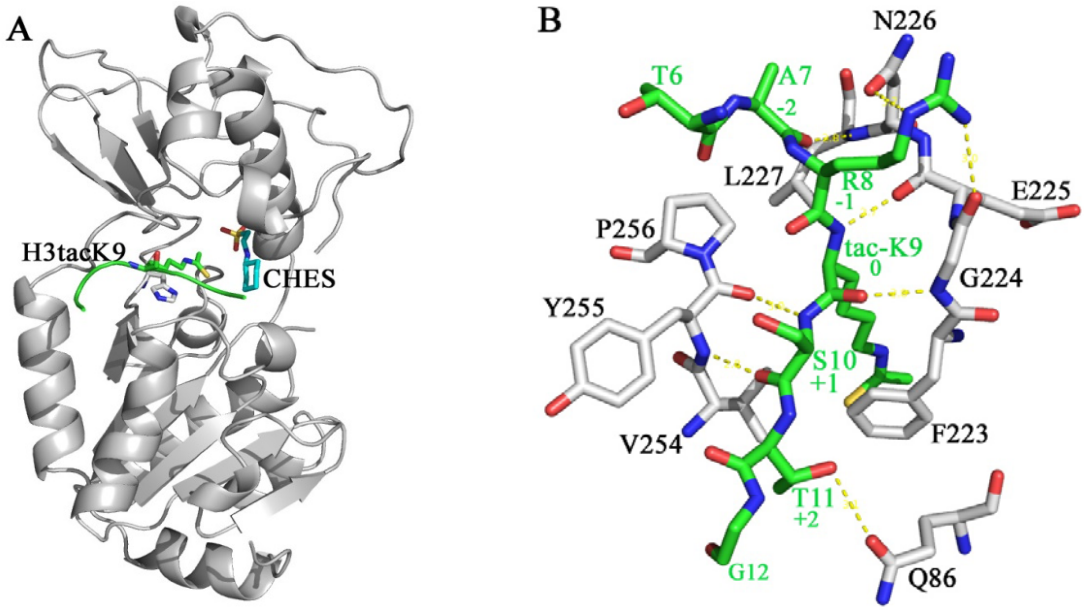

Figure 6.3 (A) Overall structure of Sirt5 in complex with an H3K9 thioacetyl peptide. The thioacetyl lysine side chain (green) and the CHES molecule (cyan) are shown in stick (cyan). (B) H-bonding interactions (dashed yellow lines) between thioacetyl peptide (green) and Sirt5 (light grey).

When the Sirt5 structure was superimposed with the structure of Sir2Tm in complex with an

acetyl peptide and NAD (PDB 2h4f) (Figure 6.2B)(*13*), the positions of the thioacetyl lysine in Sirt5 and the acetyl lysine in Sir2Tm were almost identical in the superimposed structures. The acetyl group in the Sir2Tm structure was surrounded by three hydrophobic residues, Phe48, Ile100, and Ile159. In contrast, the corresponding pocket in Sirt5 was larger and bound by CHES. The sulfate group of CHES interacted with Tyr102 and Arg105 of Sirt5 and was ~4 Å away from the thioacetyl group (Figure 6.2A). In the reported Sirt5 structure with HEPES bound(*9*), the sulfate from HEPES also interacted with Arg105 and Tyr102.

Based on the above structural analysis, we reasoned that if the acetyl group was replaced with an acyl group bearing a negatively-charged carboxylate, the acyl peptide should bind Sirt5 better than the acetyl peptide and thus may be a better substrate for Sirt5 (Figure 6.4). In cells, the most common acyl-CoA molecules with a carboxylate group are malonyl-CoA and succinyl-CoA(*14*). Malonyl-CoA, made from acetyl-CoA by acetyl-CoA carboxylase in the cytosol and the mitochondria, is a precursor for fatty acid biosynthesis(*15, 16*). Succinyl-CoA is an intermediate in the Krebs cycle in the mitochondria. Since acetyl-CoA is used to modify proteins in cells, it is possible that malonyl- and succinyl-CoA could also be used to modify proteins. Thus, H3K9 malonyl and succinyl peptides were synthesized and tested for hydrolysis by Sirt5.

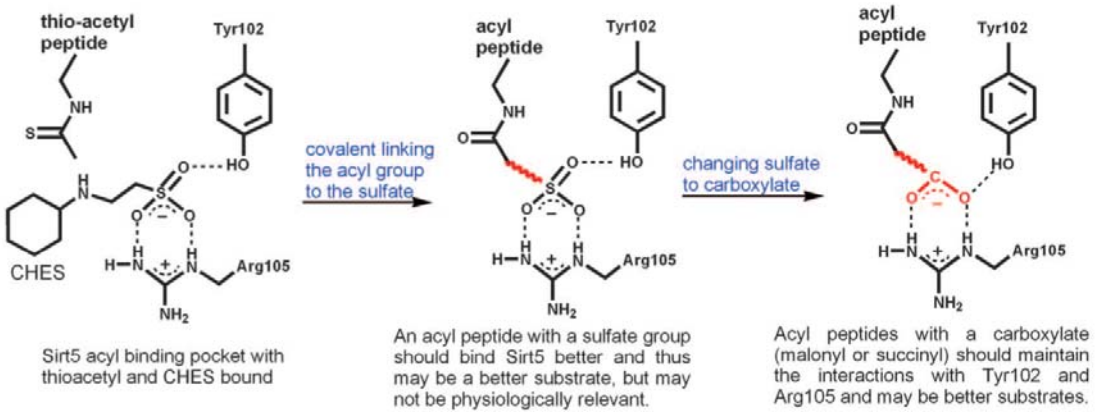

Figure 6.4 The rationale for predicting that malonyl/succinyl peptides could be better substrates for Sirt5.

Liquid chromatography–mass spectrometry (LC-MS) was used to monitor the reactions. Sirt1, 2, and 3 catalyzed the hydrolysis of the acetyl peptide, but not the malonyl or succinyl peptide (Figure 6.5A-C and 6.6-6.9). In contrast, with Sirt5, little hydrolysis of the acetyl peptide was observed, but the malonyl and succinyl peptides were hydrolyzed significantly (Figure 6.5D-F, Fig. 6.6-6.8,6.10). The deacylated peptides have identical masses to the synthetic unmodified peptide (Figure 6.6 and 6.9). Sirt6 and Sirt7 had no detectable activity on the acyl peptides under the conditions tested (Figure 6.11). Thus, Sirt5 is a desuccinylase and demalonylase.

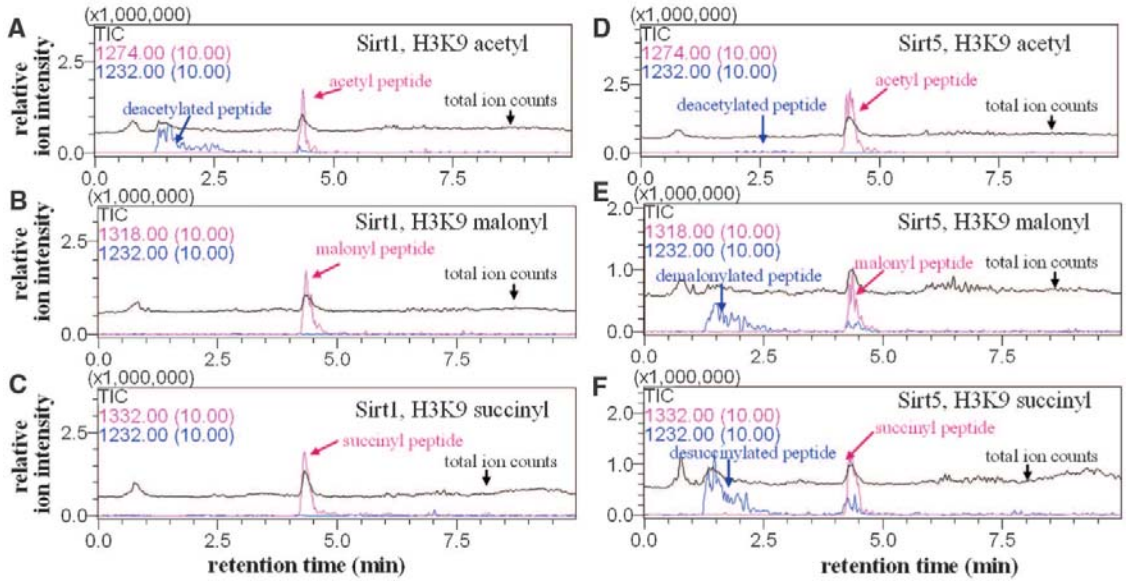

Figure 6.5 Sirt5 catalyzed the hydrolysis of malonyl and succinyl lysine. The enzymatic reactions were analyzed by LC-MS. Pink traces showed the ion intensities (10x magnified) for the masses of the acyl peptides (acetyl, m/z 1274.0; malonyl, m/z 1318.0; succinyl, m/z 1332.0) and blue traces showed the ion intensities (10x magnified) for the mass of the deacylated peptide (m/z 1232.0). Black traces showed the ion intensity for all masses from 100-2000 (total ion counts or TIC). With Sirt1, hydrolysis was observed for the acetyl peptide (A), but not malonyl (B) or succinyl (C) peptide. With Sirt5, hydrolysis of the acetyl peptide was barely detectable (D) while hydrolysis of the malonyl (E) and succinyl (F) peptides were obvious.

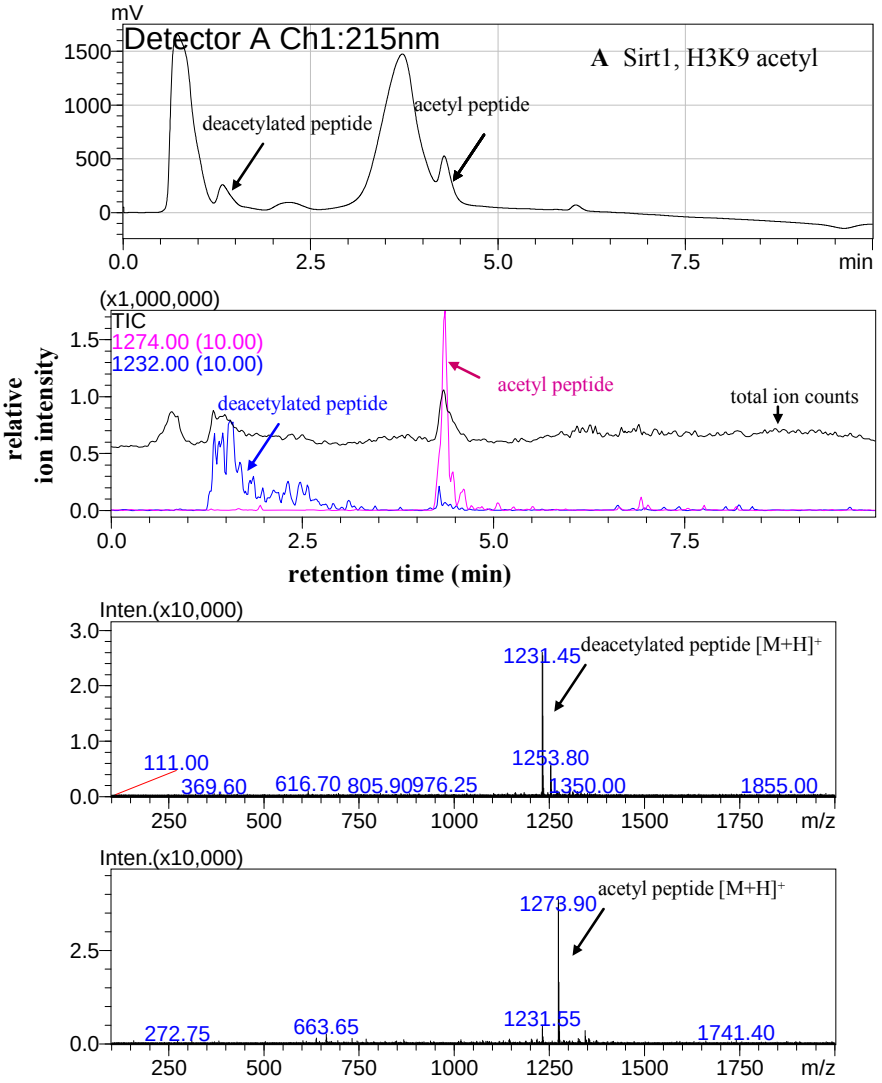
mV
Detector A Ch1:215nm
A Sirt1, H3K9 acetyl
deacetylated peptide
acetyl peptide
1500
1000
500
0
0.0
2.5
5.0
7.5
min
(x1,000,000)
TIC
1274.00 (10.00)
1232.00 (10.00)
acetyl peptide
deacetylated peptide
total ion counts
relative ion intensity
1.5
1.0
0.5
0.0
retention time (min)
Inten.(x10,000)
1231.45
deacetylated peptide [M+H]+
111.00
369.60
616.70
805.90
976.25
1253.80
1350.00
1855.00
3.0
2.0
1.0
250
500
750
1000
1250
1500
1750
m/z
Inten.(x10,000)
1273.90
acetyl peptide [M+H]+
272.75
663.65
1231.55
1741.40
2.5

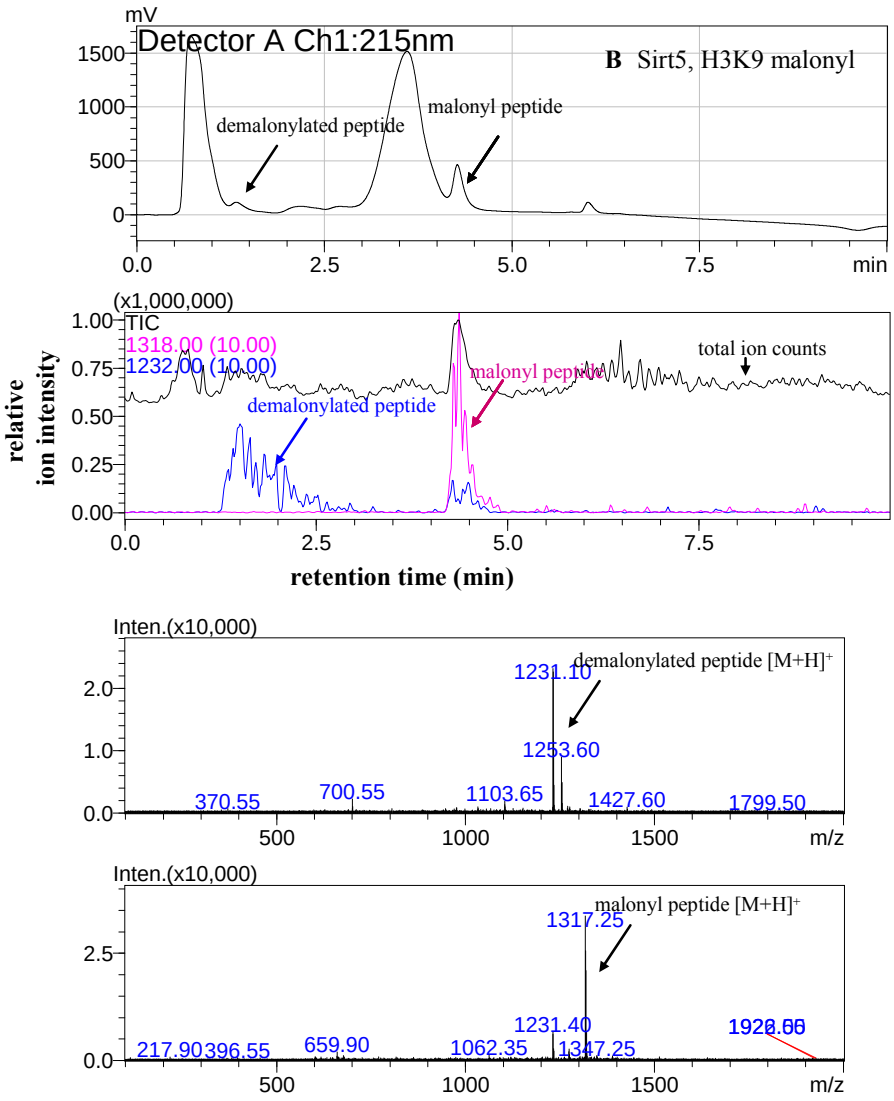
mV
Detector A Ch1:215nm
B Sirt5, H3K9 malonyl
demalonylated peptide
malonyl peptide
min
(x1,000,000)
TIC
1318.00 (10.00)
1232.00 (10.00)
total ion counts
relative ion intensity
retention time (min)
Inten.(x10,000)
demalonylated peptide [M+H]+
1231.10
1253.60
370.55
700.55
1103.65
1427.60
1799.50
m/z
Inten.(x10,000)
malonyl peptide [M+H]+
1317.25
1231.40
217.90
396.55
659.90
1062.35
1347.25
m/z

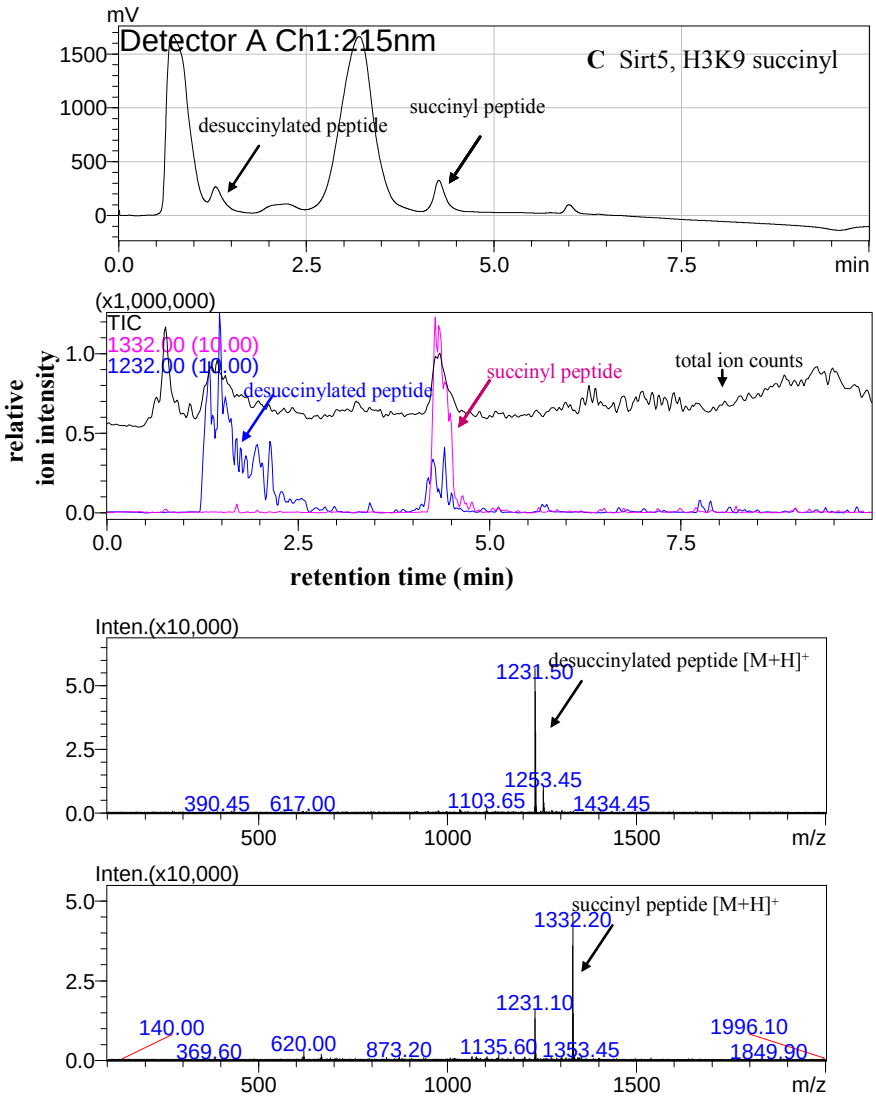

Figure 6.6 Sirt1 and Sirt5 catalyzed-hydrolysis of different acyl peptides monitored using LC-MS. For each reaction, the LC trace, MS trace, deacylated peptide mass spectra and acyl peptide mass spectra are shown. LC traces detect the UV-Vis absorption at 215 nm of compounds coming off the column, and MS traces detect the masses of the compounds coming off the column. In the MS trace, pink traces show the ion intensities (10x magnified) for the masses of the acyl peptides (acetyl, m/z 1274.0; malonyl, m/z 1318.0; succinyl, m/z 1332.0) and blue traces show the ion intensities (10x magnified) for the mass of the deacylated peptide (m/z 1232.0). Black traces show the ion intensity for all masses from 100-2000 (total ion counts or TIC). With Sirt1, the deacetylated product was detected when H3K9 acetyl peptide (A) was used as the substrate. With Sirt5, the demalonylated (B) and desuccinylated (C) products were detected.

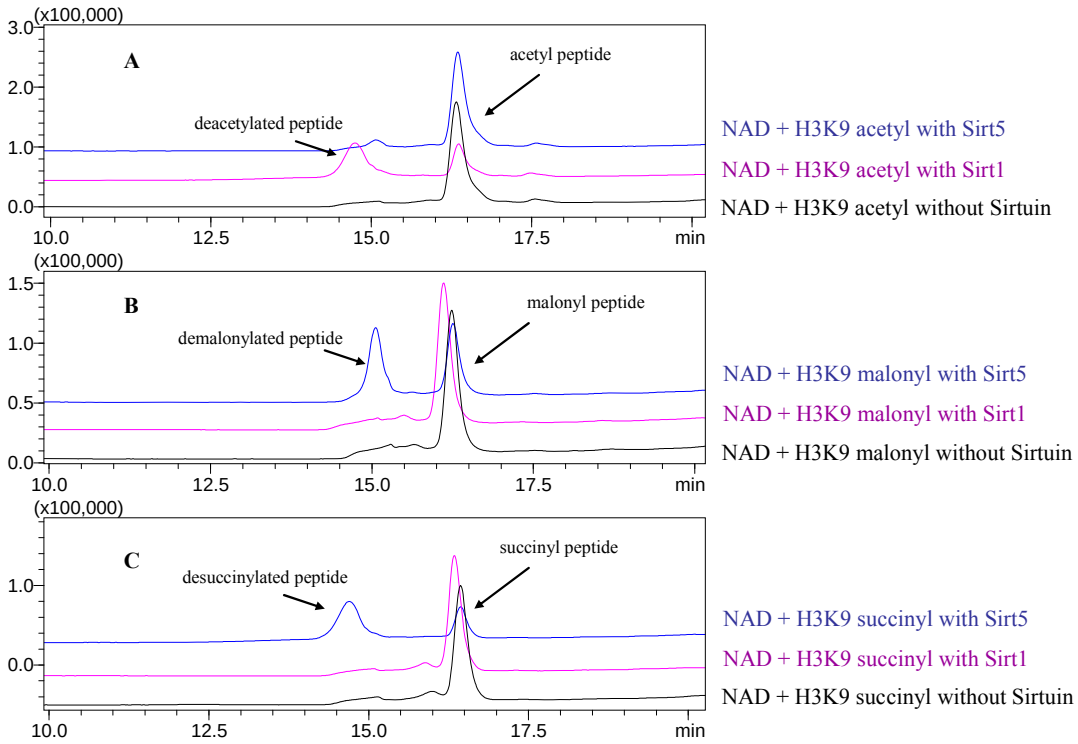

Figure 6.7 Sirt1 and Sirt5-catalyzed deacetylation, demalonylation and desuccinylation of H3 K9 peptides were examined by HPLC (monitored at 215 nm). In Figure 6.6, LC-MS was used to monitor the reactions. However, in the LC traces, the acyl peptide and deacylated peptide peaks overlapped with other peaks. Here, a longer HPLC column was used to better separate the acyl peptide and deacylated peptide. The results further confirmed that Sirt1 had better deacetylase activity, while Sirt5 had better demalonylase and desuccinylase activity.

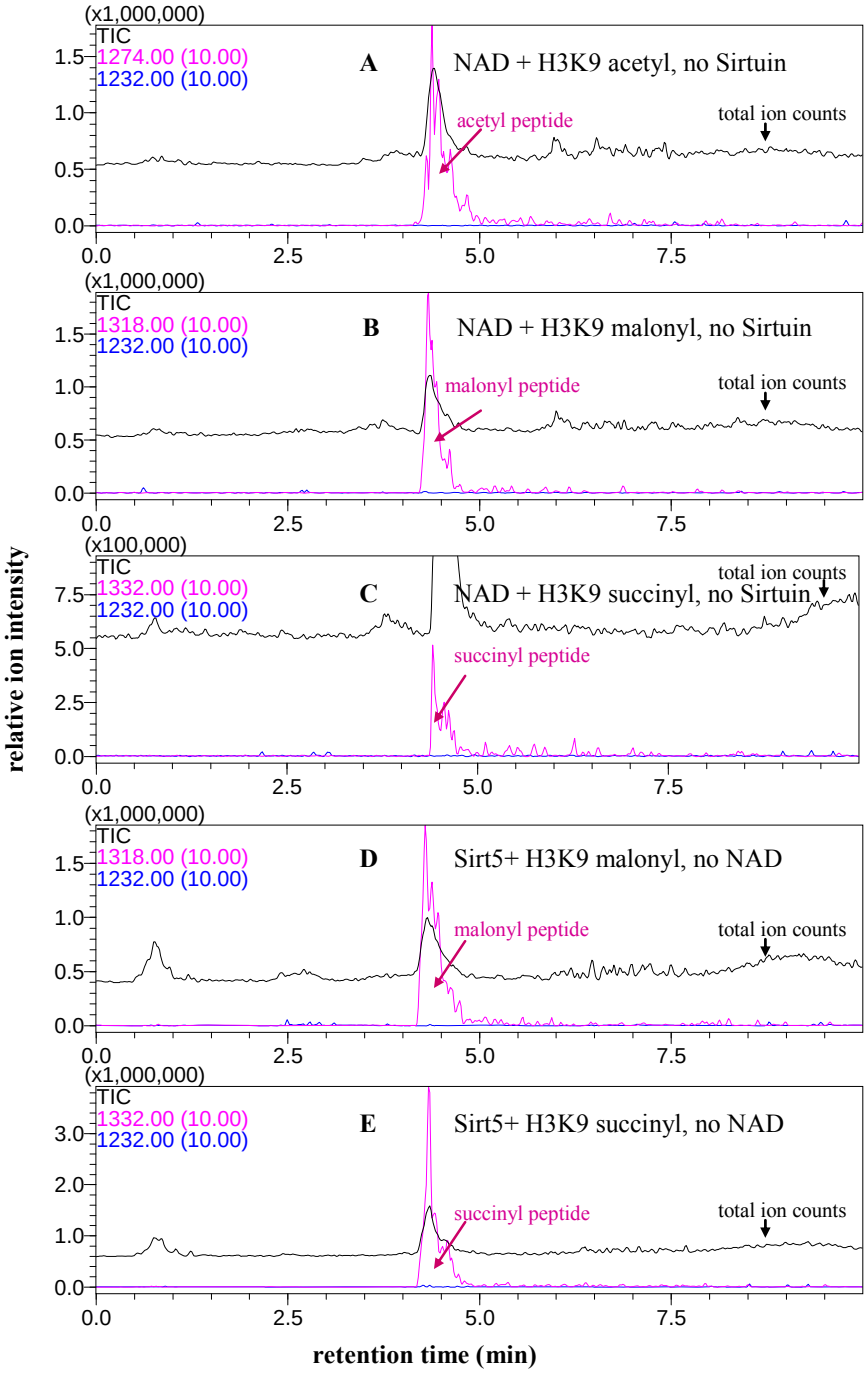

Figure 6.8 In the absence of Sirt5 or NAD, malonyl and succinyl peptides could not be hydrolyzed. Shown here are the MS traces from the LC-MS analyses for the reactions. Pink traces show the ion intensities (10x magnified) for the masses of the acyl peptides (acetyl peptide, m/z 1274.0; malonyl peptide, m/z 1318.0; succinyl peptide, m/z 1332.0) and blue traces show the ion intensities (10x magnified) for the mass of the deacylated peptide (m/z 1232.0). Black traces show the intensity for total ion counts (TIC). There was no deacylated peptide generated without

sirtuin (A, B, C) or NAD (D and E).

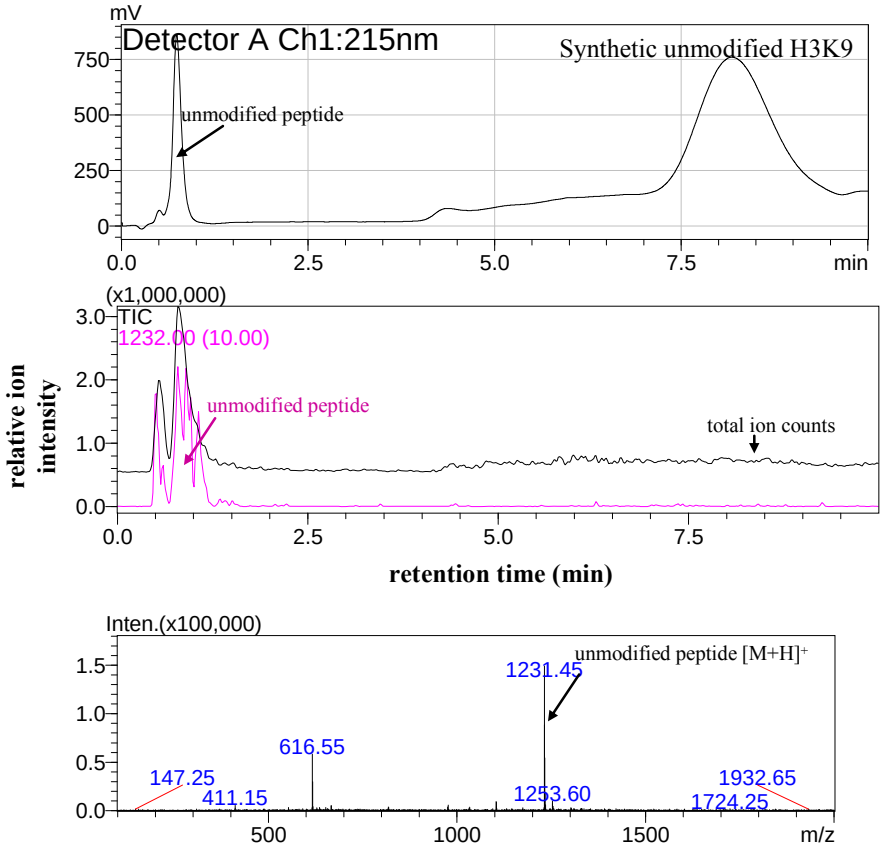

Figure 6.9 LC-MS of synthetic unmodified H3K9 peptide. The LC trace, MS trace, and mass spectra are shown from top to bottom. LC traces detect the UV-Vis absorption at 215 nm of compounds coming off the column, and MS traces detect the masses of the compounds coming off the column. Pink traces show the ion intensities (10x magnified) for the masses of the unmodified peptide (m/z 1232.0). Black traces show the ion intensity for all masses from 100-2000 (total ion counts or TIC). The demalonylated and desuccinylated peptides (Fig. S4) had identical masses to the synthetic unmodified H3K9 peptide.

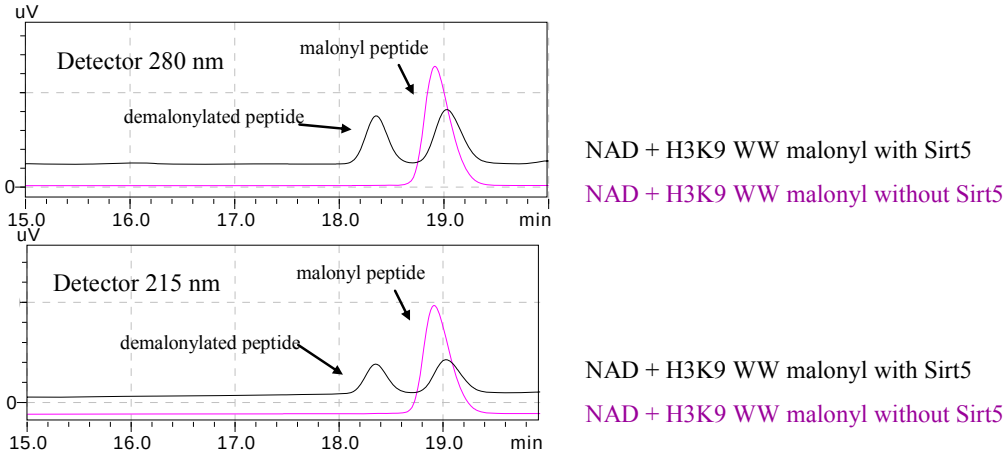

Figure 6.10 HPLC traces for the demalonylation reactions with H3K9 WW peptide were monitored at 280 nm and 215 nm. The pink traces are controls showing the peptides without Sirt5. The black traces are the reactions with Sirt5. The new peak at 18.3 min is the demalonylated product.

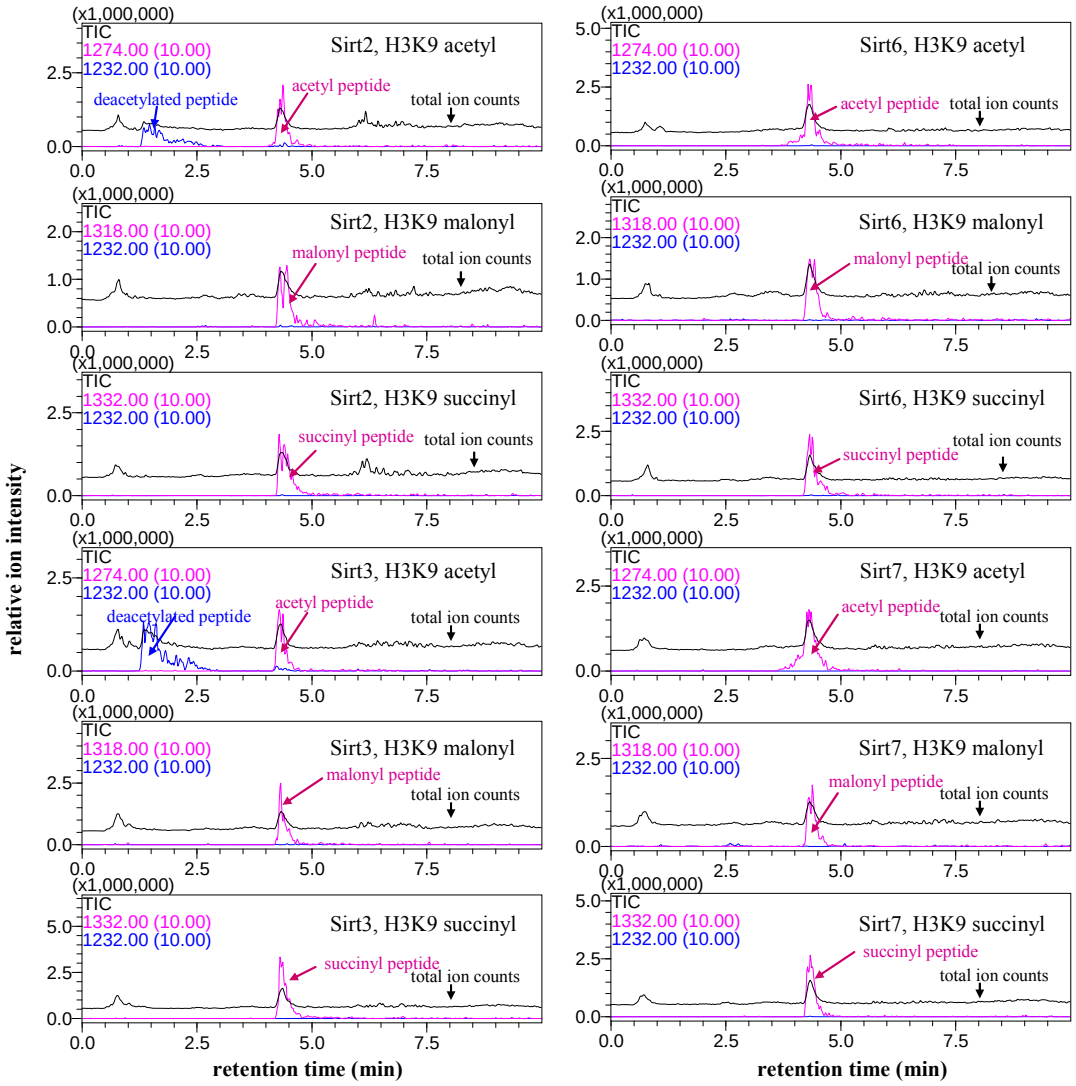

Figure 6.11 Sirt2, Sirt3, Sirt6, and Sirt7 did not catalyze the hydrolysis of malonyl and succinyl lysine. Shown here are the MS traces from the LC-MS analyses of the reactions. Pink traces show the ion intensities (10x magnified) for the masses of the acyl peptides (acetyl peptide, m/z 1274.0; malonyl peptide, m/z 1318.0; succinyl peptide, m/z 1332.0) and blue traces show the ion intensities (10x magnified) for the mass of the deacylated peptide (m/z 1232.0). Black traces show the intensity for total ion counts (TIC). Sirt2 and Sirt3 only displayed deacetylation activity, while no activity was detected for Sirt6 and Sirt7.

The k_{cat} and K_m values for Sirt5-catalyzed deacetylation, demalonylation, and desuccinylation were determined (Table 6.3, Figure 6.12) with three different peptide sequences (Table 6.4). With all three peptide sequences, the catalytic efficiencies for demalonylation and desuccinylation were

much (29 to >1000 fold) higher than that for deacetylation (Table 6.3).

Table 6.3 The kinetic parameters of Sirt5 on acetyl, malonyl, and succinyl peptides with different sequences.

Peptide		k_{cat} (s^{-1})	K_m **for peptide** (μM)	k_{cat}/K_m ($s^{-1}M^{-1}$)
H3 K9 (4-13+WW*)	**deacetylation**	ND	ND (>750)	7.8
	demalonylation	0.037 ± 0.003	6.1 ± 2.8	6.1×10^3
	desuccinylation	0.025 ± 0.002	5.8 ± 2.7	4.3×10^3
GDH K503 (498-509+WW*)	**deacetylation**	ND	ND (>750)	<2**
	demalonylation	0.014 ± 0.001	8.7 ± 1.3	1.6×10^3
	desuccinylation	0.028 ± 0.002	14 ± 4	2.0×10^3
ACS2 K628 (623-632+WW*)	**deacetylation**	ND	ND (>750)	18
	demalonylation	0.079 ± 0.008	150 ± 40	5.2×10^2
	desuccinylation	0.268 ± 0.051	450 ± 150	6.0×10^2

* Two tryptophan residues were added at the C-terminal of the peptide to facilitate the detection by UV-Vis absorption during the HPLC assay.

** No activity. The value was estimated based on the detection limit.

ND: cannot be determined either because no activity was observed or because V versus [S] was linear (even the highest [S] of 750 μM used was much smaller than the K_m).

Table 6.4 Acetyl, thioacetyl, malonyl, and succinyl peptides used for Sirt5 crystallization and kinetics studies.

Protein/lysine residue	Peptide sequence	Predicted mass (m/z)	Observed mass $[M+H]^+$ (m/z)
Histone H3 K9 (4-15)	KQTAR**(TacK)**STGGKA	1290.7 $[M+H]^+$	1290.0 $[M+H]^+$
Histone H3 K9 (4-15)	KQTAR**(MaK)**STGGKA	1318.7 $[M+H]^+$	1317.7 $[M+H]^+$
Histone H3 K9 (4-15)	KQTAR**(SuK)**STGGKA	1332.7 $[M+H]^+$	1331.3 $[M+H]^+$
Histone H3 K9 (4-13)WW	KQTAR**(AcK)**STGGWW	724.4 $[M+2H]^{2+}$	724.7 $[M+2H]^{2+}$
Histone H3 K9 (4-13)WW	KQTAR**(MaK)**STGGWW	746.4 $[M+2H]^{2+}$	746.7 $[M+2H]^{2+}$
Histone H3 K9 (4-13)WW	KQTAR**(SuK)**STGGWW	753.4 $[M+2H]^{2+}$	753.7 $[M+2H]^{2+}$
GDH K503 (498-509)WW	SGASE(**AcK**)DIVHSGWW	800.9 $[M+2H]^{2+}$	801.2 $[M+2H]^{2+}$
GDH K503 (498-509)WW	SGASE(**MaK**)DIVHSGWW	822.9 $[M+2H]^{2+}$	823.1 $[M+2H]^{2+}$
GDH K503 (498-509)WW	SGASE(**SuK**)DIVHSGWW	829.9 $[M+2H]^{2+}$	830.2 $[M+2H]^{2+}$
ACS2 K628 (623-632)WW	KTRSG**(AcK)**VMRRWW	816.9 $[M+2H]^{2+}$	817.1 $[M+2H]^{2+}$
ACS2 K628 (623-632)WW	KTRSG**(MaK)**VMRRWW	838.9 $[M+2H]^{2+}$	839.1 $[M+2H]^{2+}$
ACS2 K628 (623-632)WW	KTRSG**(SuK)**VMRRWW	845.9 $[M+2H]^{2+}$	846.4 $[M+2H]^{2+}$

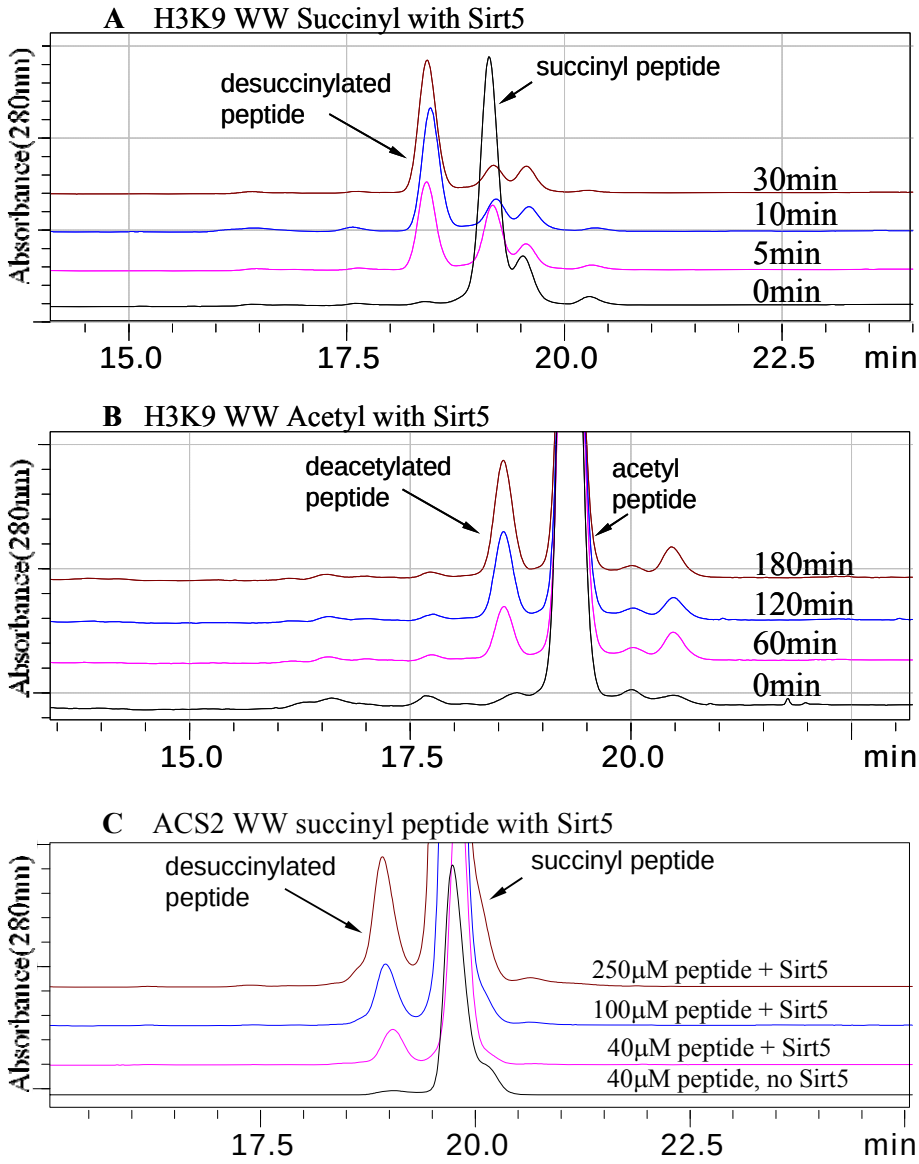

Figure 6.12 Time courses and sample HPLC traces from kinetic studies for Sirt5-catalyzed deacylation reactions. (**A**) Time course of Sirt5-catalyzed desuccinylation reaction using the H3K9 WW succinyl peptide. The desuccinylated peptide increased over time. The reaction was monitored at 280 nm. Most substrates were converted to products after 10 min. (**B**) Time course of Sirt5-catalyzed deacetylation reaction using the H3K9 WW acetyl peptide. The deacetylated peptide increased over time. The reaction was monitored at 280 nm. A very small percentage of substrate was converted to product even after 180 min. (**C**) Sample HPLC traces from Sirt5 kinetics studies.

A crystal structure of Sirt5 in complex with a succinyl peptide and NAD was obtained. The structure (Figure 6.13) showed that the carboxylate from succinyl interacted with Tyr102 and Arg105, consistent with what was predicted based on the structure of Sirt5 with CHES bound (Figure 6.4). Changing Arg105 to Met or Tyr102 to Phe significantly increased the K_m for desuccinylation (Table 6.5). Thus, Tyr102 and Arg105 were important for binding succinyl and malonyl groups.

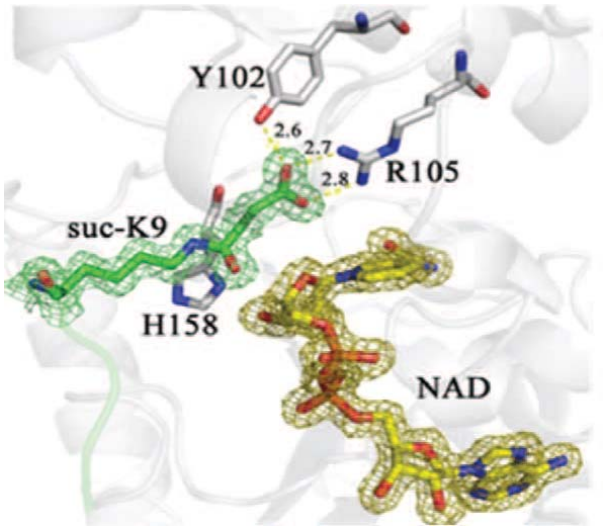

Figure 6.13 Sirt5-succinyl peptide-NAD ternary structure showing that the succinyl group interacted with Tyr102 and Arg105.

Table 6.5 The kinetic parameters of mutant Sirt5 on H3K9 acetyl and succinyl peptides

		k_{cat} (s^{-1})	K_m for peptide (μM)	k_{cat}/K_m ($s^{-1}M^{-1}$)
Sirt5	**deacetylation**	ND*	ND (> 750)*	2
	desuccinylation	0.029 ± 0.002	41 ± 11	710
Sirt5 H158Y	**deacetylation**	no activity observed	no activity observed	-
	desuccinylation	ND*	ND (> 750)*	75
Sirt5 Y102F	**deacetylation**	ND*	ND (> 750)*	2
	desuccinylation	ND*	ND (> 750)*	397
Sirt5 R105M	**deacetylation**	ND*	ND (> 750)*	0.5
	desuccinylation	ND*	ND (> 750)*	0.9

* The k_{cat} and K_m values cannot be determined because the V versus [S] plot is linear (K_m is much greater than the highest substrate concentration tested, 750 μM). Thus only k_{cat}/K_m value can be obtained.

We next determined whether lysine malonylation or succinylation exists *in vivo*. Lysine succinylation was reported to occur on *E. coli* homoserine trans-succinylase(*17*), but lysine malonylation has not been reported. We thought that detecting Sirt5-catalyzed formation of *O*-Ma-ADPR or *O*-Su-ADPR using ^{32}P-NAD could be a sensitive assay to detect the presence of malonyl or succinyl lysine. H3K9 acetyl, malonyl, and succinyl peptides were incubated with Sirt5 or Sirt1 in the presence of ^{32}P-NAD. The small molecule products were then separated by thin-layer chromatograph (TLC) and detected by autoradiography. With malonyl and succinyl peptides, Sirt5 consumed all the NAD molecules and new spots that corresponded to *O*-Ma-ADPR and *O*-Su-ADPR appeared (Figure 6.14). With the acetyl peptide, essentially no NAD was consumed by Sirt5 (Figure 6.14). Incubation of the acetyl peptide or calf thymus histones with Sirt1 produced *O*-Ac-ADPR (Figure 6.14). The *O*-Su-ADPR spot was separated from the *O*-Ac-ADPR and *O*-Ma-ADPR spots. Thus, Sirt5-catalyzed formation of *O*-Su-ADPR from the

hydrolysis of succinyl peptides could be detected using ^{32}P-NAD.

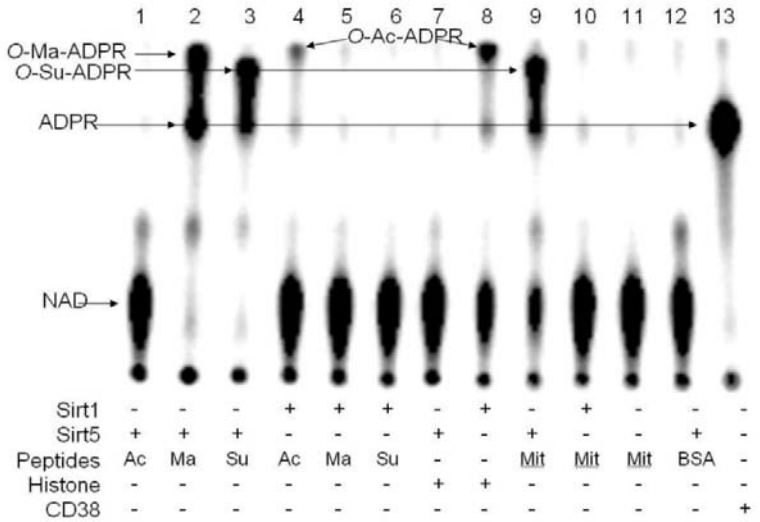

Figure 6.14 Succinyl lysine was detected in bovine liver mitochondria. Sirt5-catalyzed hydrolysis of malonyl and succinyl peptides could be detected using ^{32}P-NAD, which formed ^{32}P-labeled *O*-Ma-ADPR (lane 2) and *O*-Su-ADPR (lane 3). No reaction occurred with acetyl peptide (lane 1). The formation of *O*-Ac-ADPR catalyzed by Sirt1 was detected (lanes 4 and 8). *O*-Su-ADPR was formed when bovine liver mitochondria peptides were incubated with Sirt5 (lane 9), but not with Sirt1 (lane 10). The control with BSA peptides and Sirt5 did not generate *O*-Su-ADPR (lane 12). CD38-catalzyed hydrolysis of NAD was used to generate the standard ^{32}P-ADPR spot (lane 13).

The ^{32}P-NAD assay was then used to detect whether succinyl lysine was present in bovine liver mitochondrial proteins because Sirt5 is localized in mitochondria(*7*). When bovine liver mitochondrial peptides were treated with Sirt5 and ^{32}P-NAD, the formation of *O*-Su-ADPR was detected (Figure 6.14), suggesting that bovine liver mitochondrial proteins contained succinyl lysine. Control reactions with Sirt1, without sirtuins, or with BSA peptides did not produce *O*-Su-ADPR or *O*-Ac-ADPR (Figure 6.14).

LC-MS/MS identified succinyl lysine from three commercial mitochondrial enzymes purified

from animal tissues: glutamate dehydrogenase (GDH), malate dehydrogenase, and citrate synthase (Table 6.6 and 6.7). Thus, lysine succinylation occurs on mammalian mitochondrial proteins. Also, LC-MS/MS of commercial mitochondrial enzymes identified three and two malonyl lysine residues on GDH (Table 6.6) and malate dehydrogenase (Table 6.7), respectively. The tandem mass spectra confirmed the identities of the these peptides and modification sites. (see the online supplementary information http://www.sciencemag.org/content/suppl/2011/11/10/334.6057.806.DC1/Du-SOM.pdf). Thus, protein lysine malonylation exists in mammalian cells.

Table 6.6 Acetyl, malonyl, and succinyl GDH peptides identified by LC-MS/MS.

	Peptide sequence and modification
1	77-GASIVEDK(acetyl)LVEDLK-90
2	77-GASIVEDK(succinyl)LVEDLK-90
3	85-LVEDLK(acetyl)TR-92
4	108-IIK(acetyl)PCNHVLSLSFPIR-123
5	108-IIK(succinyl)PCNHVLSLSFPIR-123
6	152-YSTDVSVDEVK(acetyl)ALASLMTYK-171
7	152-YSTDVSVDEVK(acetyl)ALASLM(ox)TYK-171
8	152-YSTDVSVDEVK(succinyl)ALASLMTYK-171
9	172-CAVVDVPFGGAK(acetyl)AGVK-187
10	188-INPK(acetyl)NYTDNELEK-200
11	353-LQHGTILGFPK(acetyl)AK-363
12	353-LQHGTILGFPK(succinyl)AK-363
13	364-AK(acetyl)IYEGSILEVDCDILIPAASEK-386
14	366-IYEGSILEVDCDILIPAASEK(acetyl)QLTK-390
15	398-AK(acetyl)IIAEGANGPTTPEADK-415
16	398-AK(acetyl)IIAEGANGPTTPEADKIFLER-420
17	400- IIAEGANGPTTPEADK(acetyl)IFLER-420
18	400- IIAEGANGPTTPEADK(succinyl)IFLER-420
19	454-LTFK(acetyl)YER-460
20	454-LTFK(malonyl)YER-460
21	454-LTFK(succinyl)YER-460
22	478-FGK(acetyl)HGGTIPIVPTAEFQDR-496
23	497-ISGASEK(acetyl)DIVHSGLAYTMER-516
24	497-ISGASEK(malonyl)DIVHSGLAYTMER-516
25	497-ISGASEK(succinyl)DIVHSGLAYTMER-516
26	497-ISGASEK(succinyl)DIVHSGLAYTM(ox)ER-516
27	524-TAMK(acetyl)YNLGLDLR-535
28	524-TAM(ox)K(acetyl)YNLGLDLR-535
29	524-TAMK(malonyl)YNLGLDLR-535
30	524-TAMK(succinyl)YNLGLDLR-535
31	524-TAM(ox)K(succinyl)YNLGLDLR-535
32	536-TAAYVNAIEK(acetyl)VFR-548
33	536-TAAYVNAIEK(succinyl)VFR-548

Table 6.7 Acetyl, malonyl, and succinyl peptides identified on other metabolic enzymes

Proteins		Modified peptides
Malate dehydrogenase, mitochondrial	1	177-ANAFVAELK(acetyl)GLDPAR-191
	2	230-IQEAGTEVVK(succinyl)AK-241
	3	230-IQEAGTEVVK(malonyl)AK-241
	4	297-KGIEK(succinyl)NLGIGK-307
	5	298-GIEK(succinyl)NLGIGK-307
	6	302-NLGIGK(acetyl)ISPFEEK-314
	7	308-ISPFEEK(acetyl)M(ox)IAEAIPELK-324
	8	325-ASIK(acetyl)KGEEFVK-335
	9	325-ASIKK(malonyl)GEEFVK-335
	10	325-ASIK(succinyl)KGEEFVK-335
Citrate synthase, mitochondrial	1	74-GMK(acetyl)GLVYETSVLDPDEGIR-92
	2	74-GMK(succinyl)GLVYETSVLDPDEGIR-92
	3	74-GMK(succinyl)GLVYETSVLDPDEGIRFR-94

Sirt5 is known to regulate the activity of carbamoyl phosphate synthase 1 (CPS1)(*18*). We therefore sought to test whether CPS1 was a desuccinylation target of Sirt5. Trypsin-digested CPS1 peptides from bovine liver mitochondria contained succinyl lysine (Figure 6.15). To confirm that Sirt5's desuccinylase functions *in vivo*, a Sirt5 knockout (KO) mouse strain was generated using standard technology. Consistent with earlier reports(*18*), CPS1 activity was 15% higher in Sirt5 wt than in Sirt5 KO mice. Using MS, we identified three lysine residues of CPS1 that are both acetylated and succinylated: Lys44, Lys287, and Lys1291. For Lys44 and Lys287, the levels of acetylation and succinylation did not change in Sirt5 KO mice. For Lys1291, succinylation level increased 16 to >100-fold in Sirt5 KO mice compared with the level in wt mice (Figure 6.16). In contrast, acetylation levels of Lys1291 did not change in Sirt5 KO compared with wt (Figure 6.16). Thus, Sirt5 functions as a desuccinylase *in vivo*.

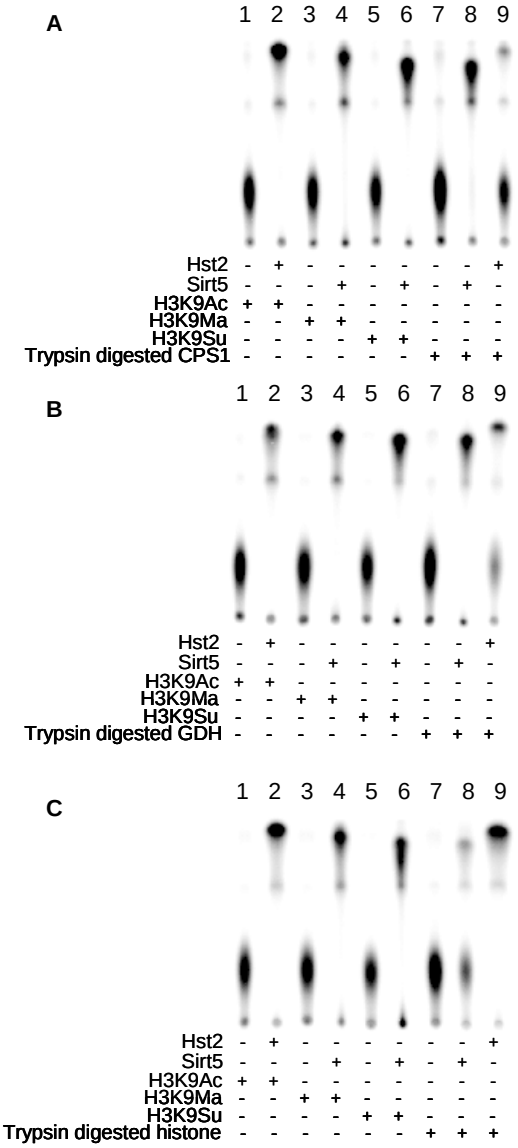

Figure 6.15 Succinyl lysine modification could be detected in CPS1 and GDH peptides. Different proteins were digested by trypsin and then incubated with ^{32}P-NAD and either Sirt5 or Hst2. For each panel, lane 1, 3 and 5 were negative controls without sirtuins. Lane 2, 4 and 6 were positive controls showing the positions of *O*-acetyl-, *O*-malonyl- and *O*-succinyl-ADP ribose on the TLC plate, respectively. Lane 7 was trypsin digested peptides without any sirtuin. Lane 8 and 9 were trypsin digested peptides treated with Sirt5 and Hst2 respectively. Lane 8 in all 3 samples showed the formation of *O*-Su-ADPR while lane 9 showed the formation of *O*-Ac-ADPR. The results showed that both CPS1 and GDH contain succinyl lysine modification. In contrast, very little succinyl lysine modification was detected on histone peptides.

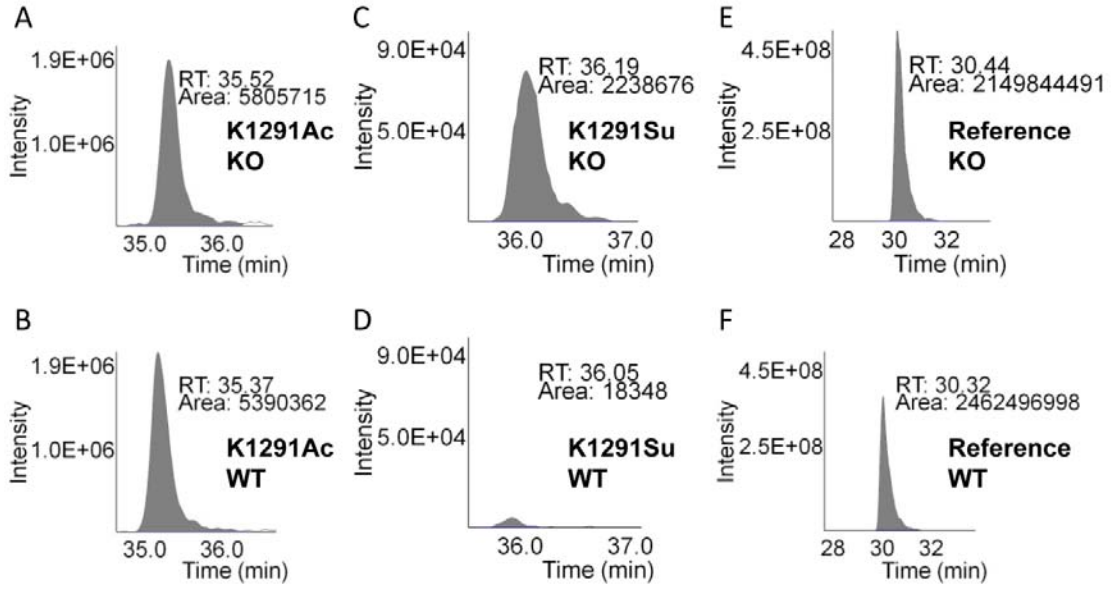

Figure 6.16 Relative quantitation analysis was achieved by extracted ion chromatograms (XICs) for peak areas of CPS1 K1291 acetyl peptides from Sirt5 KO (A) and wt mice (B); of CPS1 K1291 succinyl peptides from Sirt5 KO (C) and wt mice (D), and of a reference peptide from Sirt5 KO (E) and wt mice (F).

Here we have demonstrated that Sirt5 is an NAD-dependent demalonylase and desuccinylase. The demalonylase or desuccinylase activity is much higher than its deacetylase activity. The preference for negatively charged acyl groups can be explained by the presence of Tyr102 and Arg105 in the active site of Sirt5, which are conserved in most Class III sirtuins (Figure 6.17)(*6*). Presumably all Class III sirtuins with the conserved Arg and Tyr should have NAD-dependent desuccinylase and/or demalonylase activity.

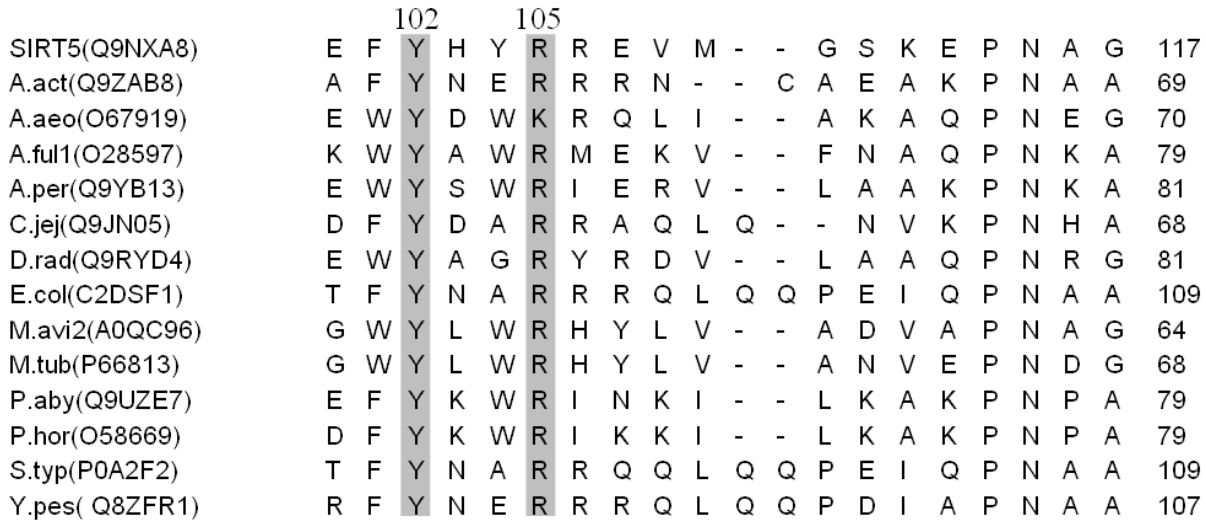

Figure 6.17 Tyr and Arg residues are conserved in most Class III sirtuins. The conservation of specific sequences motifs within the 14 Class III sirtuins were aligned and the conserved Tyr102 and Arg105 (Sirt5 numbering) residues are shaded.

We showed that lysine malonylation and succinylation occur on several mammalian proteins. Protein lysine succinylation has been observed recently in bacteria(*19*). Protein lysine malonylation has not been reported previously.

Acetylation occurs on numerous metabolic enzymes and regulates their activities in mammals and bacteria(*20, 21*). Given that succinyl-CoA and malonyl-CoA are common metabolites like acetyl-CoA(*14*), and all the succinylated and malonylated proteins we found are metabolic enzymes, it is likely that protein lysine succinylation and malonylation function similarly to acetylation and regulate metabolism(*20, 21*).

Methods

Reagents and Instrumentation.

Reagents were obtained from Aldrich or Acros in the highest purity available and used as supplied. ^{1}H NMR, ^{13}C NMR and 2D NMR were performed on INOVA 500 spectrometer. NMR data was analyzed by MestReNova (version 5.2.5). LCMS was carried out on a SHIMADZU LC-MS-QP8000α with a Sprite TARGA C18 column (40 × 2.1 mm, 5 μm, Higgins Analytical, Inc., Mountain View, CA) monitoring at 215 and 260 nm. Solvents used in LC-MS were water with 0.1% formic acid and acetonitrile with 0.1% formic acid.

Synthesis of Fmoc-Lys(*t*Bu-malonyl)-OH and Fmoc-Lys(*t*Bu-succinyl)-OH.

Mono-*t*butyl-malonate (480 mg, 3.0 mmol) or mono-*t*butyl-succinate (522.0 mg, 3 mmol) in anhydrous N,-N'-dimethylformamide (DMF, 2.0 mL) was added N-hydroxysuccinimide (334 mg, 2.9 mmol) with stirring at room temperature. Then N,N'-dicyclohexylcarbodiimide (598 mg, 2.9 mmol) in anhydrous DMF (3.0 mL) was added to the reaction. After stirring for 2 h, the reaction mixture was filtered. The filtrate was added to a solution of Fmoc-Lys-OH (736 mg, 2.0 mmol) with N, N-diisopropylethylamine (DIEA, 1.0 mL, 5.8 mmol) in anhydrous DMF (2.0 mL) at room temperature. The resulting reaction mixture was stirred for another 30 min. Then the reaction mixture was added 10 mL water and 6 mL 1 M HCl to adjust pH to 2~3. The mixture was extracted three times by 100 mL ethyl acetate and washed twice with 50 mL brine. The organic layer was dried with anhydrous sodium sulfate. After removal of the solvents *in vacuo*, the residue was purified by silica gel column using 10:1 CH_2Cl_2:CH_3OH to give the desired product in about 90% yield.

Fmoc-Lys(tBu-Malonyl)-OH. ^{1}H NMR (500 MHz, DMSO-d_6): δ 8.01 (t, 1H, *J* = 5.5 Hz), 7.89 (d, 2H, *J* = 7.0 Hz), 7.73 (dd, 2H, *J* = 2.0, 7.0 Hz), 7.46 (d, 1H, *J* = 7.0 Hz), 7.41 (t, 2H, *J* = 7.5 Hz), 7.33 (t, 2H, *J* = 7.8 Hz), 4.27 (m, 2H), 4.23 (m, 1H), 3.87 (dt, 1H, *J* = 4.5, 8.5 Hz), 3.07 (s, 2H), 3.03 (m, 2H), 1.65 (m, 2H), 1.39 (m, 2H), 1.38 (s, 9H), 1.33 (m, 2H). ^{13}C NMR (125 MHz, DMSO-d_6): δ 174.26, 167.29, 165.24, 156.08, 143.91, 143.84, 140.75, 140.73, 127.66, 127.11, 125.33, 120.15, 120.14, 80.40, 80.39, 65.57, 54.10, 46.70, 43.74, 38.51, 30.74, 28.65, 27.70, 23.02. LC-MS (ESI) calcd. for $C_{28}H_{35}N_2O_7$ [M+H$^+$] 511.3, obsd. 510.8.

Fmoc-Lys(tBu-Succinyl)-OH. ^{1}H NMR (500 MHz, CD_3OD): δ 7.75 (d, 2H, *J* = 8.0 Hz), 7.61 (dd, 2H, *J* = 4.5, 7.5 Hz), 7.35 (t, 2H, *J* = 7.3 Hz), 7.26 (t, 2H, *J* = 7.3 Hz), 4.30 (m, 2H), 4.15 (t, 1H, *J* = 7.0 Hz), 4.04 (dd, 1H, *J* = 4.5, 8.0 Hz), 3.14 (t, 2H, *J* = 7.0 Hz), 2.49 (t, 2H, *J* = 7.0 Hz), 2.38 (t, 2H, *J* = 7.3 Hz), 1.75 (m, 2H), 1.49 (m, 2H), 1.40 (s, 9H), 1.37 (m, 2H). ^{13}C NMR (125 MHz, CD_3OD): δ 180.22, 174.46, 173.72, 158.64, 145.49, 145.28, 142.69, 142.68, 128.91, 128.29, 126.38, 126.35, 121.07, 81.81, 67.97, 57.11, 48.54, 40.37, 33.23, 31.93, 31.87, 30.17, 28.48, 24.32. LC-MS (ESI) calcd. for $C_{29}H_{37}N_2O_7$ [M+H$^+$] 525.3, obsd. 524.8.

Cloning, expression and purification of human Sirtuins

Human Sirt1, 2, 3, 5, and 6 were expressed as previously described(*22*). Human *Sirt7* coding sequence was PCR-amplified using primers JT072 (5'-AGTCAGGAATTCATGGCAGCCGGGGGTCT-3') and JT073 (5'-AGTCAGCTCGAGTTACGTCACTTTCTTCCTTTTT-3'). Amplified product was digested with EcoRI and XhoI. The digested PCR product was purified and ligated into the similarly digested

expression vector pET28a. C-terminal Flag-tagged *Sirt5* (*Flag-Sirt5*) and truncated *Sirt5(34-302)* were cloned using TOPO and Gateway cloning technology (Invitrogen Corp., Carlsbad, CA) into pDEST-F1 for expression. Sirt7, Flag-Sirt5 and Sirt5(34-302) were expressed in *E. coli* and purified as described. After purification, Flag-Sirt5 and Sirt5(34-302) were digested by TEV at room temperature for 2 h and purified by HisTrap^{TM} HP Column (GE Healthcare, Piscataway, NJ) and gel filtration on a HiLoad 26/60 Superdex 75 prep grade column (GE Healthcare, Piscataway, NJ). Protein concentrations were determined by Bradford reagent.

Sirt5 X-ray diffraction data collection and structural refinement.

Sirt5-H3K9 thioacetyl peptide and Sirt5-H3K9 succinyl peptide were prepared at a 1:20 protein:peptide molar ratio and incubated for 30~60 min on ice. Crystals were grown by the method of hanging drop vapor diffusion. Sirt5-H3K9 succinyl peptide co-crystals were soaked in 10 mM NAD for 10~120 min before data collection. All the X-ray diffraction data were collected at CHESS (Cornell High Energy Synchrotron Source) A1 or F1 station. The data were processed using the programs HKL2000. The two structures of Sirt5 complexes were solved by molecular replacement using the program Molrep from the CCP4 suite of programs. The Sirt5-ADPR structure (PDB code: 2B4Y) was served as the searching template. Refinement and model building were performed with REFMAC5 and COOT from CCP4.

Synthesis of acetyl, thioacetyl, malonyl, and succinyl peptides

Acetyl, thioacetyl, malonyl and succinyl peptides were synthesized on Wang resin using standard Fmoc/*t*Bu chemistry *O*-benzotriazol-*N*,*N*,*N*',*N*'-tetramethyluronium hexafluorophosphate/1-

hydroxybenzotriazol (HBTU/HOBt) protocol(*22*). Modified lysine was incorporated using Fmoc-Lys(acetyl)-OH, Fmoc-Lys(thioacetyl)-OH, Fmoc-Lys(*t*Bu-malonyl)-OH and Fmoc-Lys(*t*Bu-succinyl)-OH. Cleavage from the resin and removal of all protecting groups were done by incubating the resin with trifluoroacetic acid (TFA) containing phenol (5%), thioanisole (5%), ethanedithiol (2.5%), and water (5%) for 2 h. The crude peptides were purified by reverse phase HPLC on BECKMAN COULTER System Gold 125P solvent module & 168 Detector with a TARGA C18 column (250 × 20 mm, 10 μm, Higgins Analytical, Inc., Mountain View, CA) monitoring at 215 nm. Mobile phases used were 0.1% aqueous TFA (solvent A) and 0.1% TFA in acetonitrile (solvent B). Peptides were eluted with a flow rate of 10 mL/min with the following gradient: 0% solvent B for 5 min, then 0 % to 25% solvent B over 25 min. The identity and purity of the peptides were verified by LC-MS. Table 6.1 and 6.4 listed the synthetic peptides.

Deacetylation, demalonylation, and desuccinylation activity assay and determination of k_{cat} and K_m.

The deacylase activity of human Sirt1, Sirt2, Sirt3, Sirt5, Sirt6 and Sirt7 were measured by detecting the deacylated peptide from the acyl peptides (Table 6.1 and 6.4) using LC-MS. Purified sirtuin was incubated with 0.3 mM acyl peptides, 1.0 mM NAD in 20 mM Tris-HCl buffer (pH 7.5) containing 1 mM DTT in 60 μL reactions for 2 h at 37°C. The reactions were stopped with 60 μL 10% TFA and analyzed by LC-MS.

For determination of k_{cat} and K_m, human Sirt1, Sirt2, Sirt3 and Sirt5 were measured by detecting the deacylated peptide from H3K9 acyl peptides using HPLC. Purified sirtuin was incubated with

1.0 mM of NAD in 20 mM Tris-HCl buffer (pH 7.5) containing acyl peptides (0–750 μM) and 1 mM DTT in 60 μL reactions at 37°C. The reactions were stopped with 100 mM HCl and 160 mM acetic acid, analyzed by HPLC with a reverse phase C18 column (250 × 4.6 mm, 90 A, 10 μm, GraceVydac, Southborough, MA), with a linear gradient of 0% to 20% B for 10 min (1 mL/min). Product quantification was based on the area of absorption monitored at 215 nm, assuming hydrolysis of the acyl group does not affect the absorption. The k_{cat} and K_m values were obtained by curve-fitting the $V_{initial}$/[E] versus [S] plot using KaleidaGraph. For Sirt5 R105M, the observed second order rate constant, k_{obs} (rate/([Sirtuin][NAD])) was detected instead of k_{cat} and K_m because of the very weak deacylation activity. The experiments were done in duplicate.

For comparing the deacetylation, demalonylation and desuccinylation activities of Sirt5 on different peptide backbones (results shown in Table 6.3), histone H3, GDH and ACS2 peptides with two tryptophan residues at the C-terminal were used to allow better detection and quantification on HPLC. The peptide sequences were listed in Table 6.4. The determination of k_{cat} and K_m was carried out essentially the same as mentioned above with slight modifications. The reactions were quenched with 60 μL 10% TFA. The chromatography gradient was 0% to 50% B for 20 min (1 mL/min). The peptides were detected and quantified on the LC by the absorption at 280 nm.

Detection of succinyl lysine from bovine liver mitochondrial proteins using the ^{32}P-NAD assay.

Bovine liver mitochondria was isolated as previously described. Mitochondria from 5 g bovine liver was lysed for 30 min at 4°C in ice-cold lysis buffer (25 mM Tris-HCl pH 8.0, 50 mM NaCl, 0.1% Triton X-100) containing protease cocktail inhibitor (P8340, Sigma). The supernatants were collected and exchanged to 25 mM Tris-HCl (pH 8.0) with 50 mM NaCl using centrifugal filter (MILLIPORE, Billerica, MA) to remove endogenous NAD. The extracts were stored at -80°C. For trypsin digestion, 1.5 mg of the bovine liver mitochondria proteins or BSA (used as the control) was dissolved in 6 M urea, 60 mM Tris-HCl (pH 8.0), 15 mM DTT in a reaction volume of 450 μL. The solution was heated at 95°C for 15 min and then cooled to room temperature. Then 22.5 μL of 1M iodoacetamide (final concentration ~50 mM) was added and the mixture was incubated at room temperature with gentle mixing for 1 h. Then 3.6 mL of 50 mM Tris-HCl (pH 7.4) with 1 mM $CaCl_2$ was added to the reaction mixture to lower the urea concentration to 0.75 M. Finally, 150 μL of 100 μg/mL modified trypsin (Promega Corporation, Madison, WI) were added and the reaction mixture was incubated at 37 °C for 12 h. After quenching the reaction by adding 65 μL 10% TFA to pH 2~3, the digested peptides were desalted by using Sep-Pak C18 cartridge 1cc/50 mg (Waters Corporation, Milford, MA) and lyophilized.

To detect the acyl-ADPR compounds formed in sirtuin-catalyzed deacylation reactions, reactions were performed in 10 μL solutions with 1 μCi ^{32}P-NAD (ARC Inc., ARP 0141, 800Ci/mmol, 0.125μM), 50 mM Tris-HCl pH 8.0, 150 mM NaCl, 10 mM DTT. The acyl peptide substrates used were 100 μM H3K9 acetyl, malonyl, or succinyl peptide, 2 μg calf thymus histones (Roche Applied Science, Indianapolis, IN), 20 μg bovine liver mitochondrial peptides, or 20 μg BSA peptides. The reactions were incubated with 1 μM Sirt5 or Sirt1 at 37°C for 1 h. CD38 catalytic

domain was used to generate ADPR as a control. A total of 0.5 μL of each reaction were spotted onto silica gel TLC plates and developed with 7:3 ethanol:ammonium bicarbonate (1 M aqueous solution). After development, the plates were air-dried and exposed to a PhosphorImaging screen (GE Healthcare, Piscataway, NJ). The signal was detected using a STORM860 phosphorimager (GE Healthcare, Piscataway, NJ).

Detection of lysine succinylation on CPS1 peptides using the ^{32}P-NAD assay

The CPS1 band was cut from a SDS-PAGE gel of the bovine liver mitochondria lysate. The protein was in-gel digested with trypsin and extracted and desalted as the following. The gel band was washed in 100 μL water for 5 min, followed by 100 μL 100 mM Ammonium bicarbonate : acetonitrile (1:1) for 10 min and finally 50 μL acetonitrile for 5 min. The acetonitrile was then discarded and the gel band was allowed to dry in the ventilated fume hood for 5-10 min. The gel slice was then rehydrated with 15 μL trypsin solution (10 μg/mL modified trypsin in 1mM HCl) on ice for 30 min. The trypsin solution was topped with 10 μL 50 mM Ammonium bicarbonate with 10% acetonitrile. The digestion reactions were kept at 30°C for 12 h. The resulting solution was acidified with formic acid (1% in final). The trypsin digested peptides were extracted twice with 30 μl of 50% acetonitrile with 0.2% TFA (45 min incubation at room temperature followed by 5 min sonication). The third extraction was done with 30 μl of 90% acetonitrile with 0.2% TFA (5 min). All the extracts were combined and lyophilized. When dried, the peptides were dissolved in 12 μl of 0.1% TFA and desalted by ZipTips (Millipore, Bedford, Massachusetts). The desalted peptides were lyophilized again and reconstituted in water. The GDH peptides from

in-gel digestion and the histone peptides from in-solution digestion were prepared as described above. The ^{32}P-NAD assays were carried out as described above. To lower the detection limit, higher concentrations of sirtuins were used. The Sirt5 was used at a final concentration of 52 μM and the Hst2 was used at 24 μM. The sample peptides were used at a concentration of 0.3 μg/μl and the control peptides were at 20 μM.

Generation of Sirt5 deficient mouse line

Sirt5 +/+ and -/- mice were generated at the Institut Clinique de la Souris (Strasbourg, France). Briefly, exon 4 of Sirt5 locus was flanked with *loxP* sites using standard genetic engineering and gene targeting procedures. The resulting Sirt5 floxed mice were bred with CMV-Cre transgenic mice to generate germline Sirt5 deficient (Sirt5 -/-) mice and control Sirt5 +/+ mice. The absence of Sirt5 mRNA in different tissues of Sirt5 -/- mice was confirmed by Q-RT-PCR analysis and the loss of Sirt5 protein expression was verified by western blot using an anti-Sirt5 antibody (Abcam ab62740)

Preparation of liver lysate from Sirt5 wt and KO mouse

The 29-week-old male Sirt5 +/+ and -/- littermates were fasted overnight (from 6:00 PM to 10:00 AM) and then provided with free access to food for four hours prior to sacrifice. Liver tissues were rapidly removed, snap-frozen with liquid nitrogen, and stored at -80°C for analysis. The liver samples were first broken into small pieces, and then homogenized in 1mL of the lysis buffer (50 mM Tris-HCl pH 8.0, 150 mM NaCl, 2 mM EDTA, 0.1% NP-40, 10% glycerol). The crude lysates were incubated at 4°C on shaker for 30 min then centrifuged at 10 000 g, 4°C

for 10 min. The concentration of the lysate was determined by Bradford assay.

CPS1 activity assay

CPS1 activities assay was carried out as described by Fahien and Cohen(*23*). The reaction was initiated by addition of the liver lysates to the rest of the reaction mixture. The reaction mixture contained 50mM Tris-HCl pH 8.0, 2.5 mM phosphoenopyruvate, 0.2 mM NADH, 30 mM NH_4Cl, 100 mM $KHCO_3$, 5 mM ATP, 10 mM MgSO4, 10 mM N-acetylglutamate, 15 U/ml pyruvate kinase / lactate dehydrogenase (SIGMA P0294). The reactions were performed at 37 degree and the decrease in absorbance at 340 nm was monitored. The initial velocity of the reaction was calculated to get the CPS1 activity. The activity assay was done with three pairs of Sirt5 wt and KO mice.

Digestion of selected proteins for nano LC-MS/MS analysis

Commercial GDH (Sigma G2626), malate dehydrogenase (Sigma M2634), citrate synthase (Sigma C3260), and pyruvate dehydrogenase (Sigma P7032) were in-solution digested with trypsin. Typically, 1.0 mg of the protein was dissolved in 6 M guanidine hydrochloride, 150 mM Tris-HCl (pH 8.0), 15 mM DTT in a reaction volume of 400 μL. The solution was incubated at room temperature for 60 min. Then 20 μL of 1M iodoacetamide (final concentration ~50 mM) was added and the mixture was incubated at room temperature with gentle mixing for another 60 min. The excess iodoacetamide was quenched with 40mM DTT. Then 3.6 mL of 50 mM Tris-HCl (pH 7.4) with 1 mM $CaCl_2$ was added to the reaction mixture to lower the guanidine hydrochloride concentration to 0.6 M. Finally, 100 μL of 100 μg/mL modified trypsin (Promega

Corporation, Madison, WI) were added and the reaction mixture was incubated at 37 °C for 12 h. After quenching the reaction by adding 65 μL 10% TFA to pH 2~3, the digested peptides were desalted by using Sep-Pak C18 cartridge 1cc/50 mg (Waters Corporation, Milford, MA) and lyophilized prior to nanoLC-MS/MS analysis.

Identification of protein acylation by nanoLC-MS/MS analyses.

The tryptic digest was reconstituted in 50 μL of 2% acetonitrile with 0.5% formic acid and about 200 ng of tryptic digest were injected for nanoLC-ESI-MS/MS analysis. The initial analysis was performed in UltiMatePlus nanoLC (Dionex, Sunnyvale, CA) coupled with to a hybrid triple quadrupole linear ion trap mass spectrometer, 4000 Q Trap from ABI/MDS Sciex (Framingham, MA) equipped with Micro Ion Spray Head II ion source. Most of final analyses were carried out using UltiMate3000 nanoLC (Dionex, Sunnyvale, CA) coupled with a LTQ Orbitrap Velos (Thermo-Fisher Scientific, San Jose, CA) mass spectrometer equipped with "Plug and Play" nano ion source device (CorSolutions LLC, Ithaca, NY).

Tryptic peptides were separated on a PepMap C-18 RP nano column (5 μm, 75 μm i.d. × 150 mm, Dionex), eluted in a 60 to 90-minute gradient of 10% to 40% acetonitrile in 0.1% formic acid at 300 nL/min. For 4000 Q Trap analysis, MS data acquisition was acquired using Analyst 1.4.2 software (AB SCIEX, Framingham, MA) in the positive ion mode for information dependent acquisition (IDA) analysis with nanospray voltage at 1.85 kV and heated interface at 150°C used for all experiments. In IDA analysis, after each survey and an enhanced resolution scan, three highest intensity ions with multiple charge states were selected for tandem MS (MS/MS) with

rolling collision energy applied for detected ions based on different charge states and *m/z* values. For Orbitrap analysis, each of tryptic digests was first acquired at CID-based parallel data-dependent acquisition (DDA) mode where FT mass analyzer was used for an MS survey scan followed by MS/MS scans on top 7 most intensity peaks with multiple charged ions above a threshold ion count of 5000 in LTQ mass analyzer. A time-based target acylated peptide inclusion list was then generated based on the preliminary results from CID mode. Finally HCD-based DDA mode with inclusion list was applied for confirmation of acylation modification, where one FT survey scan was followed by 5 MS/MS scan in FT analyzer. MS survey scans and MS/MS scans were acquired at a resolution of 60,000 and 7,500 (fwhm at *m/z* 400) respectively. The nano ion source was operated in positive ion mode with a voltage set at 1.5 kV and ion transfer tubing temperature at 225 °C. Either internal calibration using a background ion signal at m/z 445.120025 as a lock mass or external calibration using Ultramark 1621 for FT mass analyzer was performed. The normalized collision energy for CID and HCD were set at 35 % and 38% respectively. All data were acquired under Xcalibur 2.1 operation software (Thermo-Fisher Scientific).

Data analysis.

The MS/MS data generated from both 4000 Q Trap and LTQ Orbitrap Velos were submitted to Mascot 2.3 (Matrix Science, Boston, MA) for database searching using in-house licensed Mascot local server and the search was performed to query to SwissProt database (taxonomy: mammal) with three missed cleavage sites by trypsin allowed. The peptide tolerance was set to 1.2 Da and

MS/MS tolerance was set to 0.6 Da for the data from 4000 Q Trap. For Orbitrap data, the peptide tolerance was set to 10 ppm and MS/MS tolerance was set to 0.6 Da (for MS/MS spectra acquired by LTQ) and 0.05 Da (MS/MS spectra acquired by Orbitrap FT mass analyzer). A fixed carbamidomethyl modification of cysteine and several variable modifications on lysine acetylation, malonylation, succinylation, and carbamylation, deamidation of asparagine and glutamine, and methionine oxidation were applied. Only significant scores for the peptides defined by Mascot probability analysis (www.matrixscience.com/help/scoring_help.html#PBM) greater than "identity" were considered for the peptide identification and modification site determinations. All MS/MS spectra for the identified peptides with acylation modifications were manually inspected and validated using both Proteome Discoverer 1.2 and Xcalibur 2.1 software (Thermo-Fisher Scientific, San Jose, CA).

Relative quantitation of acylated peptides by nanoLC-MS/MS analysis

For relatively quantitative analysis of acylated peptides across samples, the peak areas of detected precursor ions at each specific m/z corresponding to the acylated peptides were determined by extracted ion chromatogram (XIC). The XIC of two independent (non-target), tryptic peptides identified from the same proteins in the same LC-MS/MS runs were also used as reference control for normalization of loaded sample digests. Specifically, we acquired nanoLC-MS/MS files in triplicate by Orbitrap at HCD mode as described above for identification of acylated peptides. The peak area of target acylated peptides in one LC-MS/MS data file was first extracted using Xcalibur 2.1 software with mass tolerance at 5ppm and mass precision at 4 decimal. A

layout template file was then generated and applied to all LC-MS/MS data files yielding peak area of all peptides of interest. Finally, peak area of each acylated peptide in each protein was normalized to the peak areas of the two reference peptides in each LC/MS/MS data file. The relative standard deviation (RSD) for most acylated peptides in three XIC measurements is less than 20%.

REFERENCES

1. Sauve, A. A., Wolberger, C., Schramm, V. L., and Boeke, J. D. (2006) The biochemistry of sirtuins, in *Annual Review of Biochemistry*, pp 435-465.

2. Imai, S.-i., and Guarente, L. (2010) Ten years of NAD-dependent SIR2 family deacetylases: implications for metabolic diseases, *Trends in Pharmacological Sciences 31*, 212-220.

3. Haigis, M. C., and Sinclair, D. A. (2010) Mammalian Sirtuins: Biological Insights and Disease Relevance, in *Annual Review of Pathology-Mechanisms of Disease*, pp 253-295.

4. Imai, S., Armstrong, C. M., Kaeberlein, M., and Guarente, L. (2000) Transcriptional silencing and longevity protein Sir2 is an NAD-dependent histone deacetylase, *Nature 403*, 795-800.

5. Tanner, K. G., Landry, J., Sternglanz, R., and Denu, J. M. (2000) Silent information regulator 2 family of NAD-dependent histone/protein deacetylases generates a unique product, 1-O-acetyl-ADP-ribose, *Proceedings of the National Academy of Sciences of the United States of America 97*, 14178-14182.

6. Frye, R. A. (2000) Phylogenetic classification of prokaryotic and eukaryotic Sir2-like proteins, *Biochemical and Biophysical Research Communications 273*, 793-798.

7. Michishita, E., Park, J. Y., Burneskis, J. M., Barrett, J. C., and Horikawa, I. (2005) Evolutionarily conserved and nonconserved cellular localizations and functions of human SIRT proteins, *Molecular Biology of the Cell 16*, 4623-4635.

8. Haigis, M. C., Mostoslavsky, R., Haigis, K. M., Fahie, K., Christodoulou, D. C., Murphy, A. J., Valenzuela, D. M., Yancopoulos, G. D., Karow, M., Blander, G., Wolberger, C., Prolla, T. A., Weindruch, R., Alt, F. W., and Guarente, L. (2006) SIRT4 inhibits glutamate dehydrogehase and opposes the effects of calorie restriction in pancreatic beta cells, *Cell 126*, 941-954.

9. Schuetz, A., Min, J., Antoshenko, T., Wang, C.-L., Allali-Hassani, A., Dong, A., Loppnau, P., Vedadi, M., Bochkarev, A., Sternglanz, R., and Plotnikov, A. N. (2007) Structural basis of inhibition of the human NAD(+)-dependent deacetylase SIRT5 by suramin, *Structure 15*, 377-389.

10. Liszt, G., Ford, E., Kurtev, M., and Guarente, L. (2005) Mouse Sir2 homolog SIRT6 is a nuclear ADP-ribosyltransferase, *Journal of Biological Chemistry 280*, 21313-21320.

11. Michishita, E., McCord, R. A., Berber, E., Kioi, M., Padilla-Nash, H., Damian, M., Cheung, P., Kusumoto, R., Kawahara, T. L. A., Barrett, J. C., Chang, H. Y., Bohr, V. A., Ried, T., Gozani, O., and Chua, K. F. (2008) SIRT6 is a histone H3 lysine 9 deacetylase that modulates telomeric chromatin, *Nature 452*, 492-U416.

12. Cosgrove, M. S., Bever, K., Avalos, J. L., Muhammad, S., Zhang, X. B., and Wolberger, C. (2006) The structural basis of sirtuin substrate affinity, *Biochemistry 45*, 7511-7521.

13. Hoff, K. G., Avalos, J. L., Sens, K., and Wolberger, C. (2006) Insights into the sirtuin mechanism from ternary complexes containing NAD(+) and acetylated peptide, *Structure 14*, 1231-1240.

14. Gao, L., Chiou, W., Tang, H., Cheng, X., Camp, H. S., and Burns, D. J. (2007)

Simultaneous quantification of malonyl-CoA and several other short-chain acyl-CoAs in animal tissues by ion-pairing reversed-phase HPLC/MS, *Journal of Chromatography B-Analytical Technologies in the Biomedical and Life Sciences 853*, 303-313.

15. Kim, K. H. (1997) Regulation of mammalian acetyl-coenzyme A carboxylase, *Annual Review of Nutrition 17*, 77-99.

16. Saggerson, D. (2008) Malonyl-CoA, a key signaling molecule in mammalian cells, in *Annual Review of Nutrition*, pp 253-HC253.

17. Rosen, R., Becher, D., Buttner, K., Biran, D., Hecker, M., and Ron, E. Z. (2004) Probing the active site of homoserine trans-succinylase, *Febs Letters 577*, 386-392.

18. Nakagawa, T., Lomb, D. J., Haigis, M. C., and Guarente, L. (2009) SIRT5 Deacetylates Carbamoyl Phosphate Synthetase 1 and Regulates the Urea Cycle, *Cell 137*, 560-570.

19. Zhang, Z., Tan, M., Xie, Z., Dai, L., Chen, Y., and Zhao, Y. (2011) Identification of lysine succinylation as a new post-translational modification, *Nature Chemical Biology 7*, 58-63.

20. Wang, Q., Zhang, Y., Yang, C., Xiong, H., Lin, Y., Yao, J., Li, H., Xie, L., Zhao, W., Yao, Y., Ning, Z.-B., Zeng, R., Xiong, Y., Guan, K.-L., Zhao, S., and Zhao, G.-P. (2010) Acetylation of Metabolic Enzymes Coordinates Carbon Source Utilization and Metabolic Flux, *Science 327*, 1004-1007.

21. Zhao, S., Xu, W., Jiang, W., Yu, W., Lin, Y., Zhang, T., Yao, J., Zhou, L., Zeng, Y., Li, H., Li, Y., Shi, J., An, W., Hancock, S. M., He, F., Qin, L., Chin, J., Yang, P., Chen, X., Lei, Q., Xiong, Y., and Guan, K.-L. (2010) Regulation of Cellular Metabolism by Protein

Lysine Acetylation, *Science 327*, 1000-1004.

22. Du, J., Jiang, H., and Lin, H. (2009) Investigating the ADP-ribosyltransferase activity of sirtuins with NAD analogues and 32P-NAD, *Biochemistry 48*, 2878-2890.

23. Fahien, L. A., and Cohen, P. P. (1964) A Kinetic Study of Carbamyl Phosphate Synthetase, *J Biol Chem 239*, 1925-1934.

APPENDIX A: PERMISSION FOR FULL PAPER REPRODUCTION

Chapter 2: Reprinted with permission from Su, XY et al. *J Am Chem Soc*. **2012** Jan 18; 134(2): 773-776

APPENDIX B: PERMISSION FOR FULL PAPER REPRODUCTION

Chapter 6: Reprinted with permission from Du, J et al. *Science*. **2011** Nov 11; 334(6057): 806-809

THE AMERICAN ASSOCIATION FOR THE ADVANCEMENT OF SCIENCE LICENSE TERMS AND CONDITIONS

Jan 19, 2013

This is a License Agreement between Xiaoyang Su ("You") and The American Association for the Advancement of Science ("The American Association for the Advancement of Science") provided by Copyright Clearance Center ("CCC"). The license consists of your order details, the terms and conditions provided by The American Association for the Advancement of Science, and the payment terms and conditions.

All payments must be made in full to CCC. For payment instructions, please see information listed at the bottom of this form.

License Number	3072161430547
License date	Jan 18, 2013
Licensed content publisher	The American Association for the Advancement of Science
Licensed content publication	Science
Licensed content title	Sirt5 Is a NAD-Dependent Protein Lysine Demalonylase and Desuccinylase
Licensed content author	Jintang Du, Yeyun Zhou, Xiaoyang Su, Jiu Jiu Yu, Saba Khan, Hong Jiang, Jungwoo Kim, Jimin Woo, Jun Huyn Kim, Brian Hyun Choi, Bin He, Wei Chen, Sheng Zhang, Richard A. Cerione, Johan Auwerx, Quan Hao, Hening Lin
Licensed content date	Nov 11, 2011

Volume number	334
Issue number	6057
Type of Use	Thesis / Dissertation
Requestor type	Author of the AAAS published paper
Format	Print and electronic
Portion	Full Text
Order reference number	
Title of your thesis / dissertation	THE DISCOVERY AND FUNCTIONAL STUDIES OF TWO DIPHTHAMIDE BIOSYNTHETIC GENES
Expected completion date	May 2013
Estimated size(pages)	180
Total	0.00 USD

Terms and Conditions

American Association for the Advancement of Science TERMS AND CONDITIONS

Regarding your request, we are pleased to grant you non-exclusive, non-transferable permission, to republish the AAAS material identified above in your work identified above, subject to the terms and conditions herein. We must be contacted for permission for any uses other than those specifically identified in your request above.

The following credit line must be printed along with the AAAS material: "From [Full Reference Citation]. Reprinted with permission from AAAS."

All required credit lines and notices must be visible any time a user accesses any part of the AAAS material and must appear on any printed copies and authorized user might make.

This permission does not apply to figures / photos / artwork or any other content or materials included in your work that are credited to non-AAAS sources. If the requested material is sourced to or references non-AAAS sources, you must obtain authorization from that source as well before using that material. You agree to hold harmless and indemnify AAAS against any claims arising from your use of any content in your work that is credited to non-AAAS sources.

If the AAAS material covered by this permission was published in Science during the years 1974 - 1994, you must also obtain permission from the author, who may grant or withhold permission, and who may or may not charge a fee if permission is granted. See original article for author's address. This condition does not apply to news articles.

The AAAS material may not be modified or altered except that figures and tables may be modified with permission from the author. Author permission for any such changes must be secured prior to your use.

Whenever possible, we ask that electronic uses of the AAAS material permitted herein include a hyperlink to the original work on AAAS's website (hyperlink may be embedded in the reference citation).

AAAS material reproduced in your work identified herein must not account for more than 30% of the total contents of that work.

AAAS must publish the full paper prior to use of any text.

AAAS material must not imply any endorsement by the American Association for the Advancement of Science.

This permission is not valid for the use of the AAAS and/or Science logos.

AAAS makes no representations or warranties as to the accuracy of any information contained in the AAAS material covered by this permission, including any warranties of

merchantability or fitness for a particular purpose.

If permission fees for this use are waived, please note that AAAS reserves the right to charge for reproduction of this material in the future.

Permission is not valid unless payment is received within sixty (60) days of the issuance of this permission. If payment is not received within this time period then all rights granted herein shall be revoked and this permission will be considered null and void.

In the event of breach of any of the terms and conditions herein or any of CCC's Billing and Payment terms and conditions, all rights granted herein shall be revoked and this permission will be considered null and void.

AAAS reserves the right to terminate this permission and all rights granted herein at its discretion, for any purpose, at any time. In the event that AAAS elects to terminate this permission, you will have no further right to publish, publicly perform, publicly display, distribute or otherwise use any matter in which the AAAS content had been included, and all fees paid hereunder shall be fully refunded to you. Notification of termination will be sent to the contact information as supplied by you during the request process and termination shall be immediate upon sending the notice. Neither AAAS nor CCC shall be liable for any costs, expenses, or damages you may incur as a result of the

termination of this permission, beyond the refund noted above.

This Permission may not be amended except by written document signed by both parties.

The terms above are applicable to all permissions granted for the use of AAAS material. Below you will find additional conditions that apply to your particular type of use.

FOR A THESIS OR DISSERTATION
If you are using figure(s)/table(s), permission is granted for use in print and electronic versions of your dissertation or thesis. A full text article may be used in print versions only of a dissertation or thesis.

Permission covers the distribution of your dissertation or thesis on demand by ProQuest / UMI, provided the AAAS material covered by this permission remains in situ.

If you are an Original Author on the AAAS article being reproduced, please refer to your License to Publish for rules on reproducing your paper in a dissertation or thesis.

FOR JOURNALS:
Permission covers both print and electronic versions of your journal article, however the AAAS material may not be used in any manner other than within the context of your article.

FOR BOOKS/TEXTBOOKS:
If this license is to reuse figures/tables, then permission is granted for non-exclusive world rights in all languages in both print and electronic formats (electronic formats are defined below).

If this license is to reuse a text excerpt or a full text article, then permission is granted for non-exclusive world rights in English only. You have the option of securing either print or electronic rights or both, but electronic rights are not automatically granted and do garner additional fees. Permission for translations of text excerpts or full text articles into other languages must be obtained separately.

Licenses granted for use of AAAS material in electronic format books/textbooks are valid only in cases where the electronic version is equivalent to or substitutes for the print version of the book/textbook. The AAAS material reproduced as permitted herein must remain in situ and must not be exploited separately (for example, if permission covers the use of a full text article, the article may not be offered for access or for purchase as a stand-alone unit), except in the case of permitted textbook companions as noted below.

You must include the following notice in any electronic versions, either adjacent to the reprinted AAAS material or in the terms and conditions for use of your electronic products: "Readers may view, browse, and/or download material for temporary copying purposes only, provided these uses

are for noncommercial personal purposes. Except as provided by law, this material may not be further reproduced, distributed, transmitted, modified, adapted, performed, displayed, published, or sold in whole or in part, without prior written permission from the publisher."

If your book is an academic textbook, permission covers the following companions to your textbook, provided such companions are distributed only in conjunction with your textbook at no additional cost to the user:

- Password-protected website
- Instructor's image CD/DVD and/or PowerPoint resource
- Student CD/DVD

All companions must contain instructions to users that the AAAS material may be used for non-commercial, classroom purposes only. Any other uses require the prior written permission from AAAS.

If your license is for the use of AAAS Figures/Tables, then the electronic rights granted herein permit use of the Licensed Material in any Custom Databases that you distribute the electronic versions of your textbook through, so long as the Licensed Material remains within the context of a chapter of the title identified in your request and cannot be downloaded by a user as an independent image file.

Rights also extend to copies/files of your Work (as described above) that you are required to provide for use by the visually and/or print disabled in compliance with state and federal laws.

This permission only covers a single edition of your work as identified in your request.

FOR NEWSLETTERS:
Permission covers print and/or electronic versions, provided the AAAS material reproduced as permitted herein remains in situ and is not exploited separately (for example, if permission covers the use of a full text article, the article may not be offered for access or for purchase as a stand-alone unit)

FOR ANNUAL REPORTS:
Permission covers print and electronic versions provided the AAAS material reproduced as permitted herein remains in situ and is not exploited separately (for example, if permission covers the use of a full text article, the article may not be offered for access or for purchase as a stand-alone unit)

FOR PROMOTIONAL/MARKETING USES:
Permission covers the use of AAAS material in promotional or marketing pieces such as

information packets, media kits, product slide kits, brochures, or flyers limited to a single print run. The AAAS Material may not be used in any manner which implies endorsement or promotion by the American Association for the Advancement of Science (AAAS) or Science of any product or service. AAAS does not permit the reproduction of its name, logo or text on promotional literature.

If permission to use a full text article is permitted, The Science article covered by this permission must not be altered in any way. No additional printing may be set onto an article copy other than the copyright credit line required above. Any alterations must be approved in advance and in writing by AAAS. This includes, but is not limited to, the placement of sponsorship identifiers, trademarks, logos, rubber stamping or self-adhesive stickers onto the article copies.

Additionally, article copies must be a freestanding part of any information package (i.e. media kit) into which they are inserted. They may not be physically attached to anything, such as an advertising insert, or have anything attached to them, such as a sample product. Article copies must be easily removable from any kits or informational packages in which they are used. The only exception is that article copies may be inserted into three-ring binders.

FOR CORPORATE INTERNAL USE:
The AAAS material covered by this permission may not be altered in any way. No additional printing may be set onto an article copy other than the required credit line. Any alterations must be approved in advance and in writing by AAAS. This includes, but is not limited to the placement of sponsorship identifiers, trademarks, logos, rubber stamping or self-adhesive stickers onto article copies.

If you are making article copies, copies are restricted to the number indicated in your request and must be distributed only to internal employees for internal use.

If you are using AAAS Material in Presentation Slides, the required credit line must be visible on the slide where the AAAS material will be reprinted

If you are using AAAS Material on a CD, DVD, Flash Drive, or the World Wide Web, you must include the following notice in any electronic versions, either adjacent to the reprinted AAAS material or in the terms and conditions for use of your electronic products: "Readers may view, browse, and/or download material for temporary copying purposes only, provided these uses are for noncommercial personal purposes. Except as provided by law, this material may not be further reproduced, distributed, transmitted, modified, adapted, performed, displayed, published, or sold in whole or in part, without prior written permission from the publisher." Access to any such CD, DVD, Flash Drive or Web page must be restricted to your organization's employees only.

FOR CME COURSE and SCIENTIFIC SOCIETY MEETINGS:
Permission is restricted to the particular Course, Seminar, Conference, or Meeting indicated in your

request. If this license covers a text excerpt or a Full Text Article, access to the reprinted AAAS material must be restricted to attendees of your event only (if you have been granted electronic rights for use of a full text article on your website, your website must be password protected, or access restricted so that only attendees can access the content on your site).

If you are using AAAS Material on a CD, DVD, Flash Drive, or the World Wide Web, you must include the following notice in any electronic versions, either adjacent to the reprinted AAAS material or in the terms and conditions for use of your electronic products: "Readers may view, browse, and/or download material for temporary copying purposes only, provided these uses are for noncommercial personal purposes. Except as provided by law, this material may not be further reproduced, distributed, transmitted, modified, adapted, performed, displayed, published, or sold in whole or in part, without prior written permission from the publisher."

FOR POLICY REPORTS:
These rights are granted only to non-profit organizations and/or government agencies. Permission covers print and electronic versions of a report, provided the required credit line appears in both versions and provided the AAAS material reproduced as permitted herein remains in situ and is not exploited separately.

FOR CLASSROOM PHOTOCOPIES:
Permission covers distribution in print copy format only. Article copies must be freestanding and not part of a course pack. They may not be physically attached to anything or have anything attached to them.

FOR COURSEPACKS OR COURSE WEBSITES:
These rights cover use of the AAAS material in one class at one institution. Permission is valid only for a single semester after which the AAAS material must be removed from the Electronic Course website, unless new permission is obtained for an additional semester. If the material is to be distributed online, access must be restricted to students and instructors enrolled in that particular course by some means of password or access control.

FOR WEBSITES:
You must include the following notice in any electronic versions, either adjacent to the reprinted AAAS material or in the terms and conditions for use of your electronic products: "Readers may view, browse, and/or download material for temporary copying purposes only, provided these uses are for noncommercial personal purposes. Except as provided by law, this material may not be further reproduced, distributed, transmitted, modified, adapted, performed, displayed, published, or sold in whole or in part, without prior written permission from the publisher."

Permissions for the use of Full Text articles on third party websites are granted on a case by case basis and only in cases where access to the AAAS Material is restricted by some means of password

or access control. Alternately, an E-Print may be purchased through our reprints department (brocheleau@rockwaterinc.com).

REGARDING FULL TEXT ARTICLE USE ON THE WORLD WIDE WEB IF YOU ARE AN 'ORIGINAL AUTHOR' OF A SCIENCE PAPER

If you chose "Original Author" as the Requestor Type, you are warranting that you are one of authors listed on the License Agreement as a "Licensed content author" or that you are acting on that author's behalf to use the Licensed content in a new work that one of the authors listed on the License Agreement as a "Licensed content author" has written.

Original Authors may post the 'Accepted Version' of their full text article on their personal or on their University website and not on any other website. The 'Accepted Version' is the version of the paper accepted for publication by AAAS including changes resulting from peer review but prior to AAAS's copy editing and production (in other words not the AAAS published version).

FOR MOVIES / FILM / TELEVISION:
Permission is granted to use, record, film, photograph, and/or tape the AAAS material in connection with your program/film and in any medium your program/film may be shown or heard, including but not limited to broadcast and cable television, radio, print, world wide web, and videocassette.

The required credit line should run in the program/film's end credits.

FOR MUSEUM EXHIBITIONS:
Permission is granted to use the AAAS material as part of a single exhibition for the duration of that exhibit. Permission for use of the material in promotional materials for the exhibit must be cleared separately with AAAS (please contact us at permissions@aaas.org).

FOR TRANSLATIONS:
Translation rights apply only to the language identified in your request summary above.

The following disclaimer must appear with your translation, on the first page of the article, after the credit line: "This translation is not an official translation by AAAS staff, nor is it endorsed by AAAS as accurate. In crucial matters, please refer to the official English-language version originally published by AAAS."

FOR USE ON A COVER:
Permission is granted to use the AAAS material on the cover of a journal issue, newsletter issue, book, textbook, or annual report in print and electronic formats provided the AAAS material reproduced as permitted herein remains in situ and is not exploited separately

By using the AAAS Material identified in your request, you agree to abide by all the terms and

conditions herein.

Questions about these terms can be directed to the AAAS Permissions department permissions@aaas.org.

Other Terms and Conditions:

v 2

If you would like to pay for this license now, please remit this license along with your payment made payable to "COPYRIGHT CLEARANCE CENTER" otherwise you will be invoiced within 48 hours of the license date. Payment should be in the form of a check or money order referencing your account number and this invoice number RLNK500937922.
Once you receive your invoice for this order, you may pay your invoice by credit card. Please follow instructions provided at that time.

Make Payment To:
Copyright Clearance Center
Dept 001
P.O. Box 843006
Boston, MA 02284-3006

For suggestions or comments regarding this order, contact RightsLink Customer Support: customercare@copyright.com or +1-877-622-5543 (toll free in the US) or +1-978-646-2777.

Gratis licenses (referencing $0 in the Total field) are free. Please retain this printable license for your reference. No payment is required.